Developing *in vitro* culturing methods of the Apicomplexan parasite *Cryptosporidium parvum*

Alexander J. Bones

Supervisors: Dr Anastasios D. Tsaousis, Prof Martin Michaelis

School of Biosciences

University of Kent

A thesis submitted to the University of Kent, Faculty of Sciences for the degree of MSc in Microbiology

July 2017

Acknowledgements

I would like to thank the members of the Tsaousis and Michaelis labs for their help throughout this year. I would particularly like to thank Emilie Saintas, Tom Jackson-Soutter and Edith Blackburn for locating frozen stocks of the cell lines used here; Joanna Bird, Hannah Onafuye, Helen Grimsley, Eithaar al Barwani, Basma Bahsoun and William Mosedale for kindly providing cultures of their cell lines. I would like to thank Kent Fungal Group for the use of their fluorescent microscope and Eliot Piper-Brown for providing training in its operation. I would especially like to thank Chris Miller for his expertise of *Cryptosporidium* parasites and for establishing the majority of techniques used here, and Dr Lyne Jossé for training in mammalian tissue culture techniques, general supervision and for reviewing this thesis. I would finally like to thank both of my supervisors; Dr Anastasios Tsaousis and Prof Martin Michaelis for planning this project, their supervision and for reviewing this thesis.

Contents

Abbreviations

AIDS – Acquired immunodeficiency syndrome

ATP – Adenosine triphosphate

BSA – Bovine serum albumin

$CaCl_2$ – Calcium chloride

CO_2 – Carbon dioxide

CRISPR – Clustered regularly interspaced short palindromic repeats

DAPI – 4', 6-diamidino-2-phenylindole

DEPC – Diethyl pyrocarbonate

DMSO – Dimethyl sulfoxide

DNA – Deoxyribonucleic acid

dNTPs – Deoxynucleotide triphosphates

EDTA – Ethylenediaminetetraacetic acid

FBS – Foetal bovine serum

FITC - Fluorescein isothiocyanate

GI – Gastrointestinal

HEPES – 4-(2-hydroxyethyl)-1-piperazineethanesulfonic acid

IMDM – Iscove's Modified Dulbecco's Medium

MEM – Minimal Essential Medium

$MgCl_2$ - Magnesium chloride

$NaHCO_3$ – Sodium bicarbonate

HIV – Human immunodeficiency virus

qPCR – Quantitative polymerase chain reaction

RAPD – Random amplification of polymorphic DNA

RNA – Ribonucleic acid

PBS – Phosphate buffered saline

PCR – Polymerase chain reaction

p.i. – Post-infection

SCID – Severe combined immunodeficiency

SD – Standard deviation

Abstract

Cryptosporidium is a genus of ubiquitous unicellular parasites belonging to the phylum Apicomplexa, whose members are parasites of the GI tract and airways. *Cryptosporidium* is the second largest cause of childhood diarrhoea in children under two and is associated with increased morbidity. Accompanying this is the low availability of treatment and lack of vaccines. The major barrier to developing effective treatment is the lack of reliable *in vitro* culture methods, in particular those which can support the complete growth of the parasite long term, while producing a high yield of oocysts. While numerous cell lines have been reported as maintaining the parasite, there remain no options for maintaining the parasite for longer than a week. The current cell line of choice, HCT-8, can only maintain infection for three days. Recently, our lab has successfully cultivated *C. parvum* in the oesophageal cancer derived cell line COLO-680N, and can maintain infection for over a week. Given the success of this cell line, a panel of cancer derived cell lines were grown in the presence of *C. parvum* for one week, with development assessed with fluorescent microscopy and PCR. Four cell lines were used to establish cultures for three weeks. The lung adenocarcinoma cell line, HCC4006, gave the highest oocyst yield of 5.8×10^5 oocysts per mL, a nine fold return on the initial inoculum. In addition, to tackle the issue of long term oocyst production *in vitro,* a simple, low cost bioreactor system using the COLO-680N cell line was established which produced infectious oocysts for 13 weeks. This method of oocyst production will be used to establish further cell lines as long term culture platforms. Further work aims to characterise these cell lines to establish factors which promote parasite development, and to further improve yield with media supplementation.

1.0 Introduction

1.1 General Introduction

Cryptosporidium is a genus of the phylum Apicomplexa, and are a group of small parasites which are known to invade cells of the GI tract (Tzipori *et al.* 2002) and the airways (Sponseller *et al.* 2014). From an evolutionary perspective, *Cryptosporidium* is hypothesised to present an early emerging group from the gregarines, and shares similarities with both them and the coccidia (Ryan *et al.* 2016). *Cryptosporidium* is widely believed to be an obligate intracellular parasite, and occupies an intracellular but extracytoplasmic vacuole within the host (O'Hara *et al.* 2011), and has a multi-stage life cycle typical of the Apicomplexans. These parasites are known to cause an acute, watery and non-bloody diarrhoeal disease in otherwise healthy adults, termed cryptosporidiosis. Cryptosporidiosis is particularly dangerous to the immunocompromised, where diarrhoea can become chronic and recovery is slow if at all, and infection can spread to secondary sites. *Cryptosporidium* can also cause chronic diarrhoea in children which can lead to growth stunting and delayed development (Checkley *et al.* 1998; Checkley *et al.* 2015). In severe cases, death from dehydration due to prolonged episodes of diarrhoea can also occur (Cacciò *et al.* 2014). There is only one FDA approved treatment, nitazoxanide, which shows little efficacy in the immunocompromised, and no vaccines currently exist (Checkley *et al.* 2015). In the developed world, waterborne outbreaks are common, with other common exposure routes being contact with infected livestock, individuals and food. *C. parvum* has the broadest host range of any *Cryptosporidium* species identified so far (Graczyk *et al.* 1997), and is common in livestock and humans . There is currently a major lack of methods which allow for *in vitro* culture for more than a few days (Karanis *et al.* 2011), which has hampered efforts to develop effective treatment and to understand much of its life cycle. This introduction will explore the disease cryptosporidiosis, the associated epidemiology, the cell biology of *Cryptosporidium parvum* and the current progress in developing *in vitro* culture, before describing the aims of this project.

1.2 Cryptosporidiosis

The infectious course of disease for *C. parvum* has been compared in several studies of otherwise healthy individuals. In otherwise healthy volunteers with no previous exposure to *C. parvum* a median infective dose was found to be 132 oocysts (Chappell *et al.* 1996), although other studies have found that 87 oocysts is sufficient to cause infection (Okhuysen *et al.* 1999). This low number of infectious oocysts means that a single shedding human or animal has huge infection potential. In terms of disease progression, incubation of oocysts had a 9 day incubation on average with mild disease lasting 3 days with unformed stool passing in otherwise healthy volunteers. These findings slightly contrast those found by Jokipii, which had a mean incubation period of 7.2 days and a mean

symptom duration of 12.2 days (Jokipii *et al.* 1986). Differences likely arose from the sources of infection, as no distinction was made between species of *Cryptosporidium* in the Jokipii study. A similar analysis of otherwise healthy infected individuals found that in two groups of symptomatic infected individuals there was an average incubation period of 5 and 6.43 days (Chappell *et al.* 1996). This study also found that while oocyst shedding does occur on consecutive days, certain stool samples on a given day may result in no oocysts being present in a given sample (Chappell *et al.* 1996). Isolates have varying degrees of infectivity, with the TAMU isolate having an ID_{50} of 9 oocysts, while the UCP required 1042 oocysts (Okhuysen *et al.* 1999). In adults with pre-existing IgG against *Cryptosporidium parvum* there was a > 20 fold increase in the infectious dose required to cause an infection compared with adults with no previous exposure (Chappell *et al.* 1999). Infection did not appear to resolve quicker with previous exposure, although the number of symptomatic individuals was lower, suggesting previous exposure had some protective effects (Chappell *et al.* 1999). Isolates also exhibit differing durations of diarrhoea (Okhuysen *et al.* 1999). Treating oocysts with *Lactobacillus acidophilus* and *L. reuteri* culture broth causes up to 81 % reduction in oocyst viability (Foster *et al.* 2003), suggesting that the host gut microbiota may have significant effects on disease progression and outcome. *C. parvum* has also been shown to have tumorigenic effects in a mouse model. An isolate of *C. parvum* from an immunosuppressed patient were used to experimentally infect dexamethasone suppressed and non-treated SCID mice. This led to neoplasm formation in all 18 of the tested mice (Certad *et al.* 2012). A study identifying the cause of death for calves in a Japanese dairy farm found that *C. parvum* and *Giardia intestinalis* co-infection was observed in one of the dead calves, and that *C. parvum* alone was enough to be lethal (Matsuura *et al.* 2017). Mortality in calves has also been observed by (Peeters *et al.* 1992), where experimental infections of newborn calves caused 3 of 5 calves to die. The Global Enteric Multicentre Study (GEMS) identified that infection with *C. parvum* is associated with increased mortality in children when compared to other causes of prolonged diarrhoea (Checkley *et al.* 2015). *C. parvum* shows increased mortality in numerous young animals and children, and there are much needed improvements to be made in the prevention, diagnosis, and treatment of this parasite.

1.3 Epidemiology

Cryptosporidium parvum is one of the most common etiological agents of cryptosporidiosis, along with *Cryptosporidium hominis* (Checkley *et al.* 2015). *C. parvum* has one of the most diverse ranges of host species among *Cryptosporidium* spp., being capable of infecting humans and several other mammalian species (Upton *et al.* 1985; Graczyk *et al.* 1997; Hunter *et al.* 2005). The developed world experiences seasonal outbreaks of cryptosporidiosis which are often linked to contaminated water exposure, with *Cryptosporidium* spp. being responsible for 60.3 % of protozoan waterborne

outbreaks between 2004 and 2010 (Efstratiou *et al.* 2017). The largest ever outbreak of a waterborne protozoan illness in the United States was attributed to *C. parvum*. The outbreak occurred in 1993 in Milwaukee and led to an estimated 403,000 individuals contracting cryptosporidiosis (Mac Kenzie *et al.* 1994) and an estimated 54 deaths (Hoxie *et al.* 1997). The Milwaukee outbreak was studied amongst children, and gave evidence that the southern water treatment plant was the source of the outbreak, due to a higher increase in anti-*C. parvum* IgG among children living in the southern region (McDonald *et al.* 2001). An earlier outbreak in Georgia, 1987, first drew attention to the ability of *C. parvum* to contaminate regulation compliant water supplies, in particular its resistance to commonly used purification procedures such as bleaching and filtration (Hayes *et al.* 1989). Numerous waterborne, foodborne and zoonotic outbreaks have been reported (**Table 1**). Due to the wide host range of *C. parvum,* zoonotic exposure is another common infection route (Hunter *et al.* 2005; Graczyk *et al.* 1997), with younger children and animals being particularly at risk. One study of feral pigs in California found that 5 % of the 221 sampled pigs were shedding *C. parvum* oocysts, with younger pigs (≤ 8 months old) and pigs from densely pig populated areas being the highest shedders (Atwill *et al.* 1997). A genotyping study of European hedgehogs hospitalised in Brno-Country (Czech Republic) with enteric symptoms revealed *C. parvum* subtype IIdA18G1 to be present in all 10 affected juveniles (Hofmannová *et al.* 2016). In middle Egypt, 14.19 % of 458 buffalo calves shed oocysts; 1-15 day old buffalo calves were at a significantly higher risk of infection (El-Khodery *et al.* 2008). Asymptomatic shedding of *C. parvum* oocysts in house mice, wood mice and bank voles has been identified in a Warwickshire agricultural site, and presents a potential reservoir of infection for both man and domestic livestock (Chalmers *et al.* 1997). A genotyping study of *Cryptosporidium* spp. in the United Kingdom identified that *C. parvum* was identified in 61.5 % of 1,705 human faecal samples (Mclauchlin *et al.* 2000). This study also associated *C. parvum* with increased spring cases and had a higher case rate in non-travellers, while *C. hominis* was linked to disease as a result of travelling abroad. A later study covering outbreaks from 1985 - 2000 analysed 2414 human cases and found that *C. parvum* was identified in 56.1 % of patients, *C. hominis* was identified in 41.7 % of cases and both were identified in 0.9 % of cases (Leoni *et al.* 2006). Genotyping of isolates from AIDS patients in Switzerland, Kenya and the USA found that *C. parvum* was responsible for half of the Swiss cases and one of the six Kenyan cases (Morgan *et al.* 2000). Exposure through interaction with infected livestock and/or animal reservoirs is a well-known risk factor, and adequate hygiene measures need to be taken when dealing with livestock and potentially infected animals.

Table 1 - Examples of reported cryptosporidiosis outbreaks

Outbreak (Location, Year)	Type (Waterborne, Zoonotic, Foodborne)	Affected	Cause	Reference(s)
Georgia, USA, 1987	Waterborne	Estimated 13,000	Cattle shed faeces insufficiently removed from public water supply	(Hayes *et al.* 1989)
Milawukee, USA, 1993	Waterborne	Estimated 403,000 cases, 54 deaths	Contamination of Southern water treatment plant from sewage outlet	(Mac Kenzie *et al.* 1994; McDonald *et al.* 2001; Hoxie *et al.* 1997)
Wiltshire and Oxfordshire, UK, 1989	Waterborne	516	Failure to remove oocysts in water treatment plants	(Richardson *et al.* 1991)
Oshkosh, Wisconsin, USA, 1993	Waterborne	61	Faecal accident in resort pool	(MacKenzie *et al.* 1995)
Southwest Devon, 1995	Waterborne	575	Contaminated public water supply, potentially from shedding cattle	(Patel *et al.* 1998; Peng *et al.* 1997)
Hertfordshire and North London, 1995	Waterborne	345	Contaminated public water supply, likely contamination from upriver sewage works	(Patel *et al.* 1998; Spano *et al.* 1997)
Seoul, Korea, 2012	Waterborne	126	Worn pipes allowed contamination of drinking water with waste water	(Moon *et al.* 2013)
Stockholm, Sweden, 2002	Waterborne	Estimated 800 - 1000	Insufficient removal of oocysts from swimming pool	(Insulander *et al.* 2005)
Tarrant County, Texas, USA, 2008	Waterborne	Estimated 154	Insufficient chlorine levels to kill oocysts in artificial lake	(Cantey *et al.* 2012)
Washington D.C., USA, 1998	Foodborne	92	Infected individual preparing raw food	(Quiroz *et al.* 2000)
Maine, USA, 1993	Foodborne	160	Contaminated cider, likely from shedding calf at cider farm	(Millard *et al.* 1993)
Ohio, USA, 2003	Foodborne	12	Ozonation treatment of cider insufficient to inactivate oocysts	(Blackburn *et al.* 2006)
Stockholm, Sweden, 2008	Foodborne	16	Unwashed contaminated parsley used in béarnaise sauce	(Insulander *et al.* 2008)
Sakai City, Japan, 2006	Foodborne	4	Contaminated liver and/or Yukke	(Yoshida *et al.* 2007)
New York, USA, 2000	Zoonotic	7	Veterinary students exposed to shedding calves	(Preiser *et al.* 2003)
Bologna, Italy, 2013	Zoonotic	6	Veterinary students in contact with infected new-born foals	(Galuppi *et al.* 2016)

Outbreaks in the developed world are well documented, owing to the general access to higher accuracy methods and expertise in diagnosis (Checkley *et al.* 2015). In less developed countries, cryptosporidiosis has a far greater burden and impact on health. Otherwise healthy adults tend to suffer from a mild, self-limiting infection, whereas young children in less developed areas tend to

suffer from a greater disease burden of prolonged shedding. A cross sectional case study of children in Uganda found that cryptosporidiosis was associated with persistent diarrhoea, malnutrition (underweight, wasting, and stunting), unfavourable outcome of diarrhoea and death (Tumwine *et al.* 2003). Studies in children living in slums in Brazil found that cryptosporidiosis was both highly seasonal (occurring more commonly in the months with higher rainfall) and commonly occurred in young children (mean age of first infection 11.9 months) (Newman *et al.* 1999). The prolonged burden of disease in children has been observed in Peruvian children living in a shanty town in Lima. Young children between 0 and 5 months of age who were infected demonstrated an average deficit of height of 0.95 cm (Checkley *et al.* 1998). Children who were already stunted and suffered infection had a deficit of 1.05 cm compared to uninfected stunted children. This study highlights the prolonged effects that childhood infection with cryptosporidium can have. One study of children suffering from HIV/AIDS in Jos, Nigeria, found that none of the affected children were shedding *C. parvum* oocysts in stools, whereas oocysts were found in 3.8 % of the non-HIV/AIDS suffering control group (Banwat *et al.* 2004). The low prevalence of infection may be due to analysis of a single stool sample, as oocyst shedding does not always occur on consecutive days (Chappell *et al.* 1996). A recent study highlighted the high level of infection in Australian Aboriginal people, especially children under 4 years old, who had a nearly 20 times higher notification rate compared with non-Aboriginal Australians, with *C. hominis* being particularly prevalent (Ng-Hublin *et al.* 2017). Surveillance between 2012 and 2013 in Odisha (India) found a high incidence of oocyst shedding in cattle and found contamination in 37 % of ponds and 10 % of tube wells used for drinking water (Daniels *et al.* 2015). Finally, the global enteric multicentre study (GEMS) found that *Cryptosporidium* spp. were significantly associated with disease in toddlers aged 12-23 months regardless of the HIV/AIDS rate and associated with a significant mortality risk (Kotloff *et al.* 2013). *Cryptosporidium* infectious are hugely underreported, especially in rural and remote communities (Checkley *et al.* 2015), which likely corresponds to a huge underdiagnosed global health burden. Improvements in accessibility and diagnostic tools are needed, especially in lower income countries.

1.4 Cell Biology

Cryptosporidium parvum has a multi-stage life cycle typical of apicomplexans, all stages of which are completed in a single host organism (monoxenous). Structural studies have shown the general progression of the life cycle *in vivo* and *in vitro*, however molecular studies revealing the biochemical nature of the changes undergone by the parasite, including the triggers which cause progression through the life cycle, are lacking. The difficulties maintaining *Cryptosporidium in vitro* have slowed progress in this area. The life cycle of *Cryptosporidium* is a complex and multi-stage

process (**Fig. 1**). In brief, ingestion of an oocyst results in the release of four motile sporozoites in the small intestine, which invade the ileal cells and develop into trophozoites. These divide by merogeny to generate a type I meront containing six to eight type I merozoites, which when released continue this cycle by developing into trophozoites upon invasion. At some stage, certain type I merozoites will develop into type II meronts, which contain four type II merozoites. This begins the sexual stage of multiplication, as these merozoites develop into undifferentiated gametes upon cell invasion, and will then develop into macrogamonts or microgamonts, the latter of which produces microgametes. These fertilise the macrogamont and form a zygote, which will develop into one of two types of oocyst; thin walled, which will excyst and continue the replication cycle within the same host (auto-infection), and thick walled, which are shed into the environment (Fayer *et al.* 2008). Recent studies have suggested that there may be extracellular development (Hijjawi *et al.* 2004; Rosales *et al.* 2005; Aldeyarbi *et al.* 2016b; Aldeyarbi *et al.* 2016a; Aldeyarbi *et al.* 2016c), and that sexual stages can divide by binary fission (Borowski *et al.* 2010). Developing *in vitro* culture methods which can support the parasite for over two weeks is key to understanding the life cycle and the roles extracellular stages play.

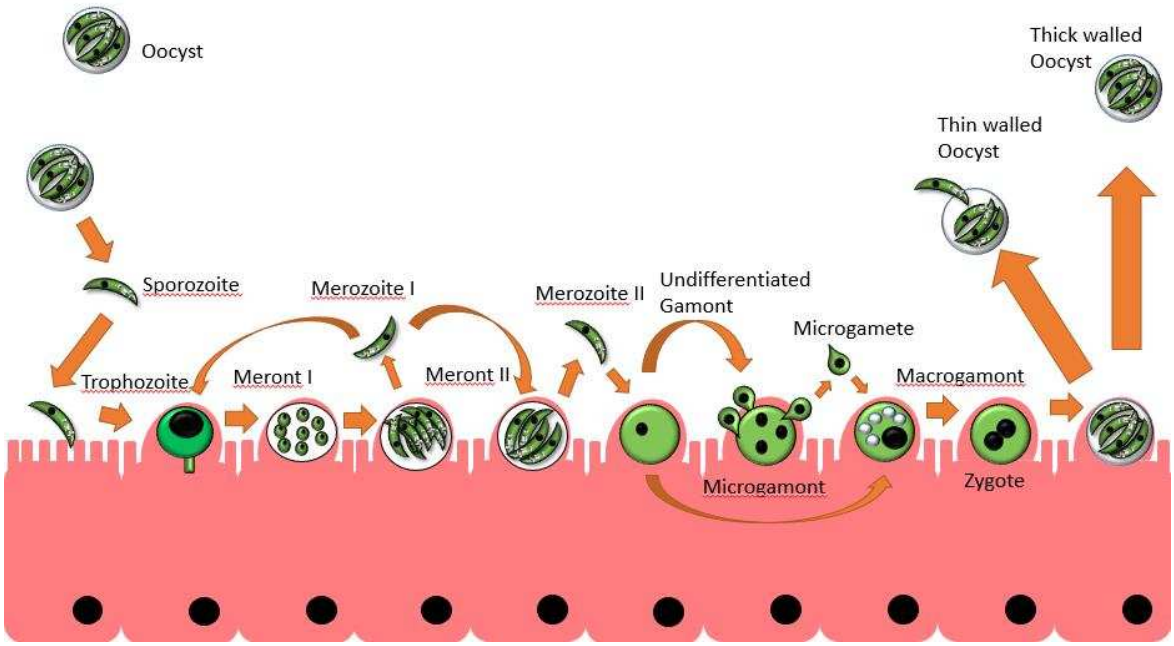

Figure 1 - Outline of the *Cryptosporidium parvum* life cycle (Thompson *et al.* 2005). Ingested oocysts release sporozoites which invade the ileum, developing into trophozoites and type I meronts, containing type I merozoites. Released type I Merozoites can become trophozoites themselves or develop into type II meronts, which release type II merozoites, these develop into undifferentiated gamonts. Gamonts differentiate into macrogamonts or microgamonts, the latter produces microgametes which fertilise macrogamonts. Sporulation occurs within the host, releasing thick walled oocysts into the environment and thin walled oocysts, which auto-infect the same host organism.

C. parvum oocysts are small, almost circular bodies measuring three to six µm in diameter. Within the oocyst are four sporozoites measuring 2 µm x 0.8 µm. Thick walled oocysts are extremely hardy and are resistant to many common disinfection methods, including 5.25 % sodium hypochlorite, and sodium hydroxide concentrations below 6 % (Barbee *et al.* 1999). Oocysts stored between 0 and 20 °C are infectious for 24 weeks (Fayer *et al.* 1998), with inactivation being reported by heating at 72.4 °C for 1 minute or 64.2 °C for 5 minutes by (Fayer 1994), but only 15 seconds at 55 °C and 60 °C and 5 seconds at 70 °C by (Fujino *et al.* 2002), indicating differences in inactivation times between strains. Oocysts can survive – 15 °C for 24 hours and –10 °C for 168 hours whilst retaining infectivity (Fayer *et al.* 1996). The highly resistant nature of the oocysts has been attributed to a complex lattice structure (Harris *et al.* 1999), a surface glycocalyx layer (Liu *et al.* 2010), carbohydrates, fatty acids and aliphatic hydrocarbons, hydrophobic proteins and an inner glycoprotein layer (Jenkins *et al.* 2010). Transcriptome analysis has revealed that oocysts are highly active in protein synthesis and translation, along with active proteasome and ubiquitin machinery (Zhang *et al.* 2012). As *C. parvum* lacks all *de novo* nutrient synthesis genes and becomes less

infectious with age (Slifko *et al.* 1999), it is likely that the parasite relies on protein recycling and its own reserves of amylopectin to survive shifts in environmental conditions (Fayer 1994; Zhang *et al.* 2012).

Upon ingestion by a host, oocysts undergo a process known as excystation. This process involves an opening in the oocyst wall, termed a "suture", which enlarges prior to sporozoite release (Reduker 1985). The opening enables release of the sporozoites and subsequent invasion of intestinal epithelia (Reduker 1985). Sporozoites exhibit gliding motility common to other apicomplexan parasites, with helical motility patterns observed just prior to cell invasion (Wetzel *et al.* 2005). Gliding motility relies on myosin motor activity, actin polymerisation and myosin light chain kinase phosphorylation of myosin (Forney *et al.* 1998). The motility trails are notably shorter than most other apicomplexans such as *Toxoplasma* and *Plasmodium*, generally being 2 to 3 times the sporozoite body length (Arrowood *et al.* 1991; Forney *et al.* 1998), with *C. parvum* sporozoites exhibiting three times faster movement than *T. gondii* tachyzoites (Wetzel *et al.* 2005). This may be attributed to oocyst adherence to the intestinal epithelia, as there is a short distance to cover for sporozoites to invade a host cell compared to *Plasmodium* and *Toxoplasma,* which migrate between several organs.

The invasion process is mediated by multiple interactions between parasite proteins and the host plasma membrane (Arrowood *et al.* 1991; Doyle *et al.* 1993; Okhuysen *et al.* 1994; Petersen *et al.* 1997; Barnes *et al.* 1998; Spano *et al.* 1998; Langer *et al.* 1999; Nesterenko *et al.* 1999; Cevallos *et al.* 2000; Langer *et al.* 2001; Pollok *et al.* 2003; Aguirre-García *et al.* 2007; Yao *et al.* 2007; Putignani *et al.* 2008; Singh *et al.* 2015). Through a still poorly understood process, invasion appears to be mediated by localisation of the apical complex to the anterior end of the sporozoite, followed by its discharge. Attachment and invasion occurs preferentially at 37 °C and at a pH of 7.4 – 7.6 (Chen *et al.* 1998; Huang *et al.* 2004), which are the conditions of the distal ileum (Evans *et al.* 1988), where infection is observed frequently. The sporozoite attaches to the plasma membrane of a host cell and is then enveloped (Chen *et al.* 1998), followed by transformation into a replicative trophozoite. Notable morphology changes are the parasite becoming rounded, and enlargement of the nucleus (Bonnin *et al.* 1999; Beyer *et al.* 2000). Internalisation of the parasite recruits vacuoles to the infected location, causing fusion and formation of the parasitophorous vacuole (Huang *et al.* 2004). The transformation from invasive sporozoite to replicative trophozoite involves both host and parasite derived factors (O'Hara *et al.* 2011). Host derived signals, which cause this transformation have recently been identified; glycoproteins present in FBS, unidentified factors secreted by HCT-8 cells and Gal-GalNAc are all capable of inducing transformation into trophozoites (Edwinson *et al.* 2016). The localisation of Gal-GalNAc to the infection site (Nelson *et al.* 2006) is

likely key to allowing the parasite to become replicative. Sporozoites, which have been pre-treated with Gal-GalNAc, showed decreased ability to enter human colorectal adenocarcinoma cells (HCT-8) and primary bovine intestinal cells (Hashim *et al.* 2006), perhaps due to the switch to trophozoites and subsequent loss of invasive cellular elements (Beyer *et al.* 2000). Trophozoite development is accompanied by the formation of the 'feeder organelle', a tube or tunnel which connects the parasite to the host cell cytoplasm (Beyer *et al.* 2000; Huang *et al.* 2004; Umemiya *et al.* 2005). Electron microscopy studies identified an 'electron dense band' at the interface between the parasite and host membrane, with the appearance of a feeder organelle visible (Bonnin *et al.* 2001). The feeder organelle has been hypothesised as a mechanism of myzocytosis engaged in by other gregarines, however no studies have shown transfer of host cytoplasm to the parasite. The ATP binding cassette protein CpABC-1 is localised to the host-parasite interface (Perkins *et al.* 1999; Zapata *et al.* 2002) and likely confers selective nutrient uptake and/or metabolite expulsion. Beyer and colleagues demonstrated replicative stages remain intracellular, but extracytoplasmic in rat ileal cells, but that the parasite can be found within the cytoplasm of intraepithelial macrophages *in vivo* (Beyer *et al.* 2000), indicating that the occupied niche may be tissue or cell type specific. The life cycle progresses through rounds of asexual merogeny followed by fertilisation of gamonts, development of zygotes and oocyst production. Scanning electron microscopy work in the HCT-8 cell line has given a rough timeline of life cycle progression, with trophozoite development occurring after 24 hours of infection, type II merozoites appearing after 48 hours of infection and gametes being found after 96 hours (Borowski *et al.* 2010).

While *Cryptosporidium* has long been considered an obligate intracellular pathogen, there is some evidence that suggests that these parasites show similar properties to gregarines in that they are capable of both replicating both within a host cell and extracellularly. The first researcher to observe this was (Hijjawi *et al.* 2004), who demonstrated through light microscopy that the entire life cycle of *C. parvum* could be completed in axenic culture. This was followed by electron microscopy studies of *C. parvum* in cell culture which demonstrated the presence of extracellular stages with similar cell structure to gregarines, such as large extracellular multinucleated stages, spores containing 8 sporozoites, motile trophozoites/gamont-like stages and of syzygy occurring (a pairing of two mature trophozoites, followed by wall formation around the cells, which develop into gametes and subsequent fertilisation and oocyst development) (Rosales *et al.* 2005). Aldeyarbi and Karanis have made similar findings in axenic culture, observing syzygy in both zoites early in culture (12 hours), gamont stages later in culture (120 hours) and syzgy of two parasites being enveloped by a double membrane at 168 hours (Aldeyarbi *et al.* 2016c). This study also highlighted the presence of protomerite and epimerite-like structures present on sporozoites. The

identification of sexual stages with transmission electron microscopy in axenic culture has also recently been reported (Aldeyarbi *et al.* 2016b). Parasites quickly entered the sexual stages of the life cycle, as early as half an hour after inoculation, which has not been observed previously in cell culture. Generated sexual stages also appeared to undergo syzygy, similarly to the observations made by (Borowski *et al.* 2010) and (Rosales *et al.* 2005) who observed microgamonts undergoing both syzygy and binary fission. The appearance of paired gamonts has also been observed, which could be undergoing binary fission (Rasmussen *et al.* 1993). Also, motile trophozoites and meronts have been observed by several groups (Hijjawi *et al.* 2004; Rosales *et al.* 2005; Borowski *et al.* 2010). In axenic culture, sporozoites generally have a banana shaped appearance, while merozoites have been described as bean shaped and rod shaped (Hijjawi *et al.* 2004; Rosales *et al.* 2005; Karanis *et al.* 2008). The work by (Karanis *et al.* 2008) claimed that the pre-treatment of bleach, used by many researchers to sterilise oocysts and prepare them for excystation, was damaging to internal sporozoites and caused death of the unusually shaped extracellular merozoites, which were observed to excyst directly from oocysts. The group attempted to maintain these stages in axenic culture but were unable to maintain them for more than 2 days. In an attempt to clarify the significance of these 'excysting merozoites' and to reveal the nature of the observed extracellular 'motile trophozoites' (Hijjawi *et al.* 2004; Aldeyarbi *et al.* 2016a) and 'gamont like stages' (Hijjawi *et al.* 2004; Rosales *et al.* 2005; Perez Cordón *et al.* 2007), (Petry *et al.* 2009) isolated sporozoites and kept them in the maintenance medium described by (Hijjawi *et al.* 2004) for 24 hours and three hours respectively, both groups observed that sporozoites became pear and oval shaped in the absence of host cells, and noted that some sporozoites appeared to have degraded (Petry *et al.* 2009). In addition, these stages were not infectious to HCT-8 cells, while freshly excysted sporozoites (< 4 hours old) were. Although the switch to trophozoites would lead to a lack of invasive capability, (Matsubayashi *et al.* 2010) have observed similar morphology changes and have shown that the change from traditional 'banana shaped' trophozoites to 'cashew nut' and 'rounded' stages was accompanied by a reduction in viability, with the final 'round' forms showing only 49.2 % viability after three hours incubation.

In light of morphological and phylogenetic similarities, *Cryptosporidium* has been reclassified from a coccidian to a gregarine (Ryan *et al.* 2016). Other evidence to support this change includes the lack of an apicoplast (a remnant plastid present in many other apicomplexans, including *Plasmodium* and *Toxoplasma)*, a similar morphology (Aldeyarbi *et al.* 2016a) and the ability to complete its life cycle in the absence of host cells (Hijjawi *et al.* 2004; Koh *et al.* 2013; Koh *et al.* 2014; Aldeyarbi *et al.* 2016b). Other phylogenetic evidence has also shown the relationship between *Cryptosporidium* and the gregarines. Sequence comparisons of the gregarines and

Cryptosporodium confirmed the view that the gregarines are an early emerging branch of the apicomplexans and that *Cryptosporodium* is a sister group of the gregarines (Carreno *et al.* 1999).

The cell biology of *Cryptosporidium* infection has been widely documented using various microscopy techniques, however live cell imaging allowing progress to be tracked in real time is still lacking. In addition, the molecular basis of the life cycle changes has yet to be discerned. In the future, with improved genetic tools such as CRISPR/Cas (Vinayak *et al.* 2015), it may be possible to routinely transfect *Cryptosporidium* to identify crucial functional genes, their roles and possible vaccine targets.

1.5 *In vitro* Culture

The major barrier which inhibits a greater understanding of this organism is a lack of a reproducible culture method capable of supporting the parasite life cycle long term (Hijjawi 2010; Ryan *et al.* 2015). The problems arise from the complex life cycle and the unclear mechanisms this parasite has for entering different stages. When selecting a suitable host cell culture, the options are generally limited to cancer derived cell lines for long term culture, due to the innate immortality of these cell lines, the availability of these cell lines from culture collections and their ease of use. The use of primary cell lines and stem cells can provide more accurate *in vivo* models of intestinal infection, and can provide higher yields of *C. parvum* stages (Castellanos-Gonzalez *et al.* 2013; Varughese *et al.* 2014; DeCicco RePass *et al.* 2017), but the short life span of these cells and finding sources of these can prove difficult. Cell lines are limited in their ability to support the parasites life cycle completely and to support continuous development, which tends to plateau after a week in culture, and often sooner (Current *et al.* 1983; Current *et al.* 1984; Flanigan *et al.* 1991). Prolonged development requires host cells which support the complete life cycle, lack a tendency to overgrow, and produce a high yield of both oocyst types to propagate new infections and to continue existing infective cycles.

The first *in vitro* culture system of *C. parvum* utilised endoderm cells of the chorioallantoic membrane of chicken embryos and completed its life cycle between three and eight days (Current *et al.* 1983). Substantial developments have been made in cell culture since, utilising several cell types, summarised in **Table 2**.

Table 2 - Summary of cell lines reported as supporting *C. parvum* replication. Where multiple cell lines are listed, subsequent data refers to those in bold.

Cell Line/Type	Oocyst Source	Media	Time Maintained	Life Cycle	Reference(s)
Chorioallantoic membrane of chicken embryos (Hubbard broiler and White Leghorn breed)	Naturally infected calf, infected AIDS patient	N/A	8 days	Complete life cycle	(Current *et al.* 1983)
Human foetal lung, Porcine kidney, Primary chicken kidney	AIDS patient	Minimal Essential Media with Earle's Salts, 2 % FBS	7 days	Complete life cycle	(Current *et al.* 1984)
HT29.74, Clone of colorectal cell line HT29	AIDS patient	RPMI-1640, 10 % FBS, 24 mM sodium bicarbonate, 1 mM sodium pyruvate, 20 mM HEPES (for undifferentiated cells), Leibovitz L-15 medium containing 5 mM galactose, 6 mM pyruvate, 1 mM L-glutamine, 20 mM HEPES, antibiotics, 10% dialyzed fetal calf serum (for differentiated cells)	13 days, rapid loss of reinfection after 5 days	Asexual stages only	(Flanigan *et al.* 1991)
Mouse peritoneal macrophages	Naturally infected calves	RPMI-1640, 10 % inactivated FBS	3 days	Asexual, few instances of gamonts or oocysts	(Martinez *et al.* 1992)
RL95-2, derived from human endometrial carcinoma	Experimentally infected calves	Dulbecco's modified Eagle's medium and Ham's F12 medium (1:1 ratio), 10 % FBS, 10 mM HEPES, 5 µg bovine insulin, 2 % $NaHCO_3$ ($^w/_v$)	4 days	Complete life cycle	(Rasmussen *et al.* 1993)
Madin-Darby canine kidney (MDCK)	Infected calves	Minimal Essential Media, 10 % FBS	5 days	Complete life cycle	(Rosales *et al.* 1993)
HRT-18 (Human rectal tumour)	Experimentally infected calves	RPMI-1640, 10 % Inactivated FBS	6 days	Asexual stages only	(Woodmansee *et al.* 1983)
Caco-2 (Colorectal adenocarcinoma)	Experimentally infected goats and lambs, AIDS patient with persistent cryptosporidiosis	N/A	5 days	Complete life cycle	(Buraud *et al.* 1991)
Madin-Darby bovine kidney (MDBK)	Naturally infected calves (Villacorta et al. 1996, Upton 1994)	Minimal Essential Media, 26 mM NaHCO3, 4 % FBS (Villacorta), RPMI-1640 with L-glutamine, 10 % FBS, 26 mM $NaHCO_3$, 15 mM HEPES (Upton)	3 days	Complete life cycle	(Villacorta *et al.* 1996; Upton, Tilley, Nesterenko, *et al.* 1994)
BALB-3T3, BT-549, Hs700t, HT-1080, RL95-2, **HCT-8** (Colorectal adenocarcinoma)	Infected cows	RPMI-1640 with L-glutamine, 10 % FBS	3 days	Not described	(Upton, Tilley and Brillhart 1994)
MRC-5 (lung fibroblast)	Clinical isolate	Medium 199, Earles salts; essential amino acids, L-glutamine, 0.075% w/v sodium bicarbonate, 10 % FBS	5 days	Not described	(Dawson *et al.* 2004)
BS-C-1 (African green monkey kidney cells)	Infected calves	Minimal Essential Media, 2 mM L-glutamine, 10 % FBS	3 days	Complete life cycle	(Qi Deng *et al.* 1998)
COLO-680N	Commercial source (infected cows)	RPMI-1640 with L-glutamine, 10 % FBS	8 weeks	Complete life cycle	(Miller, Jossé, *et al.* 2017)

It has been found that the level of HCT-8 infection can be increased with medium supplementation (Upton *et al.* 1995). With a base medium of RPMI-1640, ascorbic acid, *para*-aminobenzoic acid, folic acid and sodium pantothenate had an enhancing effect on parasite growth, as did increasing FBS from 5 % to 10 % v/v in the medium. Additional sugar supplements (glucose, maltose, galactose and mannose) and insulin also had a positive effect. The final supplemented medium, consisting of RPMI 1640 with 10% fetal bovine serum, 15 mM HEPES, 50 mM glucose, and 35 mg of ascorbic acid, 1.0 mg of folic acid, 4.0 mg of 4-aminobenzoic acid, 2.0 mg of calcium pantothenate, 0.1 U of insulin, 100 U of penicillin G, 100 mg of streptomycin, and 0.25 mg of amphotericin B per ml (pH 7.4) supported a ten-fold increase in parasite development compared to base RPMI-1640 (Upton *et al.* 1995). This medium is commonly employed when culturing *C. parvum,* although another medium formulation has been developed which can maintain HCT-8 cells and parasitism for 2 weeks (Perez Cordón *et al.* 2007). This medium formulation consists of RPMI-1640 medium with 10% heat inactivated FBS, pH 7.2 with $CaCl_2$ and $MgCl_2$ at 1 mM, and also requires the cells (HCT-8) have no medium renewal for a week prior to infection (Perez Cordón *et al.* 2007).

Another key process in *C. parvum* culture is the excystation protocol used to prepare oocysts for infection. Numerous laboratories use differing excystation protocols, with the number of excysted sporozoites vs the number of oocysts being used as a measure of viability. It has recently been established that the methods described by (Rasmussen *et al.* 1993) provides the highest rate of excsytation (Pecková *et al.* 2016). While long term culture in a single culture vessel is impossible with the HCT-8 cell line, Hijjawi reported the culture of *C. parvum* in HCT-8 cells for 25 days through sub-culturing (Hijjawi *et al.* 2001). This was attributed to maintaining the pH of the culture medium between 7.2 and 7.6 by changing the culture medium every 2-3 days. Numerous reports have described the decrease in life cycle stages after a week of culture (Current *et al.* 1984; Flanigan *et al.* 1991; Martinez *et al.* 1992; Rasmussen *et al.* 1993; Rosales *et al.* 1993; Upton, Tilley, Nesterenko, *et al.* 1994; Villacorta *et al.* 1996). The addition of fresh nutrients and maintaining physiological pH may be key to preserving the life cycle for prolonged periods of time. The success may also be attributed to HCT-8 monolayers up to 67 days old being capable of supporting infection (Sifuentes *et al.* 2007). More recently, *C. parvum* infection was maintained for 120 hours using primary human intestinal epithelial cells, which provided a significantly longer infection time compared to 48 hours using HCT-8 cells (Castellanos-Gonzalez *et al.* 2013). Primary cells provide advantages over cancer derived cell lines, such as retaining tissue markers and morphology and providing more accurate *in vivo* models (Varughese *et al.* 2014). The disadvantages are the considerable skill required to cultivate these cells, and the finite lifespan means there is need for a continued supply of these cells from animal or human tissues. Morphology of host cells has not been studied in great detail,

however some cell lines which support infection have been reported as having microvillus like extensions (Current *et al.* 1983; Upton *et al.* 1994; Flanigan *et al.* 1991). These extensions may play an important role in parasite development, as the observations that microvillus proteins localise to the parasite attachment site (Bonnin *et al.* 1999) and given the nature of encapsulation by the host cell (Chen *et al.* 2003; Borowski *et al.* 2010) host cell morphology may be worth investigating.

As an obligate intracellular pathogen, there has been considerable interest in propagating the parasite in the absence of host cells. This method has considerable advantages compared to host cell culture, overcoming the issues of host cell overgrowth and the need to purify the parasite from host cell material. The first report of *in vitro* culture was by Hijjawi in 2004, who described the entire life cycle of *C. parvum* in host cell free culture (Hijjawi *et al.* 2004). Utilising a modified version of RPMI 1640 with supplements and coagulated calf serum (Hijjawi *et al.* 2004) observed stages from inoculated sporozoites through to sporulated oocysts, along with additional extracellular stages. Previously, novel extracellular stages had been purified from the guts of infected mice (Hijjawi *et al.* 2002). Unfortunately, the results observed were not readily reproducible by other groups (Girouard *et al.* 2006; Woods *et al.* 2007). Woods and Upton observed that the figures reported as being 'extracellular gamont like stages' were more likely to be fungal contaminants (Woods *et al.* 2007) given the similar morphology and the lack of antifungals in the culture medium (Hijjawi *et al.* 2004). (Karanis *et al.* 2008) was capable of culturing the merozoite stages of the parasite, which were released directly from oocysts but could not be maintained in RPMI-1640. As discussed earlier, (Petry *et al.* 2009) and (Matsubayashi *et al.* 2010) have determined that observed 'merozoites' were in fact aged sporozoites. A recent study using the described maintenance medium (Hijjawi *et al.* 2004) to culture *C. parvum* and showed stages using scanning electron microscopy. Only stages from inoculated oocysts to type I merozoites were described, and there were no cases of either sexual stages or the previously described 'extracellular gamont like stages' (Hijjawi *et al.* 2004) in culture (Yang *et al.* 2015). Recently, Aldeyarbi and Karanis have had success in developing the complete life cycle of *C. parvum* in the absence of host cells using cell free maintenance medium Express Five™ serum free medium (Aldeyarbi *et al.* 2016b; Aldeyarbi *et al.* 2016c; Aldeyarbi *et al.* 2016a). The completion of the life cycle in serum free media is interesting, as the maintenance medium described by (Hijjawi *et al.* 2004) required coagulated newborn calf serum to form the biphasic medium, and that increasing the FBS concentration in HCT-8 medium caused a doubling of parasites visible on host cells (Upton *et al.* 1995). Woods and Upton found numerous serum free media alternatives which functioned as well as RPMI-1640 + 2 % serum, enumeration of parasites using Express Five™ serum free medium would reveal the comparative ability to develop the parasite. Unfortunately, there is still a need for long term and productive culture methods,

especially methods which maintain life cycle stages in culture. With improvements in cell culture and with optimal media design, it may be possible in the future to harvest *C. parvum* in axenic culture.

The need for long term and high yield production of oocysts has led to an interest in 3D culturing systems and organoid models. These systems allow for higher cell densities and subsequent parasite yields, along with allowing long term parasite propagation. The 3D culture environment can also provide a more accurate model of *in vivo* infection. Early efforts to develop 3D culture used HCT-8 cells in a low shear microgravity environment, incubated with porcine small intestinal grafts to promote differentiation into cuboidal epithelia and brush border formation (Alcantara Warren *et al.* 2008). This method allowed the intestinal epithelium to increase parasite numbers for 48 hours, however the infection reduced after this time, accompanied by a reduction in host cell attachment (Alcantara Warren *et al.* 2008). This provides a proof of concept, that bioreactor systems can be used to produce *C. parvum* parasites, and with the additional medium supplements described by Upton (Upton *et al.* 1995) or Cordon (Perez Cordón *et al.* 2007) this system may be adapted as a productive culture method. Following this, the culture of *C. parvum* was recently reported using a hollow fiber bioreactor system and maintained for over 6 months (Morada *et al.* 2016). This system produced 1 x 10^8 oocysts per day per mL of culture compared with a reported 1 x 10^6 oocysts produced in traditional 2D culture vessels. Another recent report described the culture of *C. parvum* in a model intestinal system developed using a silk fibre scaffold, which supported infection for two weeks (DeCicco RePass *et al.* 2017). While this method provides a good model of *in vivo* cryptosporidiosis, the use of multiple cell lines including intestinal myofibroblasts and the need for specialist equipment is a large cost barrier for many labs. For long term cryptosporidium culture, the adoption of 3D culture technology by several labs will require a low cost methodology and simple protocol which allows routine harvesting of large numbers of oocysts.

Cryptosporidium culture has seen large improvements over the last 30 years, however continuous routine propagation of *C. parvum in vitro* still eludes researchers. Assessment of cell lines which can withstand the parasite burden, avoid overgrowth and produce a high yield of oocysts is key to developing more efficient culturing techniques.

1.6 Project Aims

Given the urgent need for enhanced culture methods, this project aimed to develop the *in vitro* culture of *C. parvum.* Many researchers use HCT-8 cells when studying *C. parvum,* but this cell line has limited ability to produce oocysts for more than three days. Given the recent success in our lab cultivating the parasite for up to a week using the oesophageal adenocarcinoma derived cell line, COLO-680N, this length of time was set as the benchmark. A total of 17 cancer cell lines were tested for their ability to support the *C. parvum* life cycle. Given the undifferentiated nature of many cancer cell lines, the cell lines were picked at random for this project. These included a neuroblastoma, a melanoma, several breast cancers, colorectal cancers, lung cancers and ovarian cancers, as many of these cancer types have not been tried previously or have had only a single cell line of that type tested.

To track the progression of the life cycle, fluorescent microscopy was used, utilising a nuclear stain (DAPI), a mitochondrial marker (Mitotracker Red CMXRos™) and antibodies specific for *C. parvum* (Sporo-Glo™ and Crypt-a-Glo™). Cell lines were incubated for a week before staining and were then compared for their ability to propagate infection. In addition, the presence of parasite DNA in the media of infected cultures was tested using PCR with primers against random DNA fragments (RAPD) used for detecting *C. parvum* in environmental water supplies. Cell lines showing complete development were used to establish sub-infections of cell monolayer using *in vitro* produced oocysts with weekly passages, and the oocysts enumerated after three weeks. In addition, to address the limited long term culture methods currently available, a bioreactor system was established using COLO-680N in an attempt to culture the parasite long term i.e. over a month. Production was tracked by enumerating oocysts being produced and with fluorescent microscopy. Establishing an effective bioreactor using COLO-680N will be an important proof of concept, and will allow future work to try other cell lines and media optimisations, which if previous reports are to be believed, will conceivably give a 2 to 10 fold increase in parasite production. This will allow a wider range of labs to study *C. parvum* and will enable continuous oocyst production unrestricted by seasonal harvests. Harvesting and purifying from such a system will be far less labour intensive than current animal sources, which require lengthy purification protocols from faeces.

2.0 Methods

2.1 Cell Culture

Cell lines were revived from cryopreservation in liquid nitrogen or were subcultured from existing cultures. Cells were frozen in cryopreservation media (standard growth medium (**Table 3**) with 5 % DMSO). All reagents were warmed to 37 °C in a water bath prior to use. Foetal bovine serum (FBS) (Sigma-Aldrich, Lot No. BCBR0289V) was thawed completely before being heat-shocked at 56 °C for 30 minutes prior to use. All media (except RPMI-1640) was purchased from Thermo Fisher Scientific (IMDM Lot No. 1838127, MEM Lot No.1816890), RPMI-1640 was purchased from Sigma-Aldrich (Lot No. RNBF8560). All cell lines had antibiotics added to a final concentration of 100 U/mL penicillin and 100 µg/mL streptomycin per mL (Thermo Fisher Scientific). In the bioreactor system, 0.25 µg/mL amphotericin B (Sigma-Aldrich) was included in the culture medium.

2.2 Cell Line Revival

Cell lines were kept on dry ice until revival. Prior to revival, 4 mL of growth medium (**Table 3**) were placed in a T25 tissue culture flask (Sarstedt or Jet BioFil®) and warmed in a tissue culture incubator at 37 °C, 5 % CO_2 for at least 15 minutes. Cryovials containing cells in cryopreservation media were warmed in a 37 °C water bath while gently shaking for no more than 2 minutes. Cells were then transferred to a 15 mL falcon tube containing 3 - 4 mL standard medium (final volume 5 mL) and pelleted at 300 x g for 3 minutes. The supernatant was then discarded and the cells were resuspended in 1 mL of medium and transferred to the warmed T25 flask. After 24 hours the growth medium was carefully aspirated from the T25 flask, and replaced with warm fresh medium. Once revived, cells were passaged twice to ensure complete recovery from cryopreservation (see section 2.3).

2.3 Routine Subculture

Cells were inspected daily for contamination and to check confluency. When cells reached 80-90 % confluency, medium would be aspirated from the culture vessel. The cell monolayer was then rinsed with phosphate buffered saline (PBS - Dulbecco A, OXOID) which was then aspirated off. 0.25 % trypsin EDTA solution (Thermo Fisher Scientific) was added to the flask; 1 mL to T25s, 3 mL to T75s and 5 mL to T175s. Flasks were then placed in an incubator (37 °C, 5 % CO_2) for 3 - 5 mins to allow cells to detach. Detachment was observed by eye and light microscopy. Warm growth medium was added to the flask (4 mL for T25s, 7 mL for T75s and 10 mL for T175s) to deactivate trypsin. Solution was then transferred to a 15 mL falcon tube and pelleted at 300 x g for 3 mins. Supernatant was then discarded and the pellet resuspended in the same volume of warm medium as the previous flask (T25 – 5 mL, T75 – 15 mL, T175 – 30 mL). Warm medium was then added to a

clean culture vessel. Cell suspension was then added to the new vessel. For routine passage, cells were passaged at a split ratio (cell suspension: medium) of between 1:3 and 1:10. Fast growing cell lines (HCT-8, RKO, SW620, UFK-NB3, RKO, EFO-21 and EFO-27) were split at a lower density of 1:15 to 1:20. Cell lines were maintained at 37 °C and 5 % CO_2 in T25 flasks (Sarstedt or Jet Biofil®) in the media shown in **Table 3**.

Table 3 - Growth media used for cell lines

Cell Line	Base Medium	Foetal Bovine Serum
BT-474	IMDM	10 %
CAMA-1	IMDM	10 %
COLO-320	RPMI-1640	10 %
COLO-680N	RPMI-1640	10 %
EFM-19	IMDM	10 %
EFO-21	RPMI-1640	20 %
EFO-27	RPMI-1640	20 %
H2228	RPMI-1640	10 %
HCC4006	RPMI-1640	10 %
HCC827	RPMI-1640	10 %
HCT-8	RPMI-1640	10 %
IGR-39	IMDM	10 %
LS-174T	MEM	10 %
MDA-MB-468	IMDM	10 %
UKF-NB-3	IMDM	10 %
RKO	MEM	10 %
SW48	IMDM	10 %
SW480	IMDM	10 %
SW620	IMDM	10 %

2.4 *Cryptosporidium parvum* excystation

C. parvum oocysts (IOWA isolate) were purchased from Bunch Grass Farm, Deary, Idaho, and stored at 4 °C. For infection of the monolayer, an MOI of 2 was used (2 host cells per oocyst, equating to 2 sporozoites per host cell). Oocysts were pelleted at 5,000 x g for 8 minutes, then the supernatant was discarded. Oocysts were resuspended in excystation solution (0.01% trypsin (final concentration) in 0.5% sodium hypochlorite) for 4 hours at 37 °C. After this time, sporozoites were pelleted at 2,000 x g for 8 minutes then resuspended in PBS. This step was repeated twice to wash sporozoites, before the pellet was resuspended in PBS again and used to infect cells (see section 2.5).

2.5 *Cryptosporidium parvum* Infection of 24 well Plates

Cells were detached from flasks using 0.25 % trypsin EDTA (Thermo Fisher Scientific) incubating at 37 °C for 5 minutes. Trypsin was inactivated with the respective media (**Table 3**) and cells were pelleted at 300 x g for 3 minutes. Cells were resuspended in medium and 10 µL was counted using a Bright-Line™ haemocytometer (Sigma-Aldrich) and viability measured using trypan blue (InVitrogen™) exclusion (5 µL of 0.4% trypan blue in 45 µL cell suspension). Sterilised cover slips

were placed into 8 wells of a 24 well plate, with cell lines seeded at 1.4 x 10^5 cells per well. Cells were allowed to attach overnight. Cell lines which exhibited faster growth such as UKF-NB-3 were seeded at lower density to account for growth, with a density of ~70% upon infection observed by light microscopy. 7 x 10^4 oocysts prepared as described in section 2.4 were then added to 4 of the wells, while control wells had the equivalent volume of PBS added. Monolayers were incubated at 37 °C and 5 % CO_2 overnight to allow sporozoites to infect cells. After 16 hours the medium was discarded and 1 mL fresh medium was added to each well. Plates were incubated at 37 °C and 5 % CO_2 for a week to allow the infection to progress. Wells were inspected daily for contamination and contaminated plates were discarded.

2.6 *Cryptosporidium parvum* infection of T25 Flasks

Four T-25 flasks were detached and counted as described in section 2.5 and seeded at a cell density of 5.6 x 10^5 cells per flask. Three aliquots of 2.8 x 10^5 oocysts were excysted as described in *C. parvum* excystation and were inoculated into the flask, with one flask being inoculated with PBS to act as a control, and were left overnight. The medium was then aspirated off and replaced with 5 mL fresh growth medium.

2.7 T25 *Cryptosporidium parvum* Passage

Once a week, fresh T-25 flasks were seeded with 5.6 x 10^5 cells as described in section 2.6 and allowed to attach overnight. The following day, medium would be aspirated from an infected T-25 flask, filtered through a 40 µm cell strainer and pelleted at 5,000 x g for 8 mins. The supernatant was discarded and the pellet resuspended in fresh growth medium. The freshly seeded T-25 flask had the medium aspirated and replaced with the oocyst suspension.

2.8 Fluorescent Microscopy of Infected Monolayers

After the infection the medium was extracted (see section 2.9). Mitotracker™ Red CMXRos (Molecular Probes, InVitrogen™), was used at a 250 nM concentration in serum free base medium for the respective cell line (**Table 3**). 0.5 mL of this was added to each well, with plates wrapped in tin-foil and incubated at 37 °C and 5 % CO_2 for 15 - 45 minutes. Mitotracker™ solution was discarded and cells were fixed in 4 % paraformaldehyde for 10 minutes. Cells were permeabilised with 0.5 % Triton X-100 in PBS for 5 minutes on ice. Cells were washed twice in 0.5 mL PBS. Cells were blocked for half an hour in 3 % bovine serum albumin (BSA). BSA solution was discarded and a drop of 1 x Sporo-Glo™ antibody solution (Waterborne Inc.) was added to each infected well, and incubated for 1 hour at room temperature. Cells were then washed twice in 3 % BSA in PBS and were allowed to dry. Slides were prepared by coating with a 1:10 dilution of poly-L-lysine and left to dry at 56 °C for an hour. A drop of Fluoroshield™ with DAPI (Sigma-Aldrich) was added to the slides, and cover

slips were extracted from each well and placed with cells face down onto the slide. Cover slips were sealed with nail varnish and slides were stored at 4 °C in the dark. Slides were visualised on an Olympus IX81 and images captured using an Andor Zyla 4.2 plus sCMOS camera.

2.9 Oocyst Harvesting

After infection, medium was carefully aspirated from wells, placed into 1.5 mL microfuge tubes and pelleted at 300 x g for 3 mins. The supernatant was then transferred to a fresh tube and pelleted at 5,000 x g for 8 mins, the supernatant was discarded and 100 µL PBS was added. This process was repeated twice, before the pellet was resuspended in 50 µL PBS containing 100 U/mL penicillin and 100 µg/mL streptomycin. Samples were stored at 4 °C.

2.10 Oocyst Fluorescent Microscopy

12 well microscope slides were soaked in poly-L-lysine for 10 minutes then dried at 56 °C for 1 hour. 10 µL of oocyst suspension was then added to each well and allowed to dry in a 37 °C dry incubator. Samples were then fixed with ice cold methanol, which was allowed to dry. Once dry, samples were then blocked with 20 µL of 3 % BSA in PBS for half an hour at room temperature. Slides were rinsed once in PBS before being incubated with one drop (~ 45 µL) 1 x Crypt-a-Glo™ antibody solution (Waterborne Inc.) at 37 °C for 25 minutes or at room temperature for 1 hour, in the dark. Antibody was rinsed by adding 20 µL PBS to each well for 1 minute, then tilted to allow the PBS to drain off. This process was performed twice before being allowed to dry completely at room temperature while being kept in the dark. Once completely dry, one drop (~ 45 µL) of FluoroShield™ with DAPI (Sigma-Aldrich) was added to each well and left for 3 minutes. A coverslip was then added to each slide and slides were sealed with nail varnish (Boots). Slides were stored at 4 °C in the dark. Slides were visualised on an Olympus IX81 at 600x and 1000x magnification, and images captured using an Andor Zyla 4.2 plus sCMOS camera.

2.11 Oocyst Enumeration

Oocysts were quantified using a Bright-Line™ Hemacytometer (Sigma-Aldrich). 45 µL of oocyst suspension was mixed with 5 µL 0.4 % trypan blue (InVitrogen™), 10 µL was then added to the haemocytometer grid. Each sample had the four corner chambers counted and an average taken, 40 x objective with a 10 x eyepiece, 400 x total magnification.

2.12 Glucose Consumption

Cells were detached from culture flasks using 0.25 % trypsin EDTA (Thermo Fisher Scientific) and resuspended in culture medium. 45 µL of cell suspension was mixed with 5 µL 0.4 % trypan blue (InVitrogen™) and counted using a Bright-Line™ haemocytometer (Sigma-Aldrich). Cells were

seeded into a 24 well plate (Jet BioFil®) at a density of 2 x 10^5 cells per well and left overnight. Sporozoites were then prepared as described in excystation. Parasites were inoculated at an MOI of 2 and allowed to invade overnight. Uninfected control wells had 5 µL of PBS added. Medium was added and replaced with 1 mL fresh medium per well. Samples were taken after 6 hours, 24 hours, 48 hours, 72 hours, 96 hours, 120 hours, 144 hours and 168 hours after the medium change. 45 µL of medium was taken from each well and tested using the Accu-Chek™ Aviva glucose testing system (Roche Applied Science)

2.13 Bioreactor System

The miniPERM® SM bioreactor was purchased from Sarstedt AG & Co., Germany. Confluent T-175 flasks containing COLO-680N cells were detached and pelleted as described in section 2.3. Cell pellets were then resuspended and pooled in 50 mL of culture medium containing 36.8 x 10^6 COLO-680N cells. The cell suspension was drawn into a 50 mL syringe and inoculated into the production module through the sample port. 400 mL of culture medium warmed to 37 °C was added to the nutrient module. The bioreactor was then placed on a roller (SLS Lab Basics) in an incubator and maintained at 37 °C, 5 % CO_2 at a speed of 10 rpm. After 24 hours, oocysts were prepared as described in section at a MOI of 2, with sporozoites being resuspended in 1 mL of PBS. 1 mL of culture medium was then removed from the production module and the sporozoite suspension was inoculated into the production module before being returned to an incubator. Once a week, the nutrient module would be emptied of medium and replaced with fresh medium warmed to 37 °C.

2.14 Bioreactor Harvesting

Once a month 25 mL of production module medium was removed and replaced with fresh medium. The cell suspension was then filtered through a 40 µm nylon Corning® cell strainer (Sigma-Aldrich) to remove large clumps of cells, transferred to a 15 mL falcon tube and spun at 5,000 x g for 8 minutes. The pellet was washed twice in PBS then resuspended in PBS containing 100U/mL penicillin 100 µg/mL streptomycin. Samples were stored at 4 °C.

2.15 Bioreactor Produced Oocyst Infection

Harvested samples from the bioreactor were kept at 4 °C for at least a week. A 70 % confluent monolayer was seeded as described in *Cryptosporidium parvum* infection. Harvested samples had oocysts counted as described in section 2.11. 7x 10^4 oocysts were treated as described in section 2.4, followed by inoculation onto the monolayer as described in section 2.5, followed by overnight incubation and medium change. Infections of COLO-680N cells were allowed to incubate for a week, while HCT-8 infection was incubated for three days.

2.16 Cell Line DNA Extraction

DNA from pellets of trypsinised cell lines were isolated using the QIAamp® DNA mini kit following the manufacturer's instructions, before being eluted in DEPC treated water (Ambion). DNA was then quantified using a NanoDrop™ 1000 spectrophotometer (Thermo Fisher Scientific).

2.17 Oocyst DNA Extraction

For positive control DNA, genomic *C. parvum* DNA was extracted from commercially supplied oocysts using the QIAamp® DNA mini kit following the manufacturer's instructions. Samples were eluted in DEPC treated water (Ambion) and stored at - 20 °C.

2.18 Oocyst Preparation for PCR

Oocysts were isolated as described in oocyst harvesting. Oocyst suspension was diluted 1:10 in DEPC treated water (Ambion) and boiled at 100 °C for 20 mins. 5 µL of this was used directly as a PCR template.

2.19 PCR Reactions

Two PCR reactions were performed using the SB012 primer set (Wu *et al.* 2000) to test for *C. parvum* DNA and Hs18S (Miller *et al.* 2017) as a positive control when assessing specificity of the SB012 primers. SB012 forward primer sequence: 5'-ATAAACAAGCAGGAAAAAAGGT-3', reverse primer sequence 5'- CGCACAAGTTACAAGGATTATT-3'. Hs18S forward primer sequence: 5'-GGCGCCCCCTCGATGCTCTTAG-3', reverse primer sequence 5'-TTTCAGCTTTGCAACCATACTCC-3'.

Reactions were run with a 25 µL volume per reaction. Reaction mixture (per tube) consisted of 2.5 µL PCR buffer with 20 mM $MgCl_2$, 0.5 µL 10 mM dNTP mix (Roche Applied Science), 0.2 µL FastStart Taq Polymerase (5U/µL) (Roche Applied Science) and 10 nM of the appropriate primers. Remaining volume was made up using DEPC treated water to 25 µL. SB012 reactions had an initial denaturation of 94 °C for 6 mins, followed by 40 cycles of 94 °C for 30 seconds, annealing temperature of 51 °C for 30 seconds and an extension temperature of 72 °C for one minute. A final extension of 72 °C for 10 minutes was used. For the Hs18S sequence reaction an initial denaturation of 95 °C for 5 mins was used, followed by 36 cycles of 95 °C denaturation for 35 seconds, 52 °C extension for 20 seconds and an elongation of 72 °C for 20 seconds, with a final elongation of 72 °C for 10 minutes. The Hs18S reaction used 100 ng of extracted cell line DNA as a template.

2.20 Gel Analysis

2 % agarose gels were cast containing 7 µL ethidium bromide per 100 mL gel. 25 µL samples were mixed with 5 µL loading buffer (40% glycerol, 1mM EDTA, 0.001% bromophenol blue, 0.25% xylene

cyanol FF). 15 µL of sample was loaded per well. Images of gels were captured using a G:BOX gel imaging system (Syngene).

3.0 Results

3.1 Fluorescent Microscopy of Infected Cells

Host cells were incubated with pre-treated *C. parvum* oocysts at a ratio of 2 host cells per oocyst, with unexcysted oocysts removed after 16 hours incubation. After a week incubation, slides were prepared of infected monolayers and *C. parvum* stages visualised with fluorescent microscopy. 17 cell lines were tested, 16 of which have not been described previously and one (LS 174T) being tested previously for only three days. Three fluorescent markers were used; Mitotracker™ Red CMXRos stained mitochondria and indicates live cells and shows the area of host cell cytoplasm, 4',6-diamidino-2-phenylindole (DAPI) stained nuclei of *C. parvum* and host cells, and Sporo-Glo™ monoclonal antibody conjugated with fluorescein isothiocyanate (FITC) stained intracellular dividing stages of *C. parvum* (trophozoites, meronts I & II, gamonts and zygotes). 10 cell lines were found to contain stages of *C. parvum*, four of these showed evidence of the complete life cycle and were used to establish sub-infections (see section 3.4).

IGR-39

Melanoma cell line, active after one week, showing no visible intracellular stages of *C. parvum.*

UKF-NB-3

Neuroblastoma with a fast growth rate, active after one week but no intracellular growth of *C. parvum* was observed.

EFO-21

An ovarian cystadenocarcinoma. While cells appeared attached and showed mitochondrial activity after the week incubation, there were no visible instances of intracellular *C. parvum* infection.

EFO-27

An ovarian mucinous adenocarcinoma. Cells showed mitochondrial activity and were attached, but no intracellular *C. parvum* stages were observed.

LS 174T

LS 174T exhibits similar morphology to the COLO-680N cell line, forming colonies with large circular gaps between colonies. While cells appeared alive after the week, no *C. parvum* infection was observable after the week incubation.

HCC827

A non-small cell lung adenocarcinoma, and appeared healthy after the week incubation. Mitotracker™ and DAPI signals were present, but no evidence of Sporo-Glo™ labelled parasites could be seen.

SW48

A Dukes' type C, grade IV, colorectal adenocarcinoma. Cells appeared active at the end of the week but no intracellular stages of *C. parvum* were observed.

BT-474

A breast/duct cancer, exhibiting fairly slow growth. BT-474 showed evidence of trophozoite and merozoite replication, however no intracellular sexual stages were observed. Parasites developed in the cytoplasm (**Fig. 2**); active mitochondria can be observed in all figures indicating cells are alive. Intracellular stages appeared to be mostly limited to trophozoites (**Fig. 2**). Compared to other cell lines, this cell line showed a moderate level of infection after a week in culture. Uninfected control showing no Sporo-Glo™ signal shown in **Fig. 3**.

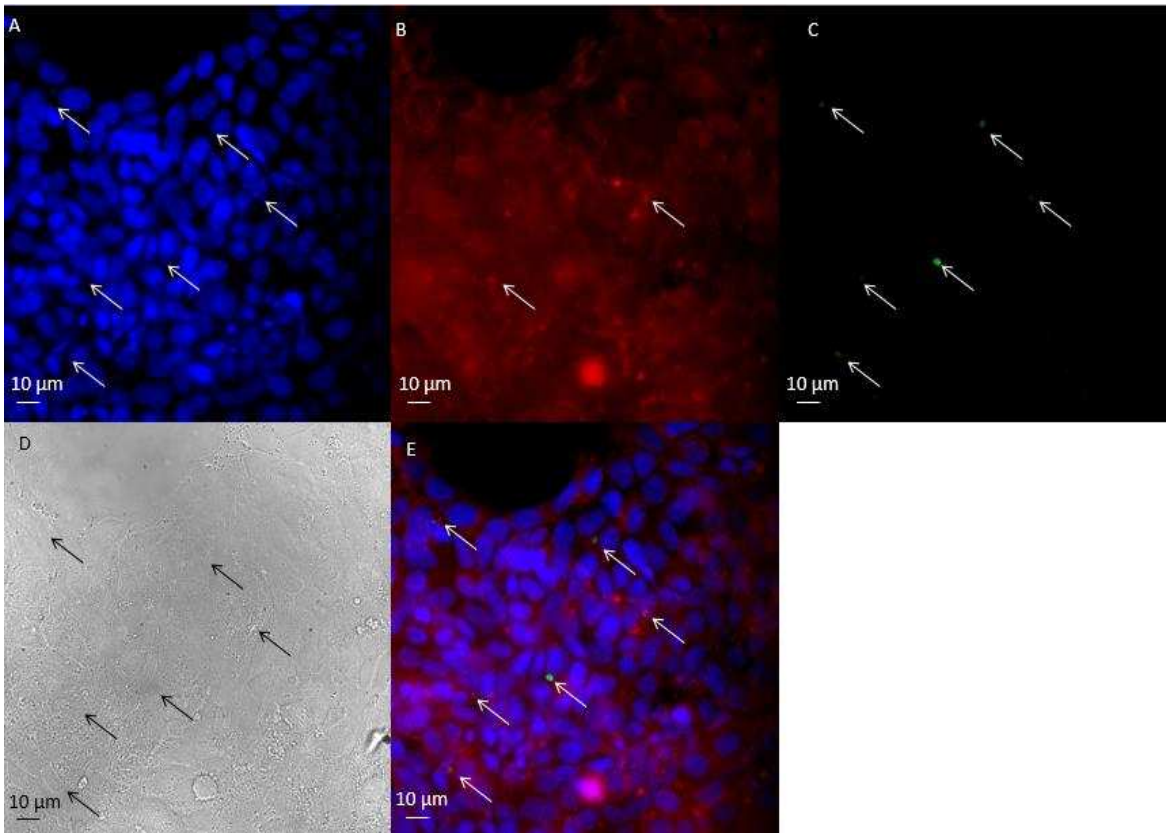

Figure 2 - **Infected BT-474 cell line**. Sporo-Glo™ filter (C) shows six regions labelled (white arrows). Mitotracker™ staining (B) shows some of these regions have signal in the Sporo-Glo™ labelled regions (white arrows). DAPI stain (A) shows distinct nuclei in regions labelled with Sporo-Glo™ (white arrows). Merged image (E) shows all channels, DIC compares with light alone (D), with outlines of parasite stages partly visible (black arrows). Stages appear limited to asexual phase of life cycle, with trophozoites and meronts I present.

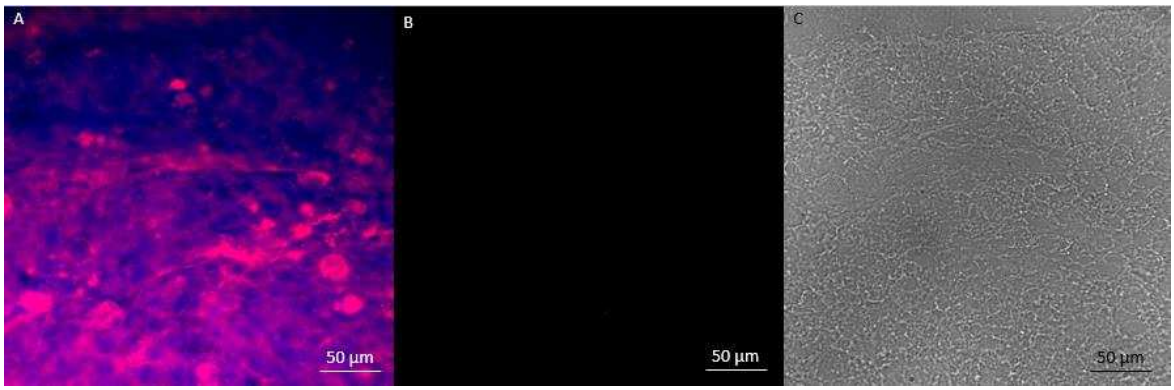

Figure 3 - Uninfected BT-474 culture. Cells have grown as a monolayer (C). Mitotracker™ shows active cells (A), but no non-specific Sporo-Glo™ binding is observed (B).

CAMA-1

CAMA-1 is a breast/duct carcinoma. This cell line had a low level of infection throughout the observed slides, with an intracellular stage and two potential oocysts present in the observed fields (**Fig. 4**). Observed in **Fig. 4** are two instances of four tightly clustered (within 5 microns) nuclei each measuring approximately half a micron in diameter. These nuclei likely belong to oocysts or type II merozoites within type II meronts, but given the lack of Sporo-Glo™ signal these are more likely to be oocysts. Uninfected cells shown in **Fig. 5**.

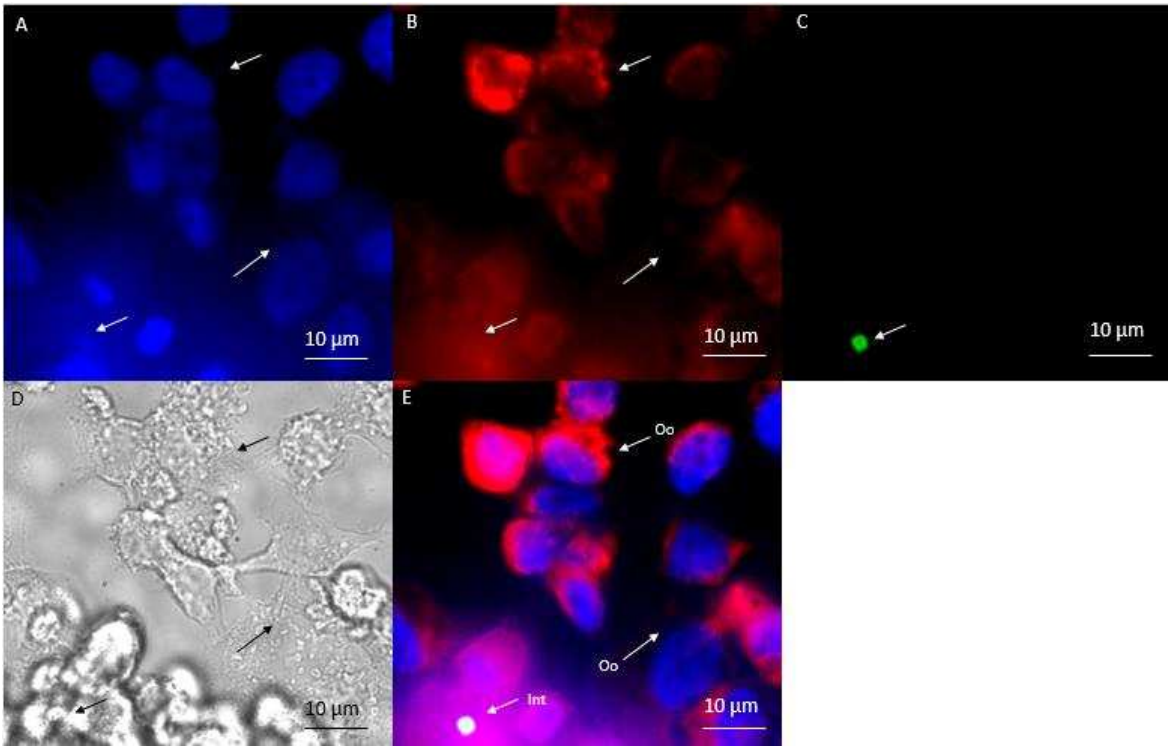

Figure 4 - Three parasite stages in CAMA-1 cells. Sporo-Glo™ staining (C) shows a single intracellular (Int) stage. DAPI staining (A) reveals two stages with multiple small nuclei (Oo) with the Sporo-Glo™ labelled region having a clouded appearance, possibly indicating a gamont or zygote stage. These regions show two rounded bodies under DIC (D, black arrows) and occupy areas devoid of mitochondria (B, white arrows).

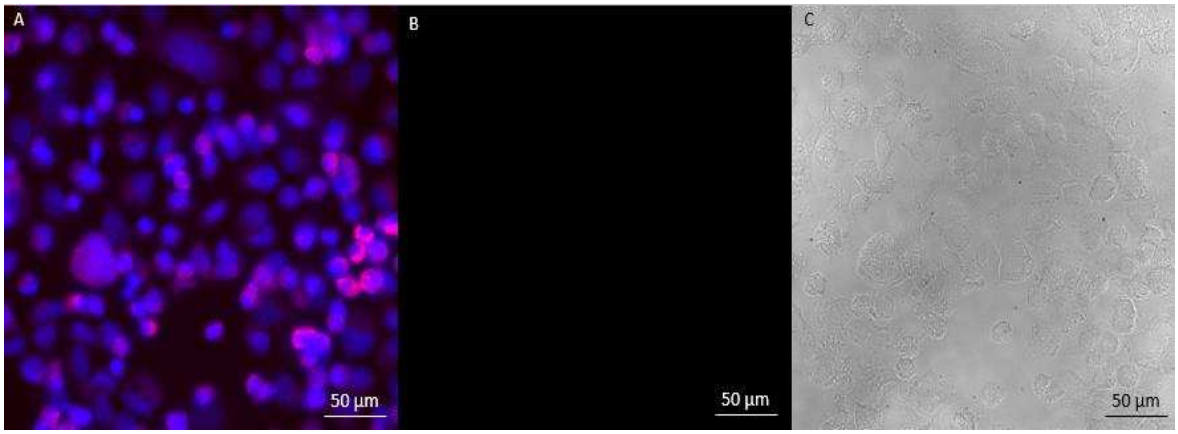

Figure 5 - Uninfected CAMA-1 cells. Mitotracker™ shows some activity (A) and cells appear nearly confluent (C), but no non-specific Sporo-Glo™ binding is observed (B).

EFM-19

A breast carcinoma, with a tendency to form colonies appearing as clumps rather than forming a continuous monolayer. This cell line had a high level of *C. parvum* infection, as seen with the Sporo-Glo™ labelling. One feature is the presence of bright mitochondrial activity around the parasites (**Figs. 6 & 7**). Three parasites can be seen within a single host cell (**Fig. 6**), which may be due to invasion by multiple merozoites, or as a result of binary fission. In this field an extremely bright Sporo-Glo™ labelled region is present, which appears to be excysting from the rounded meronts (**Fig. 6**). Alternatively, this could be a merozoite which had just invaded the host cell prior to developing into a trophozoite. A faintly Sporo-Glo™ labelled area is also present, which has a single nucleus measuring 4 µm across, indicating a trophozoite stage. All observed stages can be seen closely associating with the host nucleus (**Figs. 6 & 7**). In the second image, a mixture of sexual and asexual stages can be seen (**Fig. 7**), showing this cell line can support the complete life cycle. Uninfected cells are shown in **Fig. 8**.

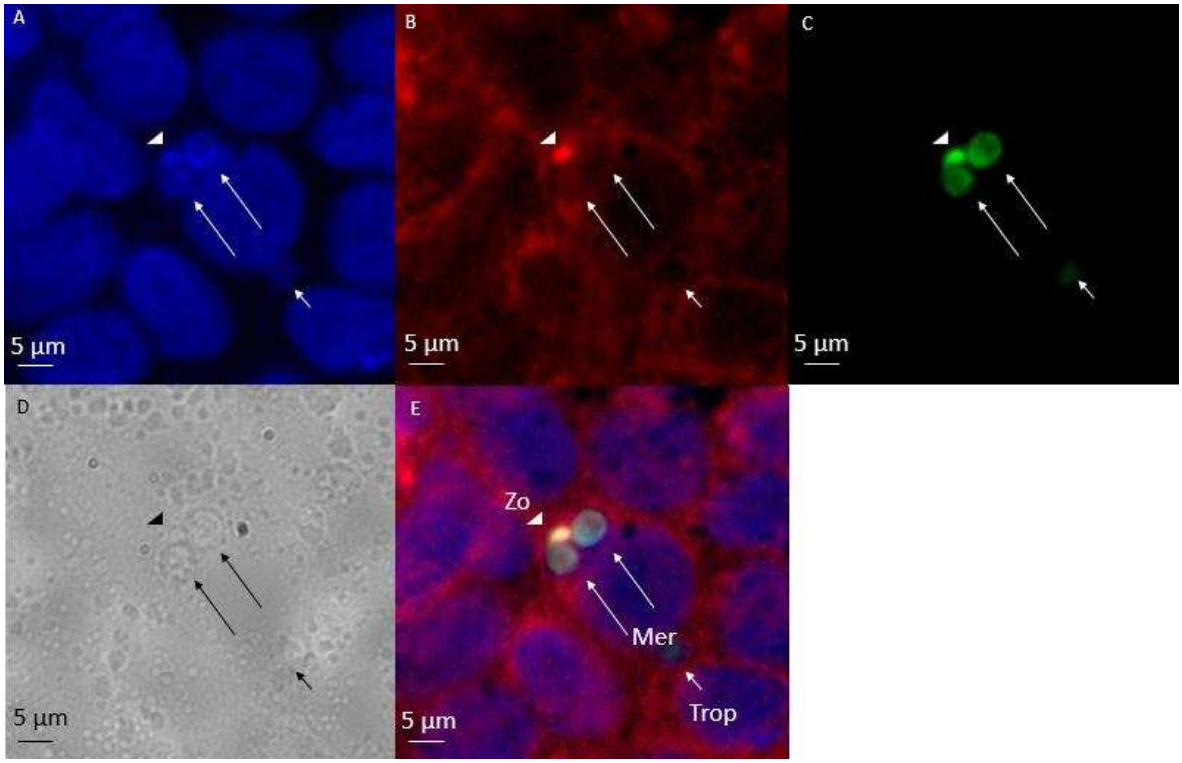

Figure 6 - Multiple parasites in EFM-19 cells. Sporo-Glo™ stain (C) shows two rounded meronts (Mer), a bright comma shaped merozoite (Zo) and a faintly labelled trophozoite (Trop). Mitotracker™ staining shows a reduced signal in these two rounded areas but a bright signal in the comma shaped region (B). DAPI stain (A) shows two distinct nuclei in the left meront and four in the top meront. A fainter Sporo-Glo™ labelled region (C) is visible at the bottom right (small arrow), with a discrete nucleus present in the DAPI field (A). Merged channels (E) show overlap of Sporo-Glo™ area, with DAPI signal within these areas. DIC shows multiple bodies visible correlating to the Sporo-Glo™ labelled regions (D).

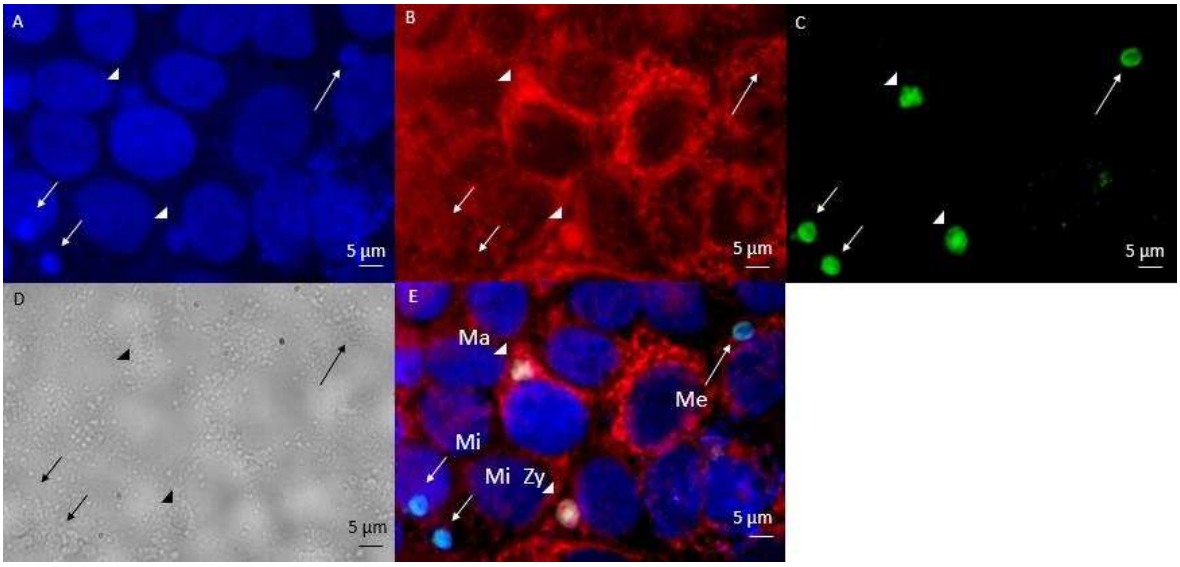

Figure 7 – Multiple *C. parvum* stages visible within EFM-19 cell culture. Sporo-Glo™ signal (C) shows five distinct labelled bodies; meront (Me), microgamonts (Mi), macrogamont (Ma) and zygote (Zy) (E). Mitotracker™ signal (B) overlaps some of the Sporo-Glo™ labelled regions (Ma, Zy). DAPI stain (A) shows distinct staining regions separate from the host cells and small nuclei in the parasite (Me, Mi stages). DIC (D) shows individual parasites are distinguishable.

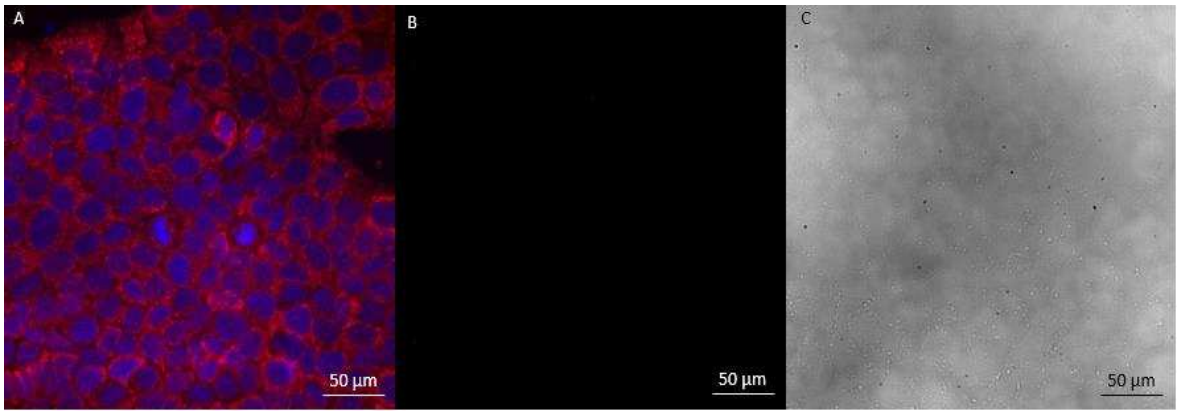

Figure 8 - Uninfected EFM-19 cells. Mitotracker™ stain (A) shows active cells, but no non-specific Sporo-Glo™ binding is observed (B). Cells have grown to confluency (C).

MDA MB 468

MDA MB 468 is a breast cancer adenocarcinoma derived from a metastatic site. This cell line supported the complete life cycle of *C. parvum*. Analysis of the host cell monolayer showed numerous stages stained with Sporo-Glo™, including sexual stages (**Fig. 9**). The infectious stages were numerous in the culture, however also present were clouded regions containing small rounded bodies (**Fig. 9**). The nature of these regions is unclear. Uninfected cells shown in **Fig. 10**.

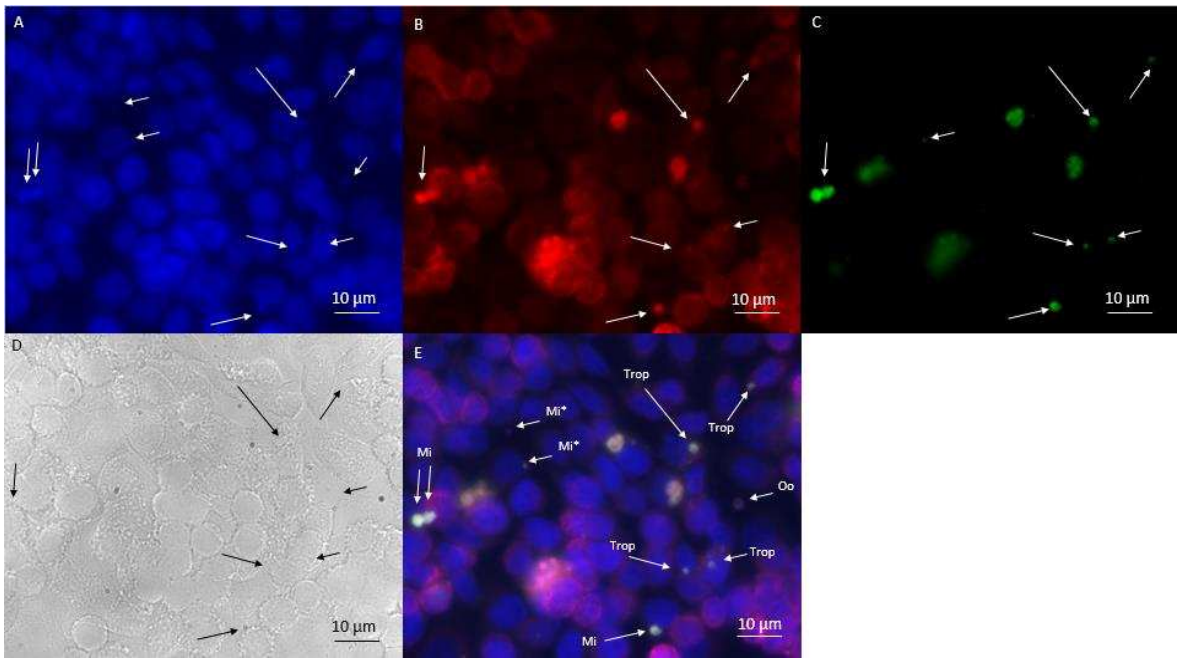

Figure 9 - Parasite stages in MDA-MB-468 cells. Sporo-Glo™ labelling (C) in this cell line appears less distinct, with more 'cloudy' appearance, and appear larger than regions observed in other cell lines. These also appear to contain multiple rounded bodies, which are visible with MitoTracker™ (B). DAPI stain (A) shows discrete nuclei at some of the Sporo-Glo™ labelled regions, but not in the larger clouded ones. White arrows show stages more similar to those seen in other cell lines; trophozoites (Trop), microgamonts (Mi), microgametes (Mi*), and an oocyst which appears to be excysting (Oo).

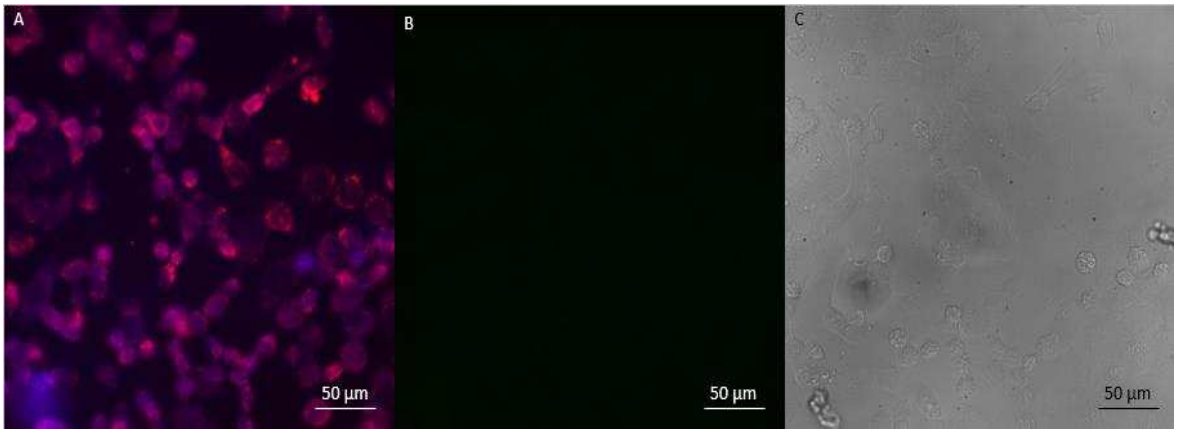

Figure 10 - Uninfected MDA MB 468 cells. Stains show active cells (A), but no non-specific Sporo-Glo™ binding is observed (B). Low confluency suggests cells may have sloughed off (C).

RKO

RKO cells are derived from a colon carcinoma and show poor differentiation. Cells showed a high level of proliferation, and as such after a week a large proportion of cells had detached leaving a low confluency slide. In addition, observed intracellular stages were few in number. These stages seem to be limited to trophozoites, with seemingly no DAPI staining of these areas (**Fig. 11**). The Mitotracker™ signal on these cell lines was extremely weak, indicating death of the cell monolayer (**Fig. 11**). Uninfected cells shown in **Fig. 12**.

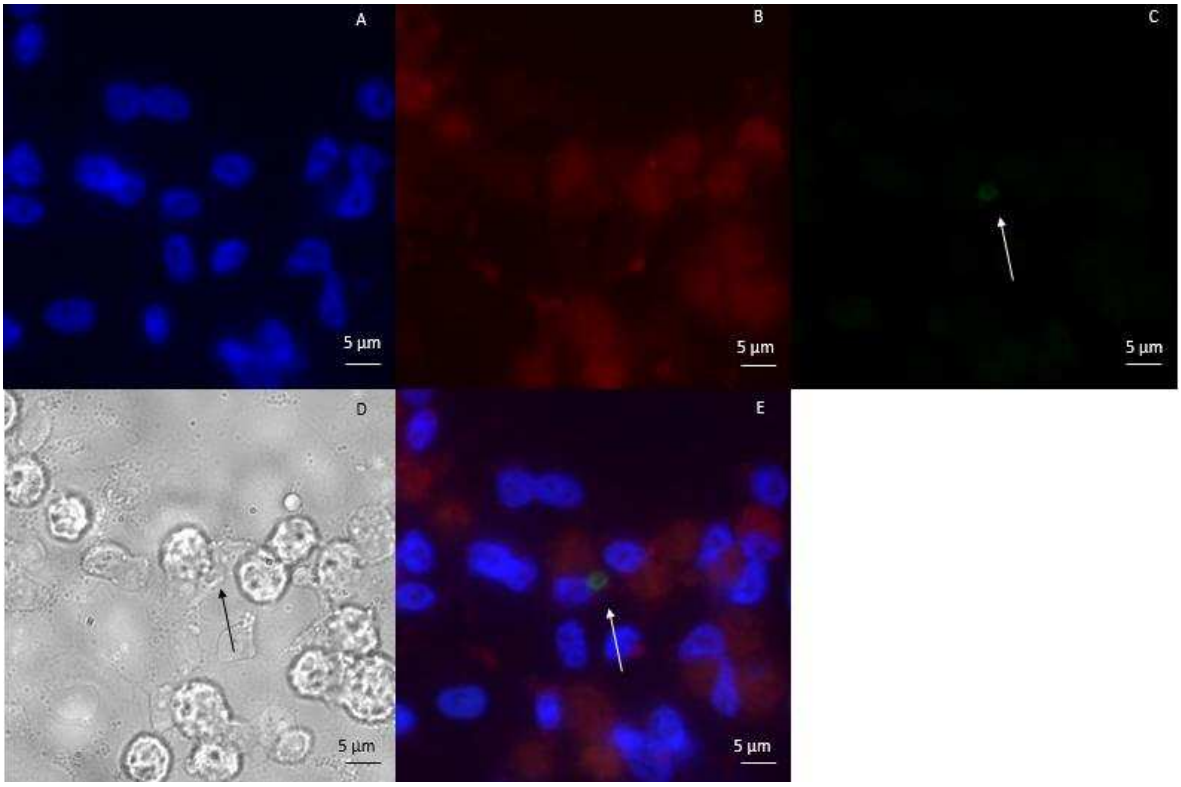

Figure 11 – RKO cell line with single *C. parvum*. Here, an extremely faintly labelled Sporo-Glo™ region (C) is visible, but this shows no corresponding DAPI stain (A). Mitotracker™ signal (B) is barely detectable. A faint outline is visible in the DIC image (D). Region appears in contact with host nucleus (E).

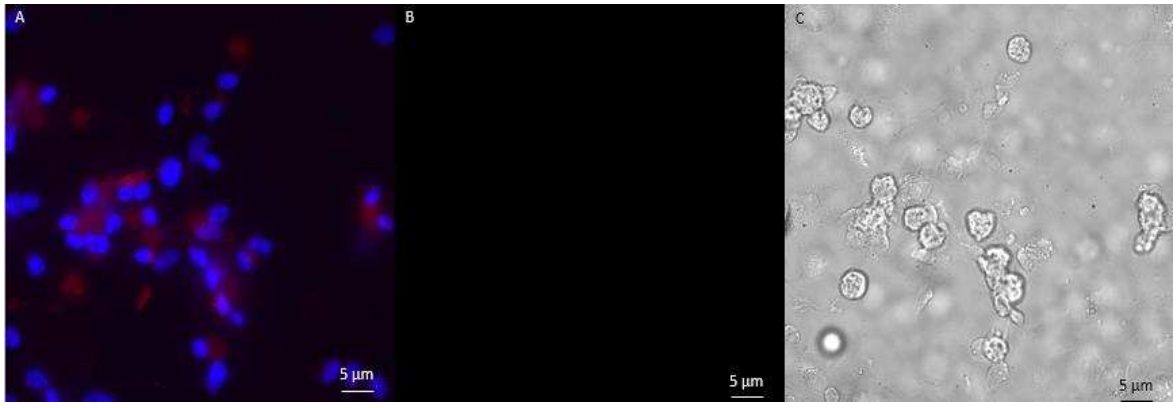

Figure 12 - Uninfected RKO cells. Cells show a similar level of detachment to the infected cells, and also show low mitochondrial activity (A, C). No Sporo-Glo™ labelling is present (B).

SW480

This cell line is derived from a Duke's type B colorectal adenocarcinoma. Screening of these cells showed evidence of oocysts or type II merozoite development within host cells (**Fig. 13**). Parasite labelling is faint, and there is a relatively low level of infection in this cell line, but the presence of type II meronts or potentially oocysts means that the complete life cycle may be present. Uninfected cells shown in **Fig. 14**, showing some level of Sporo-Glo™ cross reactivity.

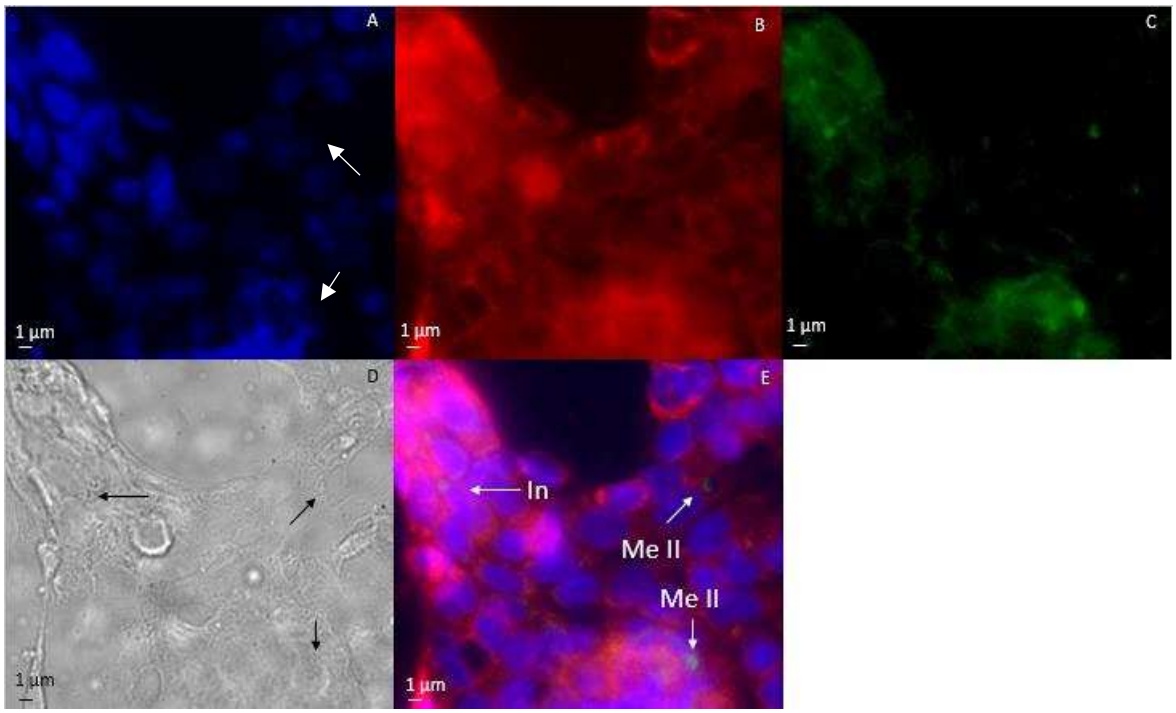

Figure 13 - SW480 cells with three parasites visible. Two type II meronts (Me II) are present to the right, shown with four nuclei (white arrows) in the DAPI field (A) along with an intracellular stage (In) which is difficult to identify. Sporo-Glo™ signal (C) is faint, but appear to occupy the vacuoles seen with Mitotracker™ (B) Outlines of the Sporo-Glo™ labelled regions are visible with DIC (D).

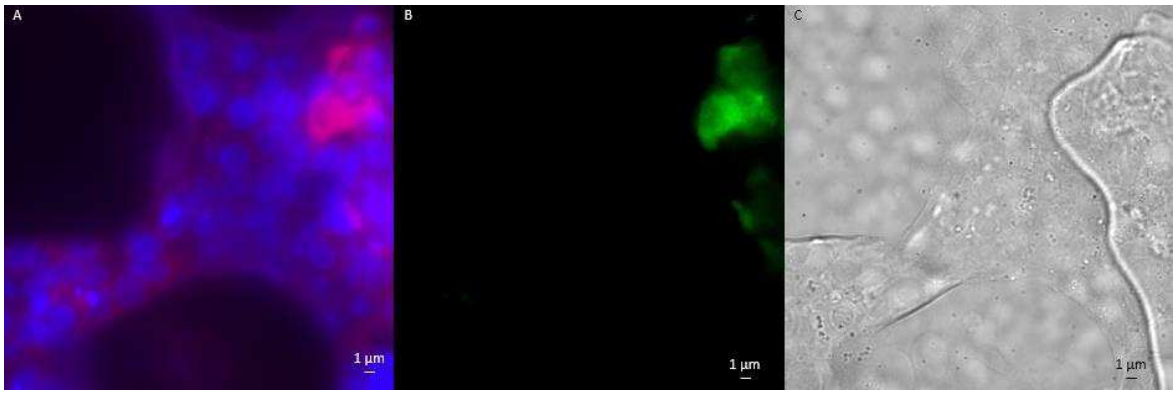

Figure 14 - Uninfected SW480 cells. Cells appear active (A). Bleed through or potential non-specific binding is visible in the Sporo-Glo™ channel (B), but this may be due to air trapped under the slide (C).

SW620

A Duke's type C colorectal carcinoma. This cell line was derived from the same patient as the SW480 cell line, a year later. This cell line was capable of supporting the *C. parvum* infection to some degree, but at a low level. This cell line also exhibited fast growth, with a tendency to become confluent within a few days. Intracellular stages were few in number, and those that were detected all appeared to be trophozoites (**Fig. 15**). Non-specific binding of the uninfected control means that this may not be *C. parvum* (**Fig. 16**) but the presence of a separate DAPI stain and the visible stage with DIC means that this particular stage is unlikely to be a false positive.

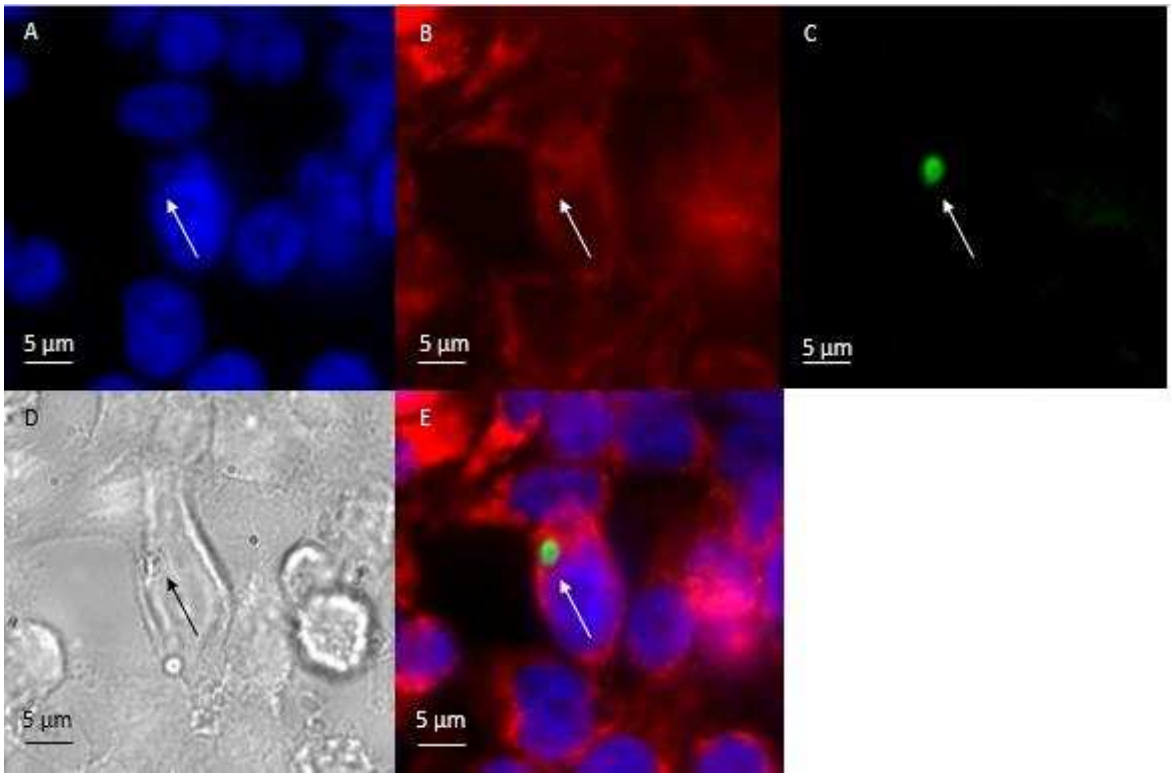

Figure 15 – SW620 cell infected with *C. parvum* trophozoite. Single Sporo-Glo™ labelled region (C) is visible (a trophozoite, white arrow). This is outlined by an area devoid of mitochondrial activity (B), the DAPI staining (A) reveals a faint outline of a distinct nuclei separate from the host nuclei. Parasite occupies vacuole like srea (E). Separate parasite is visible with DIC (D).

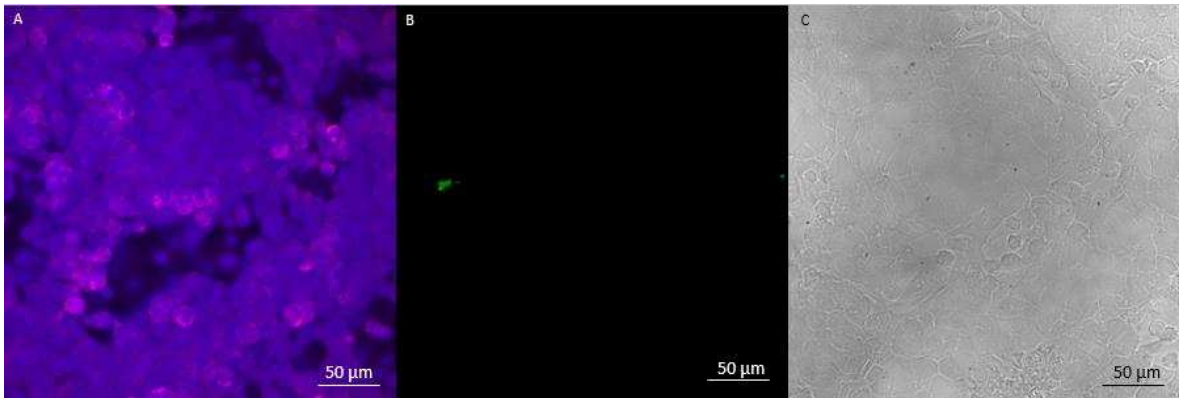

Figure 16 - Uninfected SW620 cells. Cells are at high density (A, C) and show some evidence of non-specific Sporo-Glo™ labelling (B).

COLO-320

A semi-adherent colorectal cell adenocarcinoma. No observable intracellular stages were detected, however one unique Sporo-Glo™ staining stage was visible (**Fig. 17**). Majority of monolayer was detached/in medium by the end of the week, making tracking life cycle progression difficult.

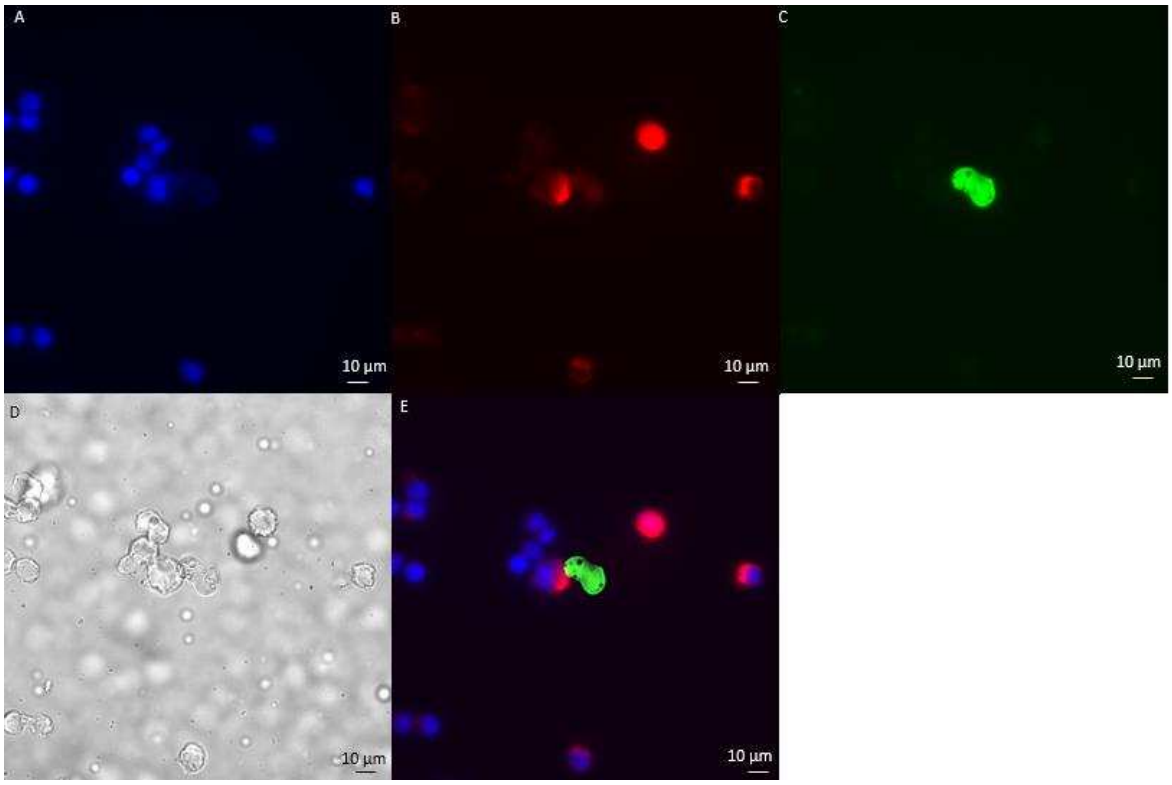

Figure 17 - **Potential extracellular stage detected in COLO-320 cell culture**. COLO-320 cells show weak Mitotracker™ staining (B), indicating probable death of monolayer, along with the low confluency (D). Stage intensely stains with Sporo-Glo™ (C) and possesses an unusual morphology, appearing similar in membrane structure to a dividing cell, however showed no uptake of DAPI stain (A) or Mitotracker™ (B). DIC (D) showssome internal organisation can be discerned. A rounded, nucleus like structure appears visible within the cytoplasm, (D, E) with additional smaller structures visible clustered around it.

H2228

A non-small cell lung cancer, which showed a moderate level of infection (**Fig. 18 (a)**). Parasites appear to occupy a vacuole area within the host cell devoid of mitochondria (**Fig. 18 (b)**). Development of stages is intracytoplasmic. Stages seen appeared limited to the asexual cycle, with no gamont stages being visible, although the presence of potential type II meronts (**Fig. 18 (b)**) suggests that sexual stages may be present in the culture. Uninfected cells shown in **Fig. 19**.

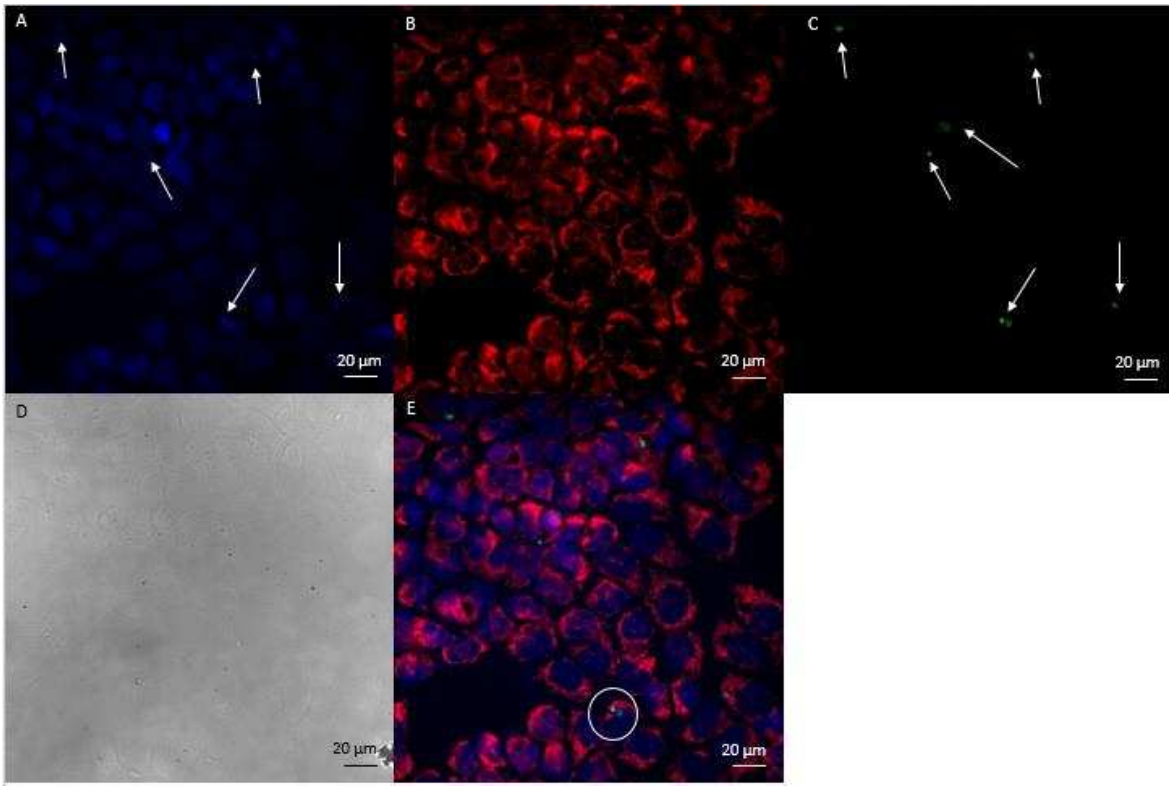

Figure 18 (a) – Infected H2228 monolayer. Sporo-Glo™ labelling (C) reveals seven parasites in the field. Mitotracker™ signal reveals vacuole like areas occupied by the parasites. DAPI signal (A) reveals brighter signal in areas labelled with Sporo-Glo™. DIC image (D) shows faint outlines of parasites. Circled area shown in **Fig. 18 (b)**. Stages here appear to be trophozoites and meronts, with no sexual stages visible.

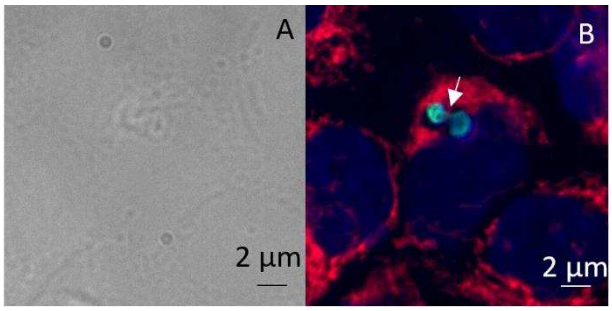

Figure 18 (b) – Two type II meronts within a H2228 cell, circled area of Figure 18 (a). Parasites appear to be in contact (white arrow, B) and occupy a vacuole lacking mitotracker signal. Stages are visible with DIC (A).

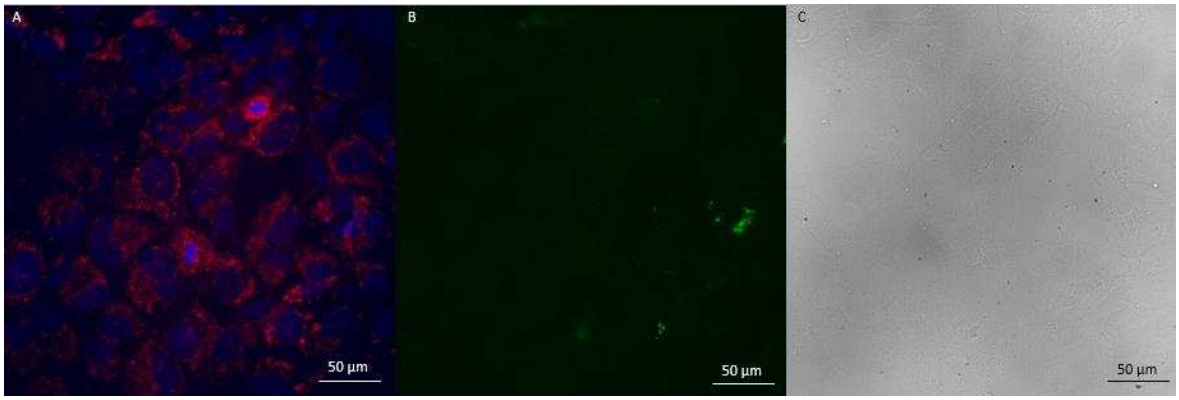

Figure 19 - Uninfected H2228 cells. Mitochondrial activity (A) and attached cells (C) visible, some background activity in Sporo-Glo™ channel (B), but rounded bodies seen in infected cells not present.

HCC4006

A lung adenocarcinoma showing several parasites present across the observed fields (**Figs. 21 & 22**). In this cell line, multiple parasites within a single cell was commonly observed (**Figs. 20 & 22**). Observed stages included a high level of gamonts and type II meronts, along with the developing zygotes (**Fig. 20**) and an oocyst (**Fig. 21**). Uninfected cells shown in **Fig. 23**.

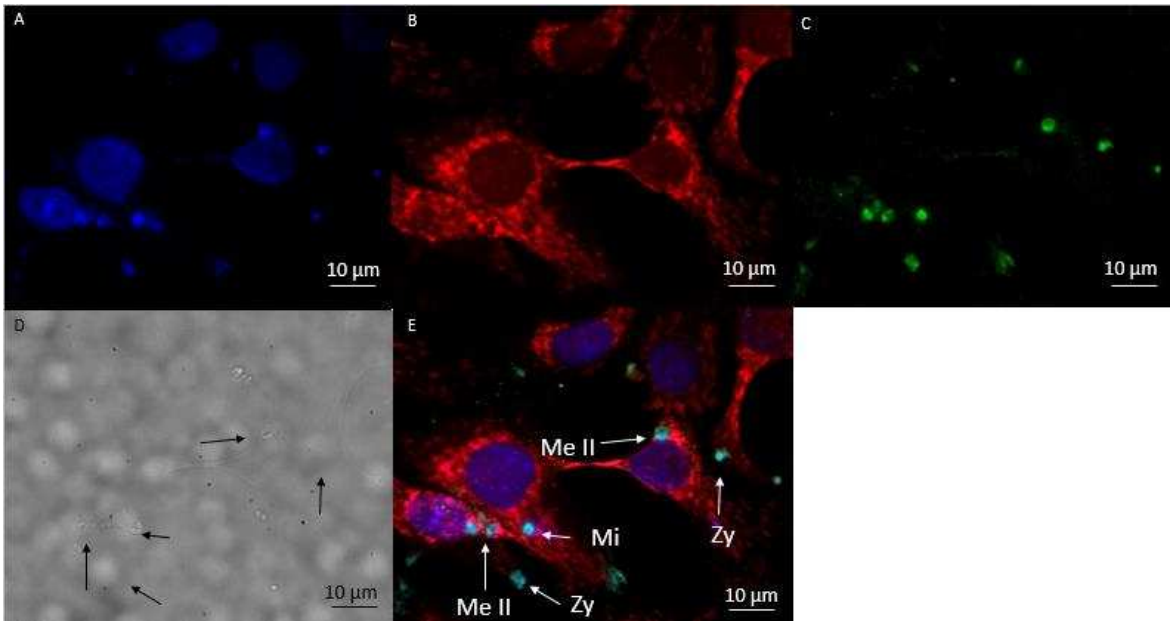

Figure 20 – Infected HCC4006 cells. Sporo-Glo™ signal (C) shows multiple parasites present in the field. Mitotracker™ staining (B) areas lacking signal which correspond to the Sporo-Glo™ labelled areas (E). DAPI staining (A) shows discrete regions corresponding to these areas. DIC imaging (D) shows outlines of the parasite are slightly visible (black arrows). Mostly sexual stages are present; meronts II (Me II), microgamonts (Mi), developing zygotes (Zy).

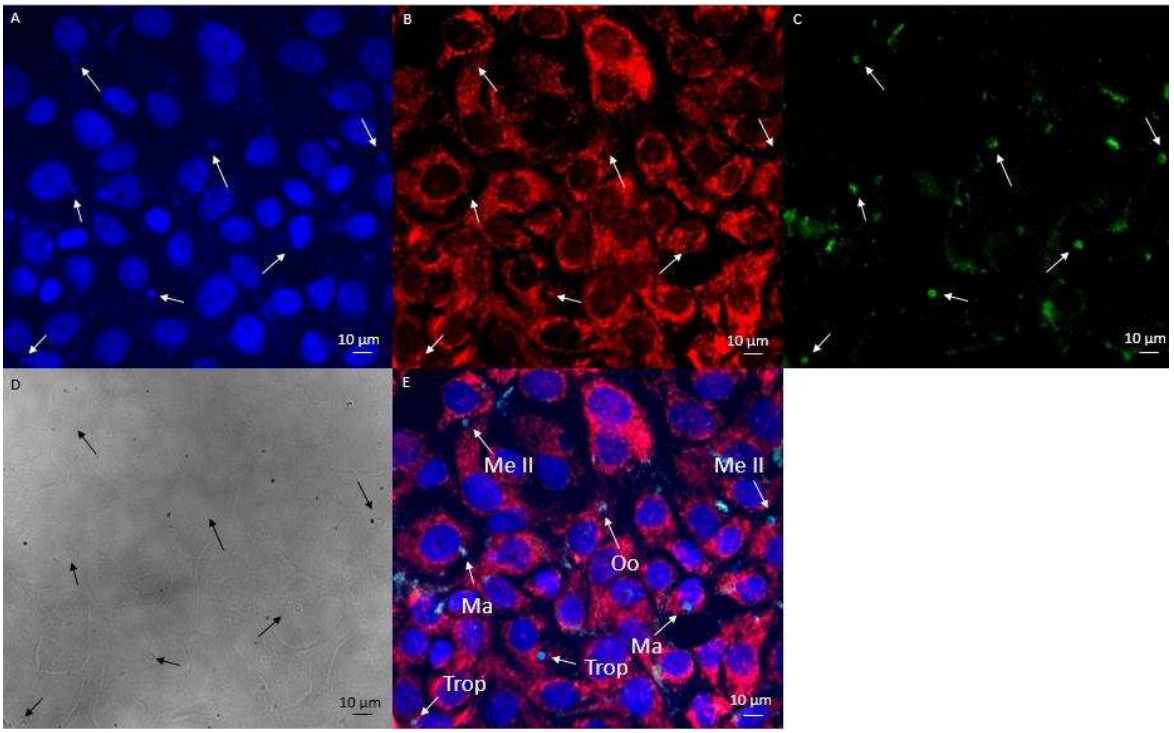

Figure 21 – Infected HCC4006 cells. Sporo-Glo™ signal (C) shows multiple parasites present (white arrows). Mitotracker™ stain (B) shows areas lacking signal which correspond to the Sporo-Glo™ labelled areas (E). DAPI staining (A) shows discrete regions corresponding to these areas. DIC imaging (D) shows outlines of the parasite are slightly visible (black arrows). Present are trophozoites (Trop) meronts II (Me II), macrogamonts (Ma) and a developing oocyst (Oo) (E).

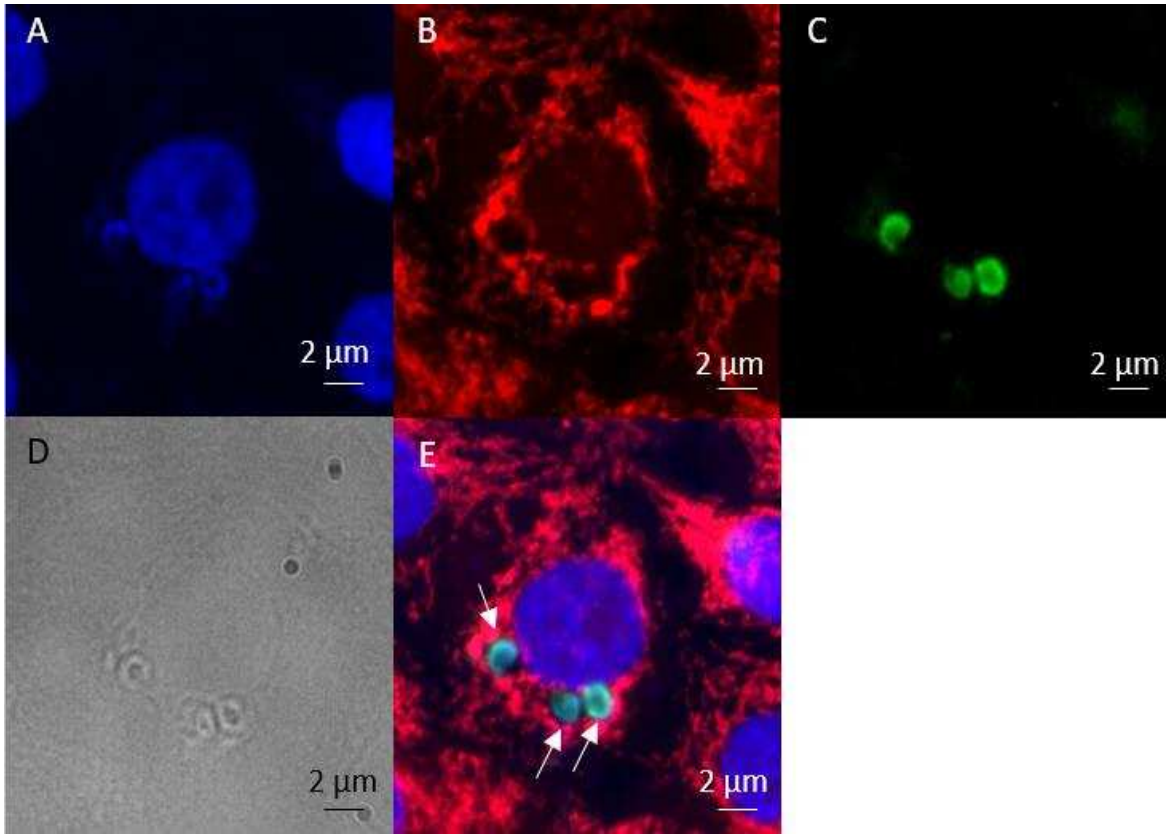

Figure 22 - Three parasites within a single HCC4006 cell. Sporo-Glo™ stained regions (C) occupy vacuoles (B, E) and have discrete nuclei (A) indicating likely type II meronts. Stages visible with DIC (D).

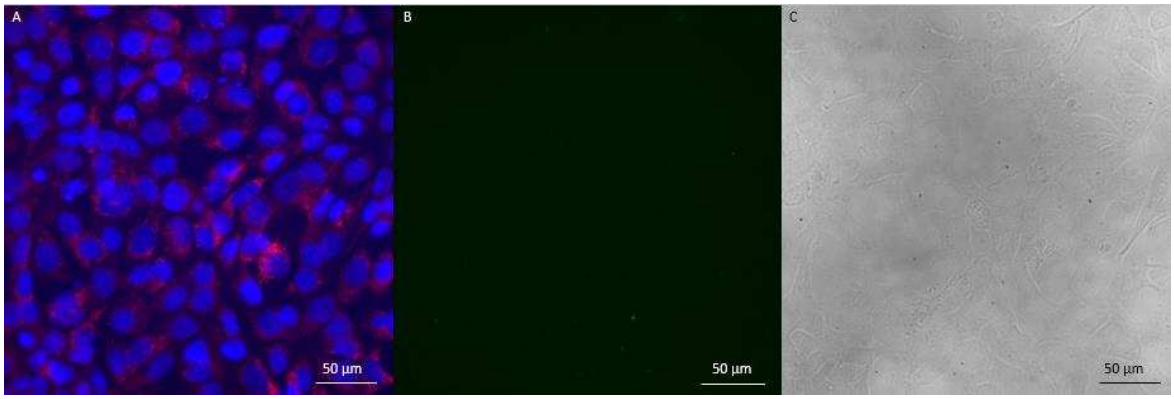

Figure 23 - Uninfected HCC4006 cells. Cells are attached (C) and show mitochondrial activity (A). Some background Sporo-Glo™ activity (B), but the corresponding parasite nuclei and vacuoles seen in infected cells are absent.

3.2 Presence of *C. parvum* DNA

The presence of extracellular oocysts in the culture medium was tested using PCR with *C. parvum* specific primers, SB012. SB012 do not target specific DNA regions, but are "RAPD" (random amplification of polymorphic DNA). Initially, primers specific for *C. parvum* Hsp70 were tried, but showed a high level of non-specific binding. While optimisation using these primers was attempted, the SB012 primers provided far clearer DNA bands when resolved on agarose gels. The PCR reaction was tested on all samples. Bands were generated at approximately the expected band size (433 bp), with purified *C. parvum* DNA acting as a positive control (**Figs. 26 & 27**). Bands were generated in at least one sample from the following cell lines; BT-474, EFM-19, MDA MB 468, HCC4006, COLO-320, SW480 and SW48. All of these stages showed some instance of intracellular infection, with the exception of COLO-320, which showed an unusual stage (see section 3.1) and SW48, where no stages were visible. Bands were absent in samples which showed no stages, and in samples were few stages were present; CAMA-1, H2228, HCC827, SW620, IGR-39, RKO and LS-174T.

As the primers used do not target a specific DNA sequence and are RAPD primers (targeting random regions of the *C. parvum* genome) they were tested for non-specific binding to human DNA. Human small ribosomal RNA coding DNA was amplified, showing successful DNA extraction and polymerisation (**Fig. 28**). Using the SB012 primers, no off-target binding was detected (**Fig. 28**). Due to time constraints, not every cell line could be tested for non-specific amplification, but the lack of binding in EFM-19 suggests SB012 binding is specific for *C. parvum.*

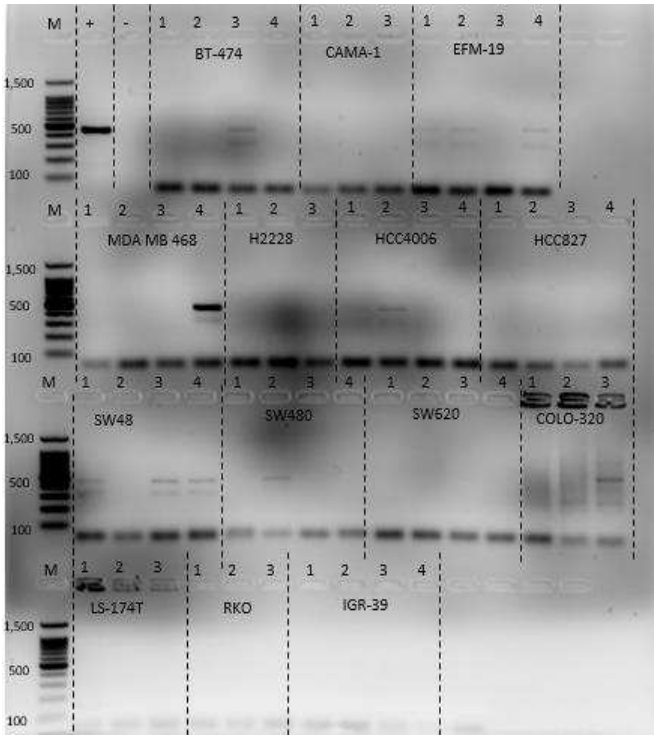

Figure 26 - PCR of media from 24 well plate infections, SB012 primer set. 2 % agarose gel stained with ethidium bromide. *C. parvum* DNA present in one of the BT-474 samples, three of the EFM-19 samples, one of the MDA-MB-468 samples, two of the HCC4006 samples, three of the SW48 samples and one of the SW480 samples. Bands generated at expected size (~450 bp). Secondary band visible at ~300 bp, the source of which is unclear, potentially due to a similar sequence elsewhere in the genome. Some samples were lost due to lids opening in storage, meaning only three samples were available for testing (CAMA-1, COLO-320, H2228, LS-174T and RKO). Positive control (+) is extracted stock oocyst DNA, negative (-) is DEPC treated water.

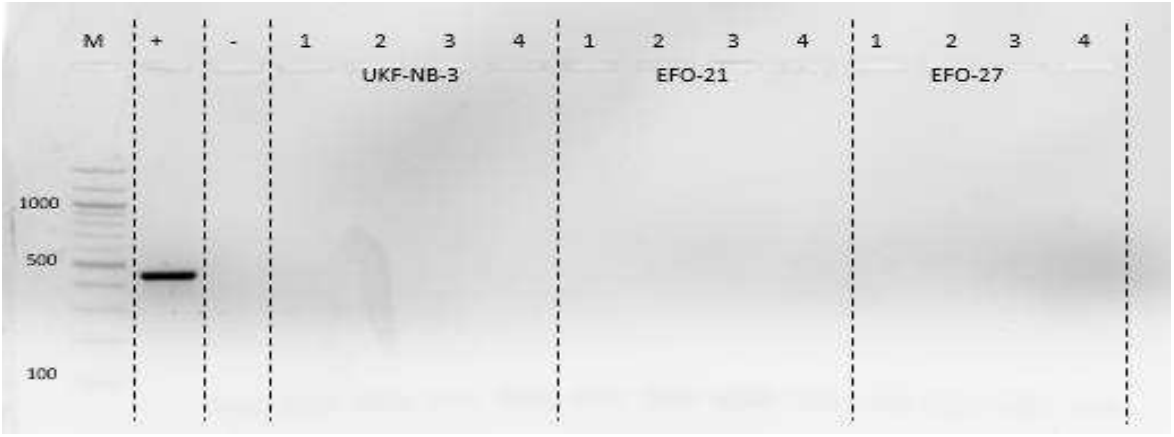

Figure 27 - PCR of UKF-NB-3, EFO-21 and EFO-27 media, SB012 primer set. All wells show no detectable *C. parvum* DNA. Positive control - extracted *C. parvum* oocyst DNA.

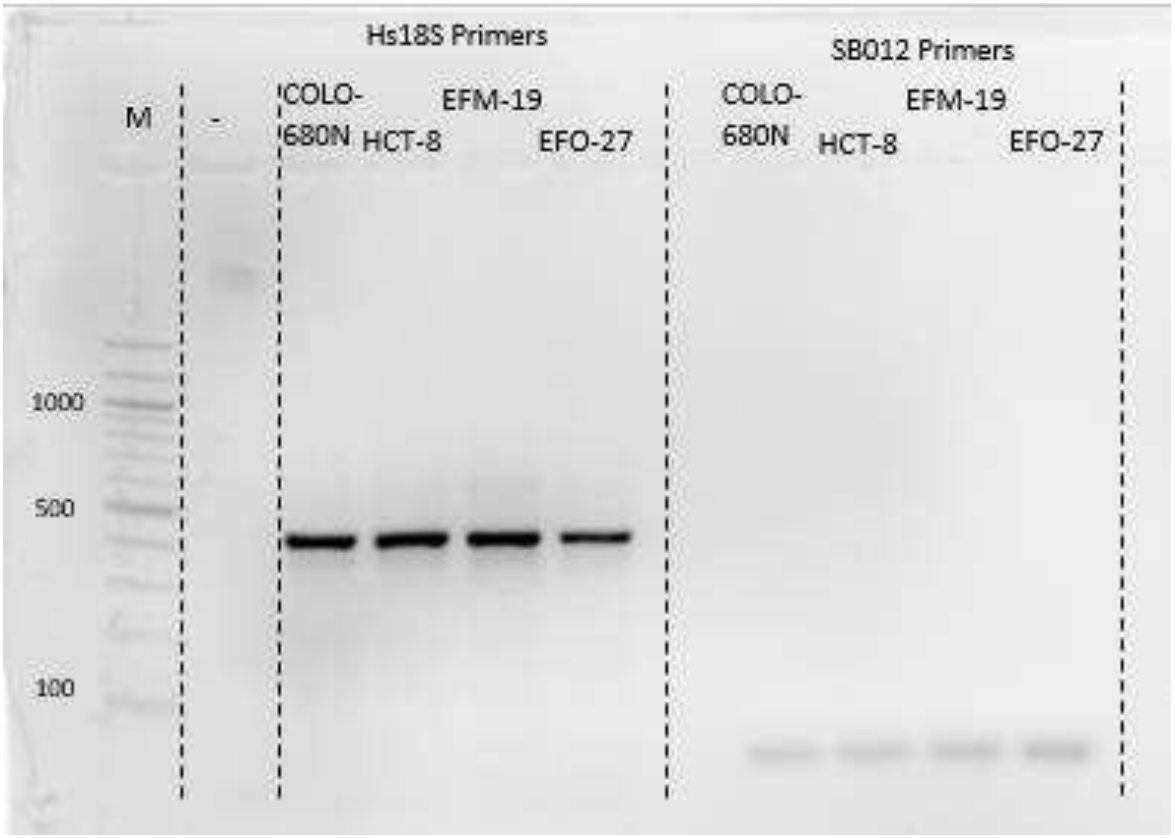

Figure 28 - Extracted DNA of four cell lines tested for non-specific SB012 primer amplification. Positive control (left hand lanes) of human 18srRNA primers. Right hand lane SB012. No non-specific binding is detected.

3.3 Glucose Consumption

Due to *C. parvum* relying on the host cell for many of its metabolic requirements, the effect of infection on the rate of glucose consumption was tested. Glucose levels were compared daily in infected and uninfected COLO-680N and HCT-8 cells. Four wells were tested under each condition, averages were taken from the four readings and plotted (**Fig. 29**). There was no difference in the rates of glucose consumption between infected and uninfected COLO-680N cells. There were large differences in the rate of glucose consumption between the cell lines, with HCT-8 depleting the medium glucose within 2 days of infection, with a higher initial rate of consumption, while COLO-680N retained glucose in the medium for a week after infection (**Fig. 29**). These differences were reflected in the growth pattern of the cells, with HCT-8 growing as multiple layers of cells, which was not observed in the COLO-680N cell line.

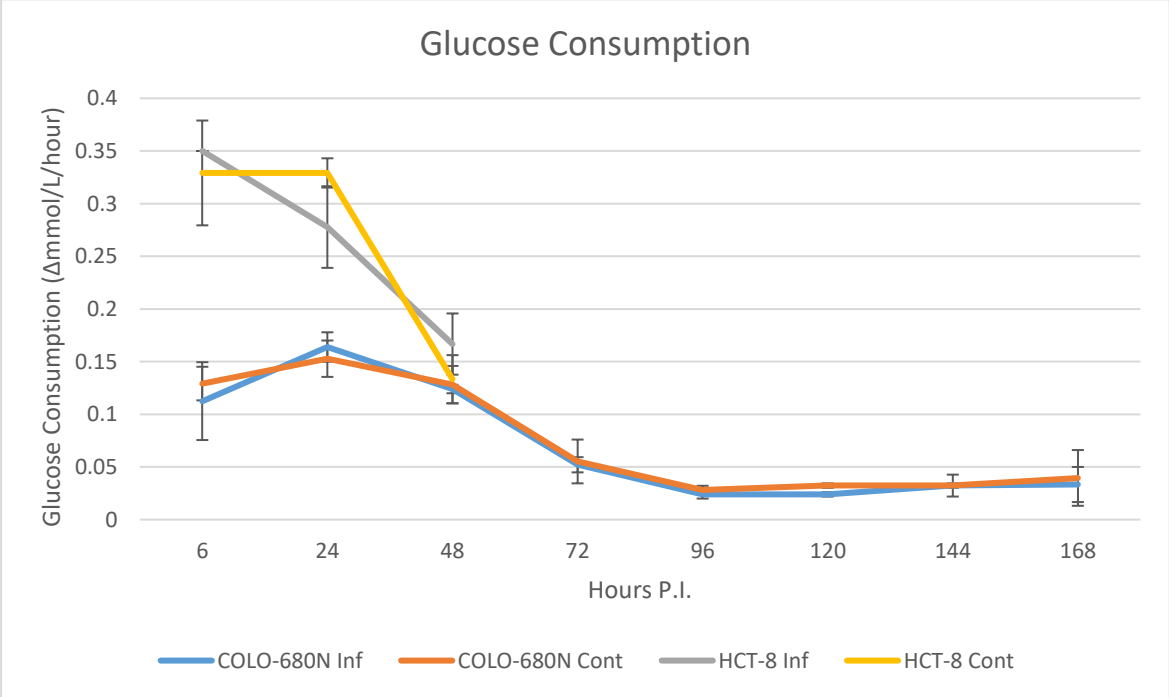

Figure 29 - Glucose Consumption of infected and uninfected COLO-680N cells and HCT-8 cells. Rate of consumption was calculated as the difference in glucose consumption since the previous reading over hours since the last reading. Error bars are SD of four experiments. In COLO-680N cells there is no difference between infected and uninfected cells. Glucose consumption initially rises, likely due to growth of monolayer and subsequently decreases, possibly due to reduced growth rate as cells reach confluency. In HCT-8 cells glucose consumption remains high initially in infected cells but drops off. Media of all HCT-8 wells was depleted of glucose by 48 hours.

3.4 Sub-Infections

Four cell lines were selected for culture in T-25 flasks, to investigate whether infection can not only be maintained but can produce oocysts which can be passaged between cell monolayers. MDA-MB-468, SW480, EFM-19 and HCC4006 were chosen as they demonstrated presence of meronts II and evidence of intracellular sexual stages (except SW480, but the presence of meronts II and detectable *C. parvum* DNA was deemed acceptable (sections 3.1 and 3.2 respectively) with fluorescent microscopy (see section 3.1). 2.8 x 10^5 oocysts were added to low confluency T-25 flasks (approximately 20 % confluency), incubated overnight followed by removal of unexcysted oocysts. Weekly, *C. parvum* in the medium was pelleted and transferred to a freshly seeded T-25 flask for three weeks. All cell lines provided a return over the initial inoculum. MDA-MB-468 and EFM-19 had counts of 1.36 x 10^5 and 1.44 x 10^5 oocysts per mL respectively (net production 0.8 x 10^5 and 0.9 x 10^5 respectively), equating to around a 1.5 x net return of oocysts. SW480 had counts of 1.8 x 10^5 oocysts per mL (net 1.2 x 10^5) provided a net gain of double the initial inoculum while HCC4006 provided 5.8 x 10^5 oocysts per mL (net 5.2 x 10^5), a nine-fold net increase over three weeks (**Fig. 30**).

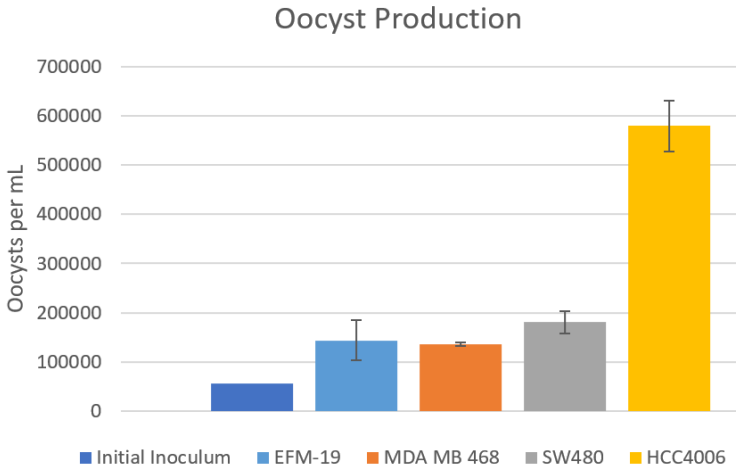

Figure 30 – Counts of oocysts per mL from sub-infection experiments. Shown are the results of average counts of three T-25 flasks.

3.3 Bioreactor

To establish an *in vitro* system which enables long term culture and convenient harvesting of oocysts, a miniPERM® SM bioreactor was inoculated with 36.8 x 10^6 COLO-680N cells and 18.4 x 10^6 treated *C. parvum* oocysts. The bioreactor was maintained for 13 weeks and produced oocysts continuously. Medium glucose reduced at a rate of approximately 1.4 mmol/L per day, and medium was replaced weekly. Microscopy of unfixed samples showed a thin walled oocysts undergoing excystation and releasing a sporozoite 10 weeks after inoculation implying the auto-infective cycle enabled continuous propagation (**Fig. 33**). Staining of samples with Crypt-a-Glo™ antibody (antibody specific for oocysts) showed production of thick walled oocysts which appeared fully intact, with excysted oocysts also present (**Fig. 32**). Enumeration of oocysts showed a fairly constant level of 1x 10^6 oocysts per mL (**Fig. 31**) across all the observed months. In order to assess the

infectivity of these oocysts, HCT-8 and COLO-680N monolayers were infected following a standard infection protocol with 7 x 10^4 oocysts after a three and seven day incubation respectively. All tested time points yielded infection, with representative images of oocysts harvested three months post infection (p.i.) are shown in **Fig. 34**. In both of these cell lines, multiple life cycle stages can be seen, indicating infectious oocyst production. COLO-680N monolayers showed a higher level of infection than HCT-8 in all observed samples.

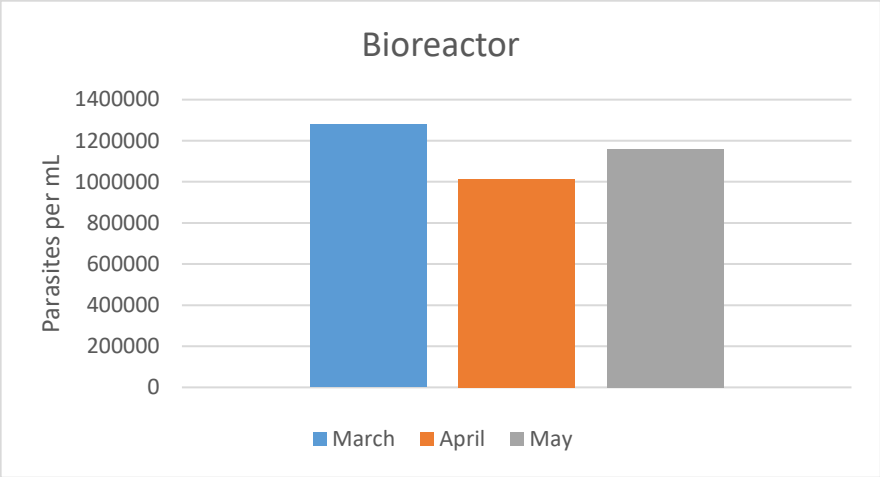

Figure 31 – Bar chart of oocyst counts from monthly bioreactor harvests. Single haemocytometer counts, levels remain fairly constant of at least 1 x 10^6 oocysts per mL.

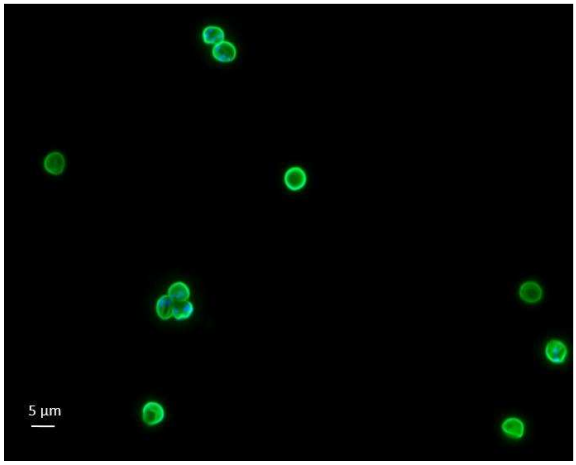

Figure 32 – Oocysts from bioreactor 1 month post infection. Varying stages of excystation are present Crypt-a-Glo™ stain (green) with DAPI (blue).

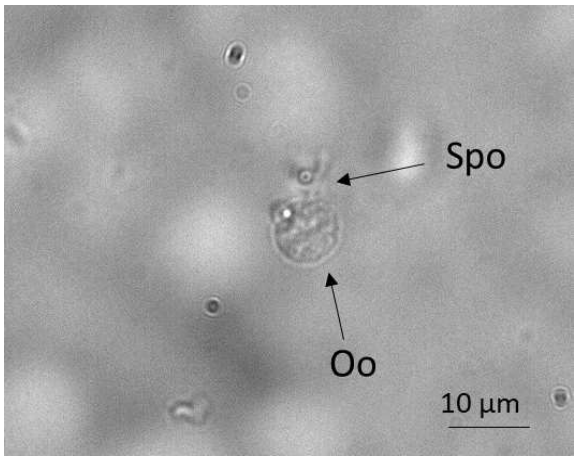

Figure 33- Unfixed sample of thin walled oocyst (Oo) with DIC microscopy. A sporozoite (Spo) stage appears to be excysting from the top, and was seen moving away from the oocyst.

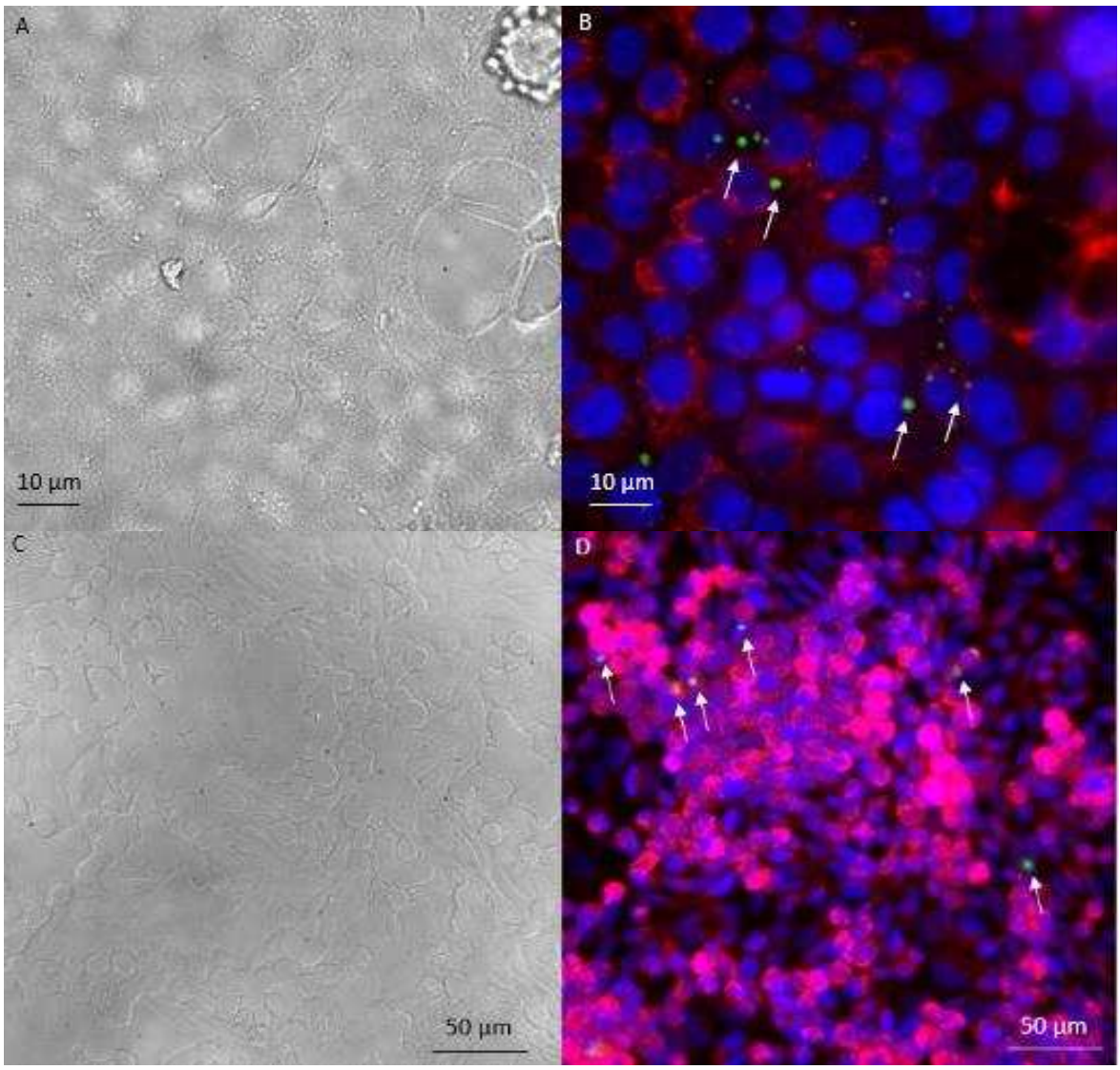

Figure 34 - Reinfection of COLO-680N cells (A, B) and HCT-8 cells (C, D) with bioreactor produced oocysts, third month harvest. Parasites visibly labelled with Sporo-Glo™ (B, D white arrows). Outlines are slightly discernible in COLO-680N cells (A) but not in HCT-8 cells (C), as cells have grown over infected cells.

4.0 Discussion

17 cell lines were tested for their ability to propagate infection, with 10 displaying some evidence of intracellular *C. parvum* development (**Table 4**). Owing to the presence of the complete life cycle and detectable *C. parvum* DNA, four of these cell lines (EFM-19, MDA MB 468, SW480 and HCC4006) were used to establish sub-infections of cell monolayers, and after three weeks all provided a net gain of oocysts. HCC4006 provided the highest yield, with a nine-fold return on the initial inoculum. In addition, a small scale bioreactor was established using COLO-680N cells, and produced infectious oocysts for 13 weeks. The development of *C. parvum* in multiple cell lines should not be considered surprising considering the number of cell lines which have been previously reported as maintaining the life cycle, but as studies have shown previously (Arrowood 2002; Hijjawi 2010; Karanis *et al.* 2011) not every cell line described here was capable of supporting the entire life cycle. The fluorescent microscopy images shown here suggest that, for the majority of the life cycle, *C. parvum* remains in an intracellular location. Apparent intracellular development has been observed previously in other cell lines, for example in macrophages and human foetal lung cells (Beyer *et al.* 2000; Current *et al.* 1984). It cannot be concluded that this development is intracytoplasmic however, as microscope slide preparation has the potential to displace cellular structures, and scanning electron or confocal microscopy will be required to confirm the parasites location. The development across multiple cell lines implies the surface markers required for invasion are expressed to some extent across multiple tissues, or that binding is relatively non-specific. Other investigators have hypothesised that initial attachment and invasion relies on specific surface proteins being expressed on the host cells, while dissemination to secondary sites is due to the overexpression of adhesion and invasion proteins on the parasite (Hijjawi 2010). These proteins allow binding to non-specific surface ligands on host surface cells, allowing invasion. The PCR results show that not all cell lines which show intracellular development produce enough of the parasite to be detectable, which requires 100 oocysts per well to give a positive result (resuspended in 50 µL = 2 oocysts per µL, diluted one in ten to give 0.2 µL, 5 µL PCR reaction template = 1 oocyst). Few of the cell lines were capable of producing this, suggesting that, although invasion and entry into the asexual phase of the life cycle can occur, both high numbers of *C. parvum* and entry into the sexual stages is a rare occurrence. Not all samples tested positive when DNA was detected, implying there is considerable variation in cell lines ability to propagate infection. An alternative explanation is that *C. parvum* was lost during processing in some samples.

Table 4 - Summary of cell line performance

Cell Line	Cell Type	Detectable *C. parvum* DNA?	Stages visible fluorescent microscopy
BT-474	Invasive ductal carcinoma	One of four samples	Asexual Stages
CAMA-1	Breast carcinoma	No	Asexual Stages, Oocysts
COLO-320	Dukes' type C, colorectal adenocarcinoma	One of three samples	Extracellular-like stage
EFM-19	Breast carcinoma	Three of four samples	Complete Life Cycle
EFO-21	Ovarian cystadenocarcinoma	No	None
EFO-27	Ovarian mucinous adenocarcinoma	No	None
H2228	Non-small cell lung cancer (adenocarcinoma)	No	Complete Life Cycle
HCC827	Lung adenocarcinoma	No	None
HCC4006	Lung adenocarcinoma	Two of four samples	Complete Life Cycle
IGR-39	Melanoma	No	None
LS-174T	Dukes' type B,colorectal adenocarcinoma	No	None
MDA-MB-468	Breast adenocarcinoma	One of four samples	Complete Life Cycle
RKO	Colon carcinoma	No	Asexual Stages
SW48	Dukes' type C, grade IV, colorectal adenocarcinoma	Three of four samples	None
SW480	Dukes' type B, colorectal adenocarcinoma	One of four samples	Complete Life Cycle
SW620	Dukes' type C, colorectal adenocarcinoma	No	Asexual Stages
UKF-NB -3	Neuroblastoma	No	None

The four tested breast cancer cell lines all showed some degree of *C. parvum* intracellular development. BT-474 and CAMA-1 were not worth pursuing further, due to a lack of sexual stages and detectable *C. parvum* DNA. The EFM-19 and MDA-MB-468 cell lines showed the complete *C. parvum* life cycle after a week, with EFM-19 having multiple samples test positive with PCR, while only one of the MDA MB 468 samples did. Both cell lines were selected for the passaging experiment and yielded 1.44×10^5 and 1.36×10^5 oocysts respectively, a net 1.6 and a 1.4 fold return in yield. There is a single reported instance of *C. parvum* development in breast cancer derived cells, with Upton reporting development in the BT-549 (breast infiltrating ductal carcinoma) cell line. The reported yields were relatively low, a quarter of the yield of HCT-8 cells (Upton, Tilley and Brillhart 1994). The breast cancer cell lines reported here are more promising, maintaining the complete life cycle for the whole week and may be suitable for further development.

Three types of cell line have not been reported previously; melanomas, neuroblastomas and ovarian adenocarcinomas. The melanoma cell line IGR-39 and the neuroblastoma cell line UKF-NB-3 both failed to provide any detectable infection with microscopy or PCR. This may not be surprising, considering the fast growth of both of these cell lines, and their morphology, which is far from that of the ileum, with cells exhibiting long projections similar to neurons. The two ovarian cancers, EFO-21 and EFO-27 also showed no intracellular development or detectable parasite DNA. Development has been previously observed in an endometrial carcinoma derived cell line (Rasmussen *et al.* 1993), but not ovarian cystadenocarcinomas or mucinous adenocarcinomas.

Of the six colorectal cell lines tested, only SW480 gave observable sexual stages after a week, with the others exhibiting either no entry into the sexual stages or no visible parasites. SW480 provided a higher yield than the breast cancer cell lines during the passaging experiments, providing double the initial inoculum. SW48 showed detectable DNA in three of four samples, but no intracellular stages were observed. This implies initial invasion was successful but subsequent rounds of replication may have failed. Previously, development in LS 174T has been described as being a quarter of that of HCT-8 (Upton 1994) after 68 hour incubations; here longer incubation does not provide higher levels of *C. parvum,* with no intracellular stages present and no *C. parvum* DNA detectable with PCR. The COLO-320 cell line, despite the low yield, gave rise to a unique staining stage not observed in other cell lines. This large region stained with Sporo-Glo™ antibody, but showed no DAPI staining. Given the single occurrence of this stage, it is difficult to determine its nature. While investigators have previously described extracellular stages of *C. parvum* (Hijjawi *et al.* 2001; Hijjawi *et al.* 2004; Rosales *et al.* 2005), this stage bears little resemblance to them, with arguably a slight resemblance to one observed in mice by (Hijjawi *et al.* 2002). If this stage is a parasite, it may be undergoing the binary fission process observed previously (Borowski *et al.* 2010), however the exact nature of this stage, and whether it is even the parasite, remains to be seen. The use of semi-adherent cells for *C. parvum* culture requires additional steps during routine cell passage and makes observing the parasite life cycle difficult, making the COLO-320 cell line unsuitable for routine infection studies. Colorectal cell lines have been the cell line of choice for *in vitro C. parvum* studies, notably the cell lines Caco-2 and HCT-8 which have been used by numerous investigators (Upton, Tilley and Brillhart 1994; Hijjawi *et al.* 2001; Woods *et al.* 2007; Morada *et al.* 2016; DeCicco RePass *et al.* 2017) for the last thirty years. The attraction of the HCT-8 cell line is the fast turnaround of 3 days (Slifko 1999, Upton 1994) the ability of aged monolayers to support infection (Sifuentes *et al.* 2007) along with *C. parvum*'s ability to complete its complete life cycle in these cells (Hijjawi *et al.* 2001). These cells are prone to overgrowth and die rapidly; previous

experiments have shown that HCT-8 shows inferior infection compared with COLO-680N, which supported far higher infection levels for eight weeks (Miller *et al.* 2017).

Two of the lung cancers tested here supported infection, with H2228 showing potential type II meronts but not observable sexual stages, or detectable *C. parvum* DNA. HCC4006 demonstrating the complete life cycle and gave detectable *C. parvum* DNA in two of four samples. Following this, the T-25 passaging over three weeks showed HCC4006 produced nine times the initial inoculum of parasites. The only previous descriptions of development in lung cell lines were human foetal lung described in 1984, the first cell line to support complete development (Current *et al.* 1984), and the MRC-5 cell line (Dawson *et al.* 2004). While efforts were made to compare COLO-680N and HCC4006 performance, unfortunately this was not possible within the time frame, given the change to fresh oocysts during the final two months of the project, which were used for the passaging studies, while COLO-680N cells were infected with older (> 6 month old) oocysts, which would have likely skewed the results in favour of HCC4006.

While this study shows that numerous cell lines can support infection, the mechanisms behind a cell lines success, or lack thereof, are still poorly understood. Characterising the cell lines described here was not realistic within the given time frame, but extensive characterisation is essential to gain insight into host-pathogen interactions and to develop more efficient *in vitro* culture methods. One avenue is the examination of protein expression and comparing infected and uninfected cell lines. While Western blotting is often used to characterise pathways in cancer cell lines, the use of single antibodies for each protein which may be impacted by *C. parvum* would be both costly and time consuming. An alternative approach is a mass spectrometry based approach, which can provide data on both a small scale and at the proteome level, including data on protein-protein interactions (Aebersold *et al.* 2003). Mass-spectrometry analysis has already been conducted on the proteome of various life cycle stages of *Plasmodium falciparum* (Lasonder *et al.* 2002). One alternative is the use of microarrays or RNA-sequencing of infected cells. The microarray approach has been used previously to demonstrate altered gene expression during infection (Liu *et al.* 2009). We may speculate as to the reasons the cell lines described here have or have not worked. Those which failed to show any infection (IGR-39, UKF-NB-3, LS-174T, EFO-21, EFO-27 and HCC827) are, with the exception of HCC827, small cells with a generally fast growth rate. The fast growth rate may not allow *C. parvum* to divert the necessary nutrients to itself, causing parasite death or arrest of the life cycle. The size of cells may also have an impact on invasion. The seeding density was altered for smaller, faster growing cells, which may lead to sporozoites having difficulty identifying a suitable host cell. Taking into account the shorter motility tails left by *C. parvum* sporozoites (Wetzel *et al.* 2005), the distance travelled to locate a host cell may be crucial in determining success of infection.

This comes with its own problems, as a higher number of host cells also means confluency will be reached sooner and that vital medium components are depleted at a higher rate. Two cell lines which showed no infection do not share features of the others; LS 174T and HCC827. Both of these cell lines grow at a similar rate and form similar structures to COLO-680N, H2228 and HCC4006 cells, with large spaces present between cells, measuring several hundred microns across. Morphology and growth rate alone are not enough to determine the success of infection, as the critical invasion process is likely key to supporting the parasite in culture, and will rely on complementary ligand expression of host markers to sporozoite adherence factors (Hijjawi 2010). As several cancers exhibit altered glycosylation of membrane proteins (Hakomori 1996), it is likely that lectins on *C. parvum* may show altered binding and subsequent invasion. Following the initial invasion, *C. parvum* relies on its host for the synthesis of a wide number of metabolites and precursors it cannot synthesise *de novo* (Abrahamsen *et al.* 2004; Ehrenman *et al.* 2013; Miller *et al.* 2017, Panagos, *et al.* 2017). As exhibited by the glucose consumption experiment, rapid glucose consumption may indicate a Warburg metabolism in some cell lines. This is a shift from oxidative phosphorylation to substrate level phosphorylation seen in certain cancers, which may have negative impacts on parasite growth, particularly if *C. parvum* relies on mitochondrial products, such as iron sulphur clusters or steroids, the latter of which is believed to be a key component of the oocyst wall (Harris *et al.* 1999; Liu *et al.* 2010; Jenkins *et al.* 2010). Metabolomics of infected and uninfected cell lines using mass spectrometry or NMR is already being investigated (Miller, Panagos, *et al.* 2017) will enable a more thorough understanding of *C. parvum* life cycle, metabolism and potentially identify areas which can be exploited as vaccine targets.

In this study, all slides were visualised at a single time point, which does not provide information regarding the progression of the life cycle and the timing of appearance of different life cycle stages. While initial processes can be observed with light microscopy, i.e. the inoculation of oocysts and the excystation process, further tracking of life cycle stages is extremely difficult. While the single time point approach is suitable for screening cell lines, true parasite growth patterns in any of these cell lines will require wither multiple time point replicates or the use of live cell imaging, such as the IncuCyte™ system. With end point assays, inferences can be made of the initial infection course. The focus detection method of assessing parasite viability relies on the parasite life cycle forming secondary infections as a result of merozoite release from type I meronts, which are generated from an initial sporozoite invasion (Slifko *et al.* 1999). Real-time data would provide information of both early invasion and the intracellular replication and progression through the life cycle. It would also allow developmental monitoring of previously described extracellular stages described by others (Hijjawi *et al.* 2004; Rosales *et al.* 2005) and the stage observed in the COLO-320 cell line.

The bioreactor system described herein is the first to use a fixed wall rotating bioreactor for culture of the parasite for over three months. Previously, a similar system was used with HCT-8 cells grown on porcine mucosal grafts (Warren 2008) however infection stopped completely after 96 hours. Our current system was maintained for a total of 13 weeks, with oocysts being present in every harvest. Our system differs in the use of a single cell type and a single inoculum, while many other protocols using 3D culture use a mixture of cell types (DeCicco RePass *et al.* 2017) or require periodical replenishment of host cells (Morada *et al.* 2016). The advantages of the approach described here are a lower cost and a far less labour intensive system. Oocysts produced appeared to be both thin and thick walled, which is likely the reason for continued propagation of the system. Thick walled oocysts could be observed via fluorescent microscopy, while thin walled oocysts could be seen in the unfixed slides undergoing excystation. As thin walled oocysts are extremely delicate and tend to rupture/excyst when handled (Current *et al.* 1984) the preparation for microscopy likely caused this. Within the bioreactor, the continuous rotation likely induced the excystation/rupture of thin walled oocysts, allowing the life cycle to begin anew.

The system relies on a single inoculum of treated oocysts, however for the first few weeks of culture the production of oocysts is debatable, as it is conceivable that extracted oocysts are simply inoculated oocysts which have not undergone development. After the first month harvest the number of parasites per millilitre had increased over the initial inoculum, indicating multiplication within the bioreactor. In addition, the infections performed with this system yielded a high level of infection in multiple cell lines, with oocysts being used three months after the initial inoculation producing infection. While the argument could still be made for the initial oocyst inoculum causing the infection, a previous study of oocyst infectivity showed that after one week of storage oocysts kept at 35 °C were only infective to two of ten mice, with no infection after longer storage times (Fayer *et al.* 1998). While a small portion of oocysts may survive long enough to retain infectivity, the high level of infection observed in these cell lines indicates the harvested oocysts were produced within a week of harvesting, implying continuous generation of oocysts. During the reinfection studies it is possible that motile infective stages (sporozoites and merozoites) were transferred to the monolayer as opposed to oocysts. In order to avoid this problem, samples were stored at 4 °C for at least a week prior to infection. Observations by Petry and colleagues have shown that sporozoites are rendered uninfectious if they fail to invade a host within 24 hours when kept at 37 °C (Petry *et al.* 2009). The reduced temperatures used here have not been tested on purified sporozoites, however given the lack of protective oocyst wall and limited amylopectin reserves (Fayer 1994) it seems unlikely that these stages can persist at 4 °C for prolonged time periods whilst retaining infectivity. The ability of oocysts to produce an infection in cultured

monolayers shows their infectivity *in vitro*. Further assessments of parasite viability would involve propidium iodide staining in combination with DAPI, which differentiates between viable and total oocysts. Infections with mice models would also confirm the infectivity of the produced oocysts *in vivo*. Another enumeration method is the focus detection method (Slifko *et al.* 1999), which measures infective oocysts based on cell invasion. In addition, enumeration may be achieved by qPCR, a method used by other investigators to quantify parasites (Zhang *et al.* 2009; Koh *et al.* 2013), and flow cytometry may allow for enumeration and assessment of infectivity (Foster *et al.* 2003).

The trialled T-25 sub-infections show that oocysts can be both produced and maintained in cell lines without the need for excystation treatment between passages. The production of thin-walled oocysts, as in the bioreactor, is likely the reason for this, allowing auto-infection of the culture. Previous descriptions of culture in traditional tissue culture flasks have utilised HCT-8 cells, however the described methods passaged infected cells directly between flasks, and had the medium changed every 2-3 days (Hijjawi *et al.* 2001). The methods described herein utilised direct passage of infectious extracellular stages, and may also involve the passage of merozoites between flasks. In addition, no fresh medium was added during except during passaging, which has been reported as resulting in higher numbers of extracellular stages and intracellular stages in HCT-8 cells when used with medium supplemented with $CaCl_2$ and $MgCl_2$ at 1 mM (Perez Cordón *et al.* 2007). Aged monolayers alone do not seem to promote invasion (Sifuentes *et al.* 2007), so any efforts to develop such a protocol will likely require supplementation of media prior to ageing experiments. In the future, both media changes and aged cells may be trialled and compared, and if in conjunction with real time visualisation techniques discussed earlier, a better idea of optimal passaging and seeding times may be established.

The yields of HCC4006 show a high return on the initial inoculum, and future development may enhance this yield. Numerous investigators have reported that media supplements can greatly improve parasite yield (Upton *et al.* 1995; Woods *et al.* 2007; Perez Cordón *et al.* 2007). While this was not trialled here, it is likely that media supplements and the base media were having an effect on the yield, if not the entire invasion process. Three of the cell lines used in the subculture experiments used IMDM with 10 % FBS as the base medium, while HCC4006 used RPMI 1640 with 10 % FBS. IMDM contains more glucose than RPMI-1640, which may encourage cell proliferation. To ascertain the effects of the base media, cell lines could be adapted to the medium before being infected. It seems likely that this would allow for better selection of base media to use for respective cell lines. The yields reported here are modest by comparison to the reported hollow fiber system (1×10^6 oocysts per mL compared with 1×10^8 oocysts per mL), (Morada *et al.* 2016) but here solely

base medium with no supplements was used. The hollow fiber system uses a base MEM medium with 15 mM HEPES buffer, described by (Upton, Tilley and Brillhart 1994) in the tubes, while mediumcirculating the main lumen space requires additional additives; 20 mg/mL glutathione, taurine, betaine and cysteine were all included, along with a lipid mixture (composed of 1.5% deoxycholate, 6.7 mg/mL oleic acid, 10 mg/mL phosphocholine, 1.6 mg/mL a-linolenic acid, 6.8 mg/mL eicosapentaenoic acid, 2mg/mL docosahexaenoic acid, 18 mg/mL cholesterol) and requires degassing of media (Morada *et al.* 2016). In addition, a set-up time is required of 11 days, and the weekly medium change requires a full litre of medium. While the reported yields may be worth the investment, anecdotal reports suggest this method is not readily reproducible, and that the system is exceptionally prone to contamination. The system described here is at lower risk due to the simpler apparatus and fewer steps involving moving the bioreactor out of the incubator environment, and the low cost means this system may be adopted by other laboratories to routinely propagate *C. parvum in vitro*. By combining the bioreactor system with the high yield cell line HCC4006 and identifying a media composition which allows high yields of oocysts, the yields may rival those reported for the hollow fiber system, at a much lower cost and with less labour intensive maintenance.

Moreover, recent focus has shifted from cell culture to axenic culture of *C. parvum* (Karanis *et al.* 2011). With the reported success establishing the complete life cycle of the parasite in host cell free culture (Hijjawi *et al.* 2004), this system would avoid nearly all of the current problems associated with *in vitro* host cell culture, however, many groups have tried and failed to replicate these findings (Woods *et al.* 2007; Girouard *et al.* 2006). While the DNA replication of *C. parvum* has been reported by several groups, there is a lack of images demonstrating the complete life cycle in axenic culture. Also, there is considerable debate as to the identity of life cycle stages seen by different groups (Hijjawi *et al.* 2004; Woods *et al.* 2007; Karanis *et al.* 2008; Petry *et al.* 2009; Koh *et al.* 2013; Karanis *et al.* 2011) by light microscopy, confocal microscopy and electron microscopy. The axenic culture reported by (Hijjawi *et al.* 2004) included images of extracellular stages which had not been observed previously, and many of the described stages of the normal life cycle have been identified by others as being yeast and other contaminants (Woods *et al.* 2007). In addition, the development of the extracellular stages described by Hijjawi and Rosales have not been seen by other groups (Karanis *et al.* 2011; Aldeyarbi *et al.* 2016a; Aldeyarbi *et al.* 2016b). A recent study validating the original axenic culture system reported the identification of some stages of the life cycle, however these were limited to the asexual stages (Yang *et al.* 2015). The described 'merozoites' show similar morphology to the aged sporozoites described by (Petry *et al.* 2009). Stages identified by other investigators as merozoites (Karanis *et al.* 2008) also have similar morphology.

Another recent paper demonstrated *C. parvum* DNA replication in a model biofilm system, and used confocal microscopy to demonstrate life cycle progression (Koh *et al.* 2013; Koh *et al.* 2014). The presented confocal images show little similarities to the stages identified during this study here and bear little similarity to the stages shown by (Aldeyarbi *et al.* 2016a). Identifying *C. parvum* stages in axenic culture remains difficult, as there is no widely agreed upon reference images with which to identify stages. The reports of multiplication in cell free systems mean these are a promising area for future development, and recently many investigators are reporting the multiplication of *C. parvum* in host cell free systems (Zhang *et al.* 2009; Koh *et al.* 2013). With the exception of (Aldeyarbi *et al.* 2016b), no investigators provide evidence of the complete life cycle being present. A recent paper describing the multiplication of *C. parvum* in an aquatic biofilm system claims to show type II meront development (Koh *et al.* 2013), however these stages, while similar to those observed by (Hijjawi *et al.* 2004), have been identified by others as fungal contaminants and debris (Woods *et al.* 2007). While it is conceivable that *C. parvum* has differing morphology in cell free systems, these stages are not the same as observed by (Aldeyarbi *et al.* 2016a), which show similar ultrastructure to *in vivo* stages. Description of multiplication in cell free culture observed by Zhang provides qPCR evidence of parasite multiplication and evidence of stages present with fluorescent microscopy, but the complete life cycle still appears absent (Zhang *et al.* 2009). While the replication of *C. parvum* has recently been observed in axenic culture with transmission electron microscopy (Aldeyarbi *et al.* 2016c; Aldeyarbi *et al.* 2016b; Aldeyarbi *et al.* 2016a), these stages and the development of oocysts has not been quantified. Adaptation of this system may be the first step toward axenic *in vitro* culture. For the moment, complete development in high numbers seems to be seen only in host cell culture, and will likely remain so until a better understanding of this parasite is achieved.

5.0 Conclusion

In summary, the complete life cycle of *C. parvum* has been shown to occur in four of the tested cell lines, however there is still the problem of low yields in three of these. A cell line has been identified which can support the entire life cycle and produce a high yield of oocysts, the lung adenocarcinoma HCC4006. The HCC4006 cell line is a suitable candidate for further development owing to its ability to produce an increase over the initial inoculum of oocysts and its ability to survive for a week with no medium change in a single culture vessel. This cell line is generally user friendly, requiring a medium change once weekly and generally a weekly passage when seeded at a 1:4 split ratio. The establishment of a low cost bioreactor with a simple protocol will enable researchers to cultivate *C. parvum* continuously to supplement their commercial supplies, and further development of this system will enable higher yields to be generated. Productive and routine culture of *C. parvum in vitro* may be within reach, and by further developing cell lines with high potential such as COLO-680N and HCC4006 and using them with low cost and simple 3D culture systems, a truly reproducible and long term system will enable *in vitro* harvesting of parasites at a level which can be used for experiments, and potentially enable the first maintenance of clonal *C. parvum* populations *in vitro*. While axenic culture is a tantalising prospect, for the foreseeable future it is likely that host cell culture will remain the only option for reproducible parasite propagation until a better understanding of *C. parvum'*s biology is achieved.

References

Abrahamsen, M.S. *et al.* (2004). Complete Genome Sequence of the Apicomplexan, Cryptosporidium parvum. *Science* **304**:441–445.

Aebersold, R. and Mann, M. (2003). Mass spectrometry-based proteomics. *Nature* [Online] **422**:198–207. Available at: http://www.ncbi.nlm.nih.gov/pubmed/12634793.

Aguirre-García, M.M. and Okhuysen, P.C. (2007). Cryptosporidium parvum: Identification and characterization of an acid phosphatase. *Parasitology Research* **101**:85–89.

Alcantara Warren, C. *et al.* (2008). Detection of Epithelial-Cell Injury, and Quantification of Infection, in the HCT-8 Organoid Model of Cryptosporidiosis. *The Journal of Infectious Diseases* [Online] **198**:143–149. Available at: https://academic.oup.com/jid/article-lookup/doi/10.1086/588819.

Aldeyarbi, H.M. and Karanis, P. (2016a). Electron microscopic observation of the early stages of Cryptosporidium parvum asexual multiplication and development in in vitro axenic culture. *European Journal of Protistology* [Online] **52**:36–44. Available at: http://dx.doi.org/10.1016/j.ejop.2015.07.002.

Aldeyarbi, H.M. and Karanis, P. (2016b). The fine structure of sexual stage development and sporogony of Cryptosporidium parvum in cell-free culture. *Parasitology* [Online] **143**:749–761. Available at: http://www.journals.cambridge.org/abstract_S0031182016000275.

Aldeyarbi, H.M. and Karanis, P. (2016c). The Ultra-Structural Similarities between Cryptosporidium parvum and the Gregarines. *Journal of Eukaryotic Microbiology* **63**:79–85.

Arrowood, M.J. (2002). In Vitro Cultivation of Cryptosporidium Species In Vitro Cultivation of Cryptosporidium Species. *In Vitro* **15**:390–400.

Arrowood, M.J., Sterling, C.R. and Healey, M.C. (1991). Immunofluorescent microscopical visualization of trails left by gliding Cryptosporidium parvum sporozoites. *J Parasitol* [Online] **77**:315–317. Available at: http://www.ncbi.nlm.nih.gov/entrez/query.fcgi?cmd=Retrieve&db=PubMed&dopt=Citation&list_uids=2010865.

Atwill, E.R. *et al.* (1997). Prevalence of and associated risk factors for shedding Cryptosporidium parvum oocysts and Giardia cysts within feral pig populations in California . Prevalence of and Associated Risk Factors for Shedding Cryptosporidium parvum Oocysts and Giardia Cysts wi. *American Society for Microbiology* **63**:10–14.

Banwat, E.B. *et al.* (2004). Cryptosporidium infection in undernourished children with HIV / AIDS in Jos, Nigeria. TT -. *Annals of African Medicine* **3**:80–82.

Barbee, S.L. *et al.* (1999). Inactivation of Cryptosporidium parvum oocyst infectivity by disinfection and sterilization processes. *Gastrointestinal Endoscopy* **49**:605–611.

Barnes, D.A. *et al.* (1998). A novel multi-domain mucin-like glycoprotein of Cryptosporidium parvum mediates invasion. *Molecular and Biochemical Parasitology* **96**:93–110.

Beyer, T. V *et al.* (2000). Cryptosporidium parvum (Coccidia, apicomplexa): Some new ultrastructural observations on its endogenous development. *European Journal of Protistology* [Online] **36**:151–159. Available at: http://dx.doi.org/10.1016/S0932-4739(00)80034-6.

Blackburn, B.G. *et al.* (2006). Cryptosporidiosis associated with ozonated apple cider. *Emerging Infectious Diseases* **12**:684–686.

Bonnin, A. *et al.* (2001). Characterization of a monoclonal antibody reacting with antigen-4 domain of gp900 in Cryptosporidium parvum invasive stages. *Parasitology Research* **87**:589–592.

Bonnin, A. *et al.* (1999). Immunodetection of the microvillous cytoskeleton molecules villin and ezrin in the parasitophorous vacuole wall of Cryptosporidium parvum (Protozoa: Apicomplexa). *European journal of cell biology* [Online] **78**:794–801. Available at: http://www.ncbi.nlm.nih.gov/pubmed/10604656.

Borowski, H. *et al.* (2010). Morphological characterization of Cryptosporidium parvum life-cycle stages in an in vitro model system. *Parasitology* [Online] **137**:13–26. Available at: http://www.ncbi.nlm.nih.gov/pubmed/19691870.

Buraud, M. *et al.* (1991). Sexual stage development of Cryptosporidia in the Caco-2 cell line. *Infection and Immunity* **59**:4610–4613.

Cacciò, S.M. and Widmer, G. (2014). Cryptosporidium: Parasite and disease. *Cryptosporidium: Parasite and Disease*:1–564.

Cantey, P.T. *et al.* (2012). Outbreak of cryptosporidiosis associated with a man-made chlorinated lake--Tarrant County, Texas, 2008. *Journal of environmental health* [Online] **75**:14–9. Available at: http://www.ncbi.nlm.nih.gov/pubmed/23210393.

Carreno, R.A., Matrin, D.S. and Barta, J.R. (1999). Cryptosporidium is more closely related to the gregarines than to coccidia as shown by phylogenetic analysis of apicomplexan parasites inferred using small-subunit ribosomal RNA gene sequences. *Parasitology Research* [Online] **85**:899–904. Available at: http://link.springer.com/10.1007/s004360050655.

Castellanos-Gonzalez, A. *et al.* (2013). Human primary intestinal epithelial cells as an improved in vitro model for cryptosporidium parvum infection. *Infection and Immunity* **81**:1996–2001.

Certad, G. *et al.* (2012). Fulminant cryptosporidiosis after near-drowning: A human Cryptosporidium parvum strain implicated in invasive gastrointestinal adenocarcinoma and cholangiocarcinoma in an experimental model. *Applied and Environmental Microbiology* **78**:1746–1751.

Cevallos, A.M. *et al.* (2000). Mediation of Cryptosporidium parvum Infection In Vitro by Mucin-Like Glycoproteins Defined by a Neutralizing Monoclonal Antibody Mediation of Cryptosporidium parvum Infection In Vitro by Mucin-Like Glycoproteins Defined by a Neutralizing Monoclonal Antibo. **68**:5167–5175.

Chalmers, R.M. *et al.* (1997). The prevalence of Cryptosporidium parvum and C. muris in Mus domesticus Apodemus sylvaticus and Clethrionomys glareolus in an agricultural system. *Parasitology Research* **83**:478–482.

Chappell, C.L. *et al.* (1996). Cryptosporidium parvum: intensity of infection and oocyst excretion patterns in healthy volunteers. *The Journal of infectious diseases* [Online] **173**:232–6. Available at: http://www.ncbi.nlm.nih.gov/pubmed/8537664.

Chappell, C.L. *et al.* (1999). Infectivity of Cryptosporidium parvum in healthy adults with pre-existing anti-C. parvum serum immunoglobulin G. *The American journal of tropical medicine and hygiene* [Online] **60**:157–64. Available at: http://www.ncbi.nlm.nih.gov/pubmed/9988341.

Checkley, W. *et al.* (2015). A review of the global burden, novel diagnostics, therapeutics, and vaccine targets for cryptosporidium. *The Lancet Infectious Diseases* **15**:85–94.

Checkley, W. *et al.* (1998). Effects of Cryptosporidium parvum Infection in Peruvian Children: Growth Faltering and Subsequent Catch-up Growth. *American Journal of Epidemiology* [Online] **148**:497–506. Available at: https://academic.oup.com/aje/article-lookup/doi/10.1093/oxfordjournals.aje.a009675.

Chen, X.M. *et al.* (2003). Cryptosporidium parvum invasion of biliary epithelia requires host cell tyrosine phosphorylation of cortactin via c-Src. *Gastroenterology* **125**:216–228.

Chen, X.M. *et al.* (1998). Cryptosporidium parvum is cytopathic for cultured human biliary epithelia via an apoptotic mechanism. *Hepatology* **28**:906–913.

Current, W.L. and Haynes, T.B. (1984). Complete Development of Cryptosporidium in Cell Culture. *Science* **224**:603–605.

Current, W.L. and Long, P.L. (1983). Development of Human and Calf Cryptosporidium in Chicken Embryos Author (s): William L . Current and Peter L . Long Published by : Oxford University Press Stable URL : http://www.jstor.org/stable/30133841 Development of Human and Calf Cryptosporidium in. *The*

Journal of infectious diseases **148**:1108–1113.

Daniels, M.E. *et al.* (2015). Cryptosporidium and giardia in humans, domestic animals, and village water sources in rural India. *American Journal of Tropical Medicine and Hygiene* **93**:596–600.

Dawson, D.J. *et al.* (2004). Survival of Crytosporidium species in environments relevant to foods and beverages. *Journal of Applied Microbiology* **96**:1222–1229.

DeCicco RePass, M.A. *et al.* (2017). Novel bioengineered three-dimensional human intestinal model for long-term infection of Cryptosporidium parvum. *Infection and Immunity* **85**.

Doyle, P.S., Crabb, J. and Petersen, C. (1993). Anti-Cryptosporidium parvum antibodies inhibit infectivity in vitro and in vivo. *Infection and Immunity* **61**:4079–4084.

Edwinson, A., Widmer, G. and McEvoy, J. (2016). Glycoproteins and Gal-GalNAc cause Cryptosporidium to switch from an invasive sporozoite to a replicative trophozoite. *International Journal for Parasitology* [Online] **46**:67–74. Available at: http://linkinghub.elsevier.com/retrieve/pii/S0020751915002532.

Efstratiou, A., Ongerth, J.E. and Karanis, P. (2017). Waterborne transmission of protozoan parasites: Review of worldwide outbreaks - An update 2011–2016. *Water Research* [Online] **114**:14–22. Available at: http://dx.doi.org/10.1016/j.watres.2011.10.013.

Ehrenman, K. *et al.* (2013). Cryptosporidium parvum scavenges LDL-derived cholesterol and micellar cholesterol internalized into enterocytes. *Cellular Microbiology* **15**:1182–1197.

El-Khodery, S.A. and Osman, S.A. (2008). Cryptosporidiosis in buffalo calves (Bubalus bubalis): Prevalence and potential risk factors. *Tropical Animal Health and Production* **40**:419–426.

Evans, D.F. *et al.* (1988). Measurement of gastrointestinal pH profiles in normal ambulant human subjects. *Gut* **29**:1035–41.

Fayer, R. (1994). Effect of High Temperature on Infectivity of Cryptosporidium parvum Oocysts in Water. *Applied and Environmental Microbiology* **60**:2732–2735.

Fayer, R. and Nerad, T. (1996). Effects of low temperatures on viability of Cryptosporidium parvum oocysts. *Appl. Environ. Microbiol* **62**:1431–1433.

Fayer, R., Trout, J.M. and Jenkins, M.C. (1998). Infectivity of Cryptosporidium parvum Oocysts Stored in Water at Environmental Temperatures. *The Journal of Parasitology* [Online] **84**:1165. Available at: http://www.jstor.org/stable/3284666?origin=crossref.

Fayer, R. and Xiao, L. (2008). *Cryptosporidium and Cryptosporidiosis*. 2nd Editio. Boca Raton, FL, USA: CRC Press.

Flanigan, T.P. *et al.* (1991). Asexual Development of Cryptosporidium-Parvum within a Differentiated Human Enterocyte Cell-Line. *Infection and Immunity* **59**:234–239.

Forney, J.R. *et al.* (1998). Actin-dependent motility in Cryptosporidium parvum sporozoites. *Journal of Parasitology* [Online] **84**:908–913. Available at: http://www.ncbi.nlm.nih.gov/pubmed/9794629.

Foster, J.C. *et al.* (2003). Effect of Lactobacillus and Bifidobacterium on Cryptosporidium parvum oocyst viability. *Food Microbiology* **20**:351–357.

Fujino, T. *et al.* (2002). The effect of heating against Cryptosporidium oocysts. *Journal of Veterinary Medical Science* **64**:199–200.

Galuppi, R. *et al.* (2016). Cryptosporidium parvum: From foal to veterinary students. *Veterinary Parasitology* [Online] **219**:53–56. Available at: http://dx.doi.org/10.1016/j.vetpar.2016.02.001.

Girouard, D. *et al.* (2006). Failure to Propagate Cryptosporidium spp . in Cell-Free Culture. *Journal of Parasitology* **92**:399–400.

Graczyk, T.K., Fayer, R. and Cranfield, M.R. (1997). Zoonotic transmission of Cryptosporidium parvum: Implications for water- borne cryptosporidiosis. *Parasitology Today* **13**:348–351.

Hakomori, S. (1996). Tumor Malignancy Defined by Aberrant Glycosylation and Sphingo (glyco) lipid Metabolism Tumor Malignancy Defined by Aberrant Glycosylation and Sphingo (glyco) lipid Metabolism ’. *Cancer research* **56**:5309–5318.

Harris, J.R. and Petry, F. (1999). Cryptosporidium parvum: structural components of the oocyst wall. *The Journal of parasitology* [Online] **85**:839–49. Available at: http://www.ncbi.nlm.nih.gov/pubmed/10577718.

Hashim, A. *et al.* (2006). Interaction of Cryptosporidium hominis and Cryptosporidium parvum with Primary Human and Bovine Intestinal Cells Interaction of Cryptosporidium hominis and Cryptosporidium parvum with Primary Human and Bovine Intestinal Cells. *Infection and Immunity* **74**:99–107.

Hayes, E.B. *et al.* (1989). Large community outbreak of cryptosporidiosis due to contamination of a filtered public water supply. *The New England Journal of Medicine* **320**:1372–1376.

Hijjawi, N. (2010). Cryptosporidium: New developments in cell culture. *Experimental Parasitology* [Online] **124**:54–60. Available at: http://dx.doi.org/10.1016/j.exppara.2009.05.015.

Hijjawi, N.S. *et al.* (2001). Complete development and long-term maintenance of Cryptosporidium parvum human and cattle genotypes in cell culture. *International Journal for Parasitology* **31**:1048–1055.

Hijjawi, N.S. *et al.* (2004). Complete development of Cryptosporidium parvum in host cell-free culture. *International Journal for Parasitology* **34**:769–777.

Hijjawi, N.S. *et al.* (2002). Successful in vitro cultivation of Cryptosporidium andersoni: Evidence for the existence of novel extracellular stages in the life cycle and implications for the classification of Cryptosporidium. *International Journal for Parasitology* **32**:1719–1726.

Hofmannová, L. *et al.* (2016). Cryptosporidium erinacei and C. parvum in a group of overwintering hedgehogs. *European Journal of Protistology* **56**:15–20.

Hoxie, N.J. *et al.* (1997). Cryptosporidiosis-associated mortality following a massive waterborne outbreak in Milwaukee, Wisconsin. *American Journal of Public Health* **87**:2032–2035.

Huang, B.Q., Chen, X.-M. and LaRusso, N.F. (2004). Cryptosporidium parvum attachment to and internalization by human biliary epithelia in vitro: a morphologic study. *The Journal of parasitology* [Online] **90**:212–21. Available at: http://www.ncbi.nlm.nih.gov/pubmed/15165040.

Hunter, P.R. and Thompson, R.C.A. (2005). The zoonotic transmission of Giardia and Cryptosporidium. *International Journal for Parasitology* **35**:1181–1190.

Insulander, M. *et al.* (2005). An outbreak of cryptosporidiosis associated with exposure to swimming pool water. *Scandinavian Journal of Infectious Diseases* [Online] **37**:354–360. Available at: http://www.tandfonline.com/doi/full/10.1080/00365540410021072.

Insulander, M., Jong, B. De and Svenungsson, B. (2008). *A Food-Borne Outbreak of Cryptosporidiosis among Guests and Staff at a Hotel Restaurant in Stockholm County, Sweden, September 2008*.

Jenkins, M.B. *et al.* (2010). Significance of wall structure, macromolecular composition, and surface polymers to the survival and transport of Cryptosporidium parvum oocysts. *Applied and Environmental Microbiology* **76**:1926–1934.

Jokipii, L. and Jokipii, A. (1986). Timing of symptoms and oocyst excretion in human cryptosporidiosis. *The New England Journal of Medicine* **315**:1643–6.

Karanis, P. *et al.* (2008). Observations on Cryptosporidium Life Cycle Stages During Excystation. *Journal of Parasitology* [Online] **94**:298–300. Available at: http://www.bioone.org/doi/abs/10.1645/GE-3348RN.

Karanis, P. and Aldeyarbi, H.M. (2011). Evolution of Cryptosporidium in vitro culture. *International Journal for Parasitology* [Online] **41**:1231–1242. Available at: http://dx.doi.org/10.1016/j.ijpara.2011.08.001.

Mac Kenzie, W.R. *et al.* (1994). A massive oubreak in Milawukee of Cryptosporidium infection transmitted through the public water supply. *The New England Journal of Medicine* **331**:161–167.

Koh, W. *et al.* (2014). Extracellular excystation and development of Cryptosporidium: tracing the fate of oocysts within Pseudomonas aquatic biofilm systems. *BMC microbiology* [Online] **14**:281. Available at: http://www.pubmedcentral.nih.gov/articlerender.fcgi?artid=4236811&tool=pmcentrez&rendertype=abstract.

Koh, W. *et al.* (2013). Multiplication of the waterborne pathogen Cryptosporidium parvum in an aquatic biofilm system. *Parasites & vectors* [Online] **6**:270. Available at: http://www.pubmedcentral.nih.gov/articlerender.fcgi?artid=3848567&tool=pmcentrez&rendertype=abstract.

Kotloff, K.L. *et al.* (2013). Burden and aetiology of diarrhoeal disease in infants and young children in developing countries (the Global Enteric Multicenter Study, GEMS): A prospective, case-control study. *The Lancet* **382**:209–222.

Langer, R.C. *et al.* (2001). Characterization of an Intestinal Epithelial Cell Receptor Recognized by the Cryptosporidium parvum Sporozoite Ligand CSL Downloaded from http://iai.asm.org/ on November 29 , 2014 by VIRGINIA COMMONWEALTH UNIV. **69**:1661–1670.

Langer, R.C. and Riggs, M.W. (1999). Cryptosporidium parvum Apical Complex Glycoprotein CSL Contains a Sporozoite Ligand for Intestinal Epithelial Cells Cryptosporidium parvum Apical Complex Glycoprotein CSL Contains a Sporozoite Ligand for Intestinal Epithelial Cells. **67**:5282–5291.

Lasonder, E. *et al.* (2002). Analysis of the Plasmodium falciparum proteome by high-accuracy mass spectrometry. *Nature* [Online] **419**:537–42. Available at: http://www.ncbi.nlm.nih.gov/pubmed/12368870.

Leoni, F. *et al.* (2006). Genetic analysis of Cryptosporidium from 2414 humans with diarrhoea in England between 1985 and 2000. *Journal of Medical Microbiology* **55**:703–707.

Liu, J. *et al.* (2009). Biphasic modulation of apoptotic pathways in Cryptosporidium parvum-infected human intestinal epithelial cells. *Infection and immunity* [Online] **77**:837–49. Available at: http://www.pubmedcentral.nih.gov/articlerender.fcgi?artid=2632021&tool=pmcentrez&rendertype=abstract.

Liu, Y. *et al.* (2010). Composition and conformation of cryptosporidium parvum oocyst wall surface macromolecules and their effect on adhesion kinetics of oocysts on quartz surface. *Biomacromolecules* **11**:2109–2115.

MacKenzie, W.R., Kazmierczak, J.J. and Davis, J.P. (1995). An outbreak of cryptosporidiosis associated with swimming pools. *Kansenshogaku Zasshi. Journal of the Japanese Association for Infectious Diseases* [Online] **1**:545–553. Available at: http://www.ncbi.nlm.nih.gov/pubmed/18306673.

Martinez, F. *et al.* (1992). In vitro multiplication of cryptosporidium parvum in mouse peritoneal macrophages. *Veterinary Parasitology* **42**:27–31.

Matsubayashi, M. *et al.* (2010). Morphological changes and viability of Cryptosporidium parvum sporozoites after excystation in cell-free culture media. *Parasitology* [Online] **137**:1861–1866. Available at: http://www.ncbi.nlm.nih.gov/pubmed/20800015.

Matsuura, Y. *et al.* (2017). Report of fatal mixed infection with Cryptosporidium parvum and Giardia intestinalis in neonatal calves. **62**:214–220.

McDonald, A.C. *et al.* (2001). *Cryptosporidium parvum*– Specific Antibody Responses among Children Residing in Milwaukee during the 1993 Waterborne Outbreak. *The Journal of Infectious Diseases* [Online] **183**:1373–1379. Available at: https://academic.oup.com/jid/article-lookup/doi/10.1086/319862.

Mclauchlin, J., Amar, C. and Nichols, G.L. (2000). Molecular Epidemiological Analysis of Cryptosporidium spp . in the United Kingdom : Results of Genotyping Samples from Humans and 105 Fecal Samples from Livestock Animals Molecular Epidemiological Analysis of Cryptosporidium spp . in the United Kingdom : . **38**:3984–3990.

Millard, P.S. *et al.* (1993). An outbreak of cryptosporidiosis from fresh-pressed apple cider. *JAMA : the journal of the American Medical Association* [Online] **272**:1592–6. Available at: http://www.ncbi.nlm.nih.gov/pubmed/7966869.

Miller, C.N., Jossé, L., *et al.* (2017). A cell culture platform for Cryptosporidium that enables long-term cultivation and new tools for the systematic investigation of its biology. [Online]. Available at: http://dx.doi.org/10.1101/134270.

Miller, C.N., Panagos, C.G., *et al.* (2017). Metabolic changes of the host-pathogen environment in a Cryptosporidium infection. *bioRxiv*.

Moon, S. *et al.* (2013). Epidemiological characteristics of the first water-borne outbreak of cryptosporidiosis in seoul, korea. *Journal of Korean Medical Science* **28**:983–989.

Morada, M. *et al.* (2016). Continuous culture of Cryptosporidium parvum using hollow fiber technology. *International Journal for Parasitology* [Online] **46**:21–29. Available at: http://dx.doi.org/10.1016/j.ijpara.2015.07.006.

Morgan, U. *et al.* (2000). Molecular Characterization of Cryptosporidium Isolates Obtained from Human Immunodeficiency Virus-Infected Individuals Living in Switzerland , Kenya , and the United States Molecular Characterization of Cryptosporidium Isolates Obtained from Human Immunod. *Society* **38**:1180–1183.

Nelson, J.B. *et al.* (2006). Cryptosporidium parvum infects human cholangiocytes via sphingolipid-enriched membrane microdomains. *Cellular Microbiology* **8**:1932–1945.

Nesterenko, M. V., Woods, K. and Upton, S.J. (1999). Receptor/ligand interactions between Cryptosporidium parvum and the surface of the host cell. *Biochimica et Biophysica Acta - Molecular Basis of Disease* **1454**:165–173.

Newman, R.D. *et al.* (1999). Longitudinal study of Cryptosporidium infection in children in northeastern Brazil. *The Journal of infectious diseases* **180**:167–175.

Ng-Hublin, J.S.Y. *et al.* (2017). Differences in the occurrence and epidemiology of cryptosporidiosis in Aboriginal and non-Aboriginal people in Western Australia (2002 − 2012). *Infection, Genetics and Evolution* [Online] **53**:100–106. Available at: http://linkinghub.elsevier.com/retrieve/pii/S1567134817301788.

O'Hara, S.P. and Chen, X.M. (2011). The cell biology of cryptosporidium infection. *Microbes and Infection* **13**:721–730.

Okhuysen, P.C. *et al.* (1994). Arginine Aminopeptidase, an Integral Membrane Protein of the Cryptosporidium parvum Sporozoite. **31**:635–638.

Okhuysen, P.C. *et al.* (1999). Virulence of Three Distinct *Cryptosporidium parvum* Isolates for Healthy Adults. *The Journal of Infectious Diseases* [Online] **180**:1275–1281. Available at: https://academic.oup.com/jid/article-lookup/doi/10.1086/315033.

Patel, S. *et al.* (1998). Molecular characterisation of Cryptosporidium parvum from two large suspected waterborne outbreaks. Outbreak Control Team South and West Devon 1995, Incident Management Team and Further Epidemiological and Microbiological Studies Subgroup North Thames 199. *Communicable Disease and Public Health* **1**:231–233.

Pecková, R. *et al.* (2016). Statistical comparison of excystation methods in Cryptosporidium parvum oocysts. *Veterinary Parasitology* [Online] **230**:1–5. Available at: http://linkinghub.elsevier.com/retrieve/pii/S0304401716304058.

Peeters, J.E. *et al.* (1992). Cryptosporidium-Parvum in Calves - Kinetics and Immunoblot Analysis of Specific Serum and Local Antibody-Responses (Immunoglobulin a [Iga], Igg, and Igm) after Natural and Experimental Infections. *Infection and Immunity* **60**:2309–2316.

Peng, M.M. *et al.* (1997). Genetic Polymorphism among Cryptosporidium parvum Isolates: Evidence of Two

Distinct Human Transmission Cycles. *Emerging Infectious Diseases* **3**:567–573.

Perez Cordón, G. *et al.* (2007). More productive in vitro culture of Cryptosporidium parvum for better study of the intra- and extracellular phases. *Memorias do Instituto Oswaldo Cruz* **102**:567–571.

Perkins, M.E. *et al.* (1999). CpABC, a Cryptosporidium parvum ATP-binding cassette protein at the host-parasite boundary in intracellular stages. *Proceedings of the National Academy of Sciences of the United States of America* **96**:5734–5739.

Petersen, C., Barnes, D.A. and Gousset, L. (1997). Cryptosporidium parvum GP900, a unique invasion protein. *The Journal of eukaryotic microbiology* [Online] **44**:89S–90S. Available at: http://www.ncbi.nlm.nih.gov/pubmed/9508468.

Petry, F., Kneib, I. and Harris, J.R. (2009). Morphology and In Vitro Infectivity of Sporozoites of Cryptosporidium parvum. *J. Parasitol.* **95**:1243–1246.

Pollok, R.C.G. *et al.* (2003). The role of Cryptosporidium parvum-derived phospholipase in intestinal epithelial cell invasion. *Parasitology research* [Online] **90**:181–6. Available at: http://www.ncbi.nlm.nih.gov/pubmed/12783305.

Preiser, G., Preiser, L. and Madeo, L. (2003). An Outbreak of Cryptosporidiosis Among Veterinary Science Students Who Work With Calves. *Journal of American College Health* [Online] **51**:213–215. Available at: http://www.ncbi.nlm.nih.gov/pubmed/12822713%0Ahttp://www.tandfonline.com/doi/abs/10.1080/07448480309596353.

Putignani, L. *et al.* (2008). The thrombospondin-related protein CpMIC1 (CpTSP8) belongs to the repertoire of micronemal proteins of Cryptosporidium parvum. *Molecular and Biochemical Parasitology* **157**:98–101.

Qi Deng, M. and Cliver, D.O. (1998). Cryptosporidium parvum Development in the BS-C-1 Cell Line Published by : Allen Press on behalf of The American Society of Parasitologists Stable URL : http://www.jstor.org/stable/3284519 REFERENCES Linked references are available on JSTOR for this articl. *The Journal of parasitology* **84**:8–15.

Quiroz, E.S. *et al.* (2000). An outbreak of cryptosporidiosis linked to a foodhandler. *The Journal of infectious diseases* [Online] **181**:695–700. Available at: http://www.ncbi.nlm.nih.gov/pubmed/10669357.

Rasmussen, K.R., Larsen, N.C. and Healey, M.C. (1993). Complete development of Cryptosporidium parvum in a human endometrial carcinoma cell line. *Infection and immunity* [Online] **61**:1482–5. Available at: http://www.pubmedcentral.nih.gov/articlerender.fcgi?artid=281389&tool=pmcentrez&rendertype=abstract.

Reduker, D., Speer, C. and Blixt, J. (1985). Ultrastructural changes in the oocyst wall during excystation of Cryptosporidium parvum (Apicomplexa; Eucoccidiorida). *Can. J. Zool* **63**:1892–1896.

Reduker, D.W., Speer, C. a and Blixt, J. a (1985). Ultrastructure of Cryptosporidium parvum oocysts and excysting sporozoites as revealed by high resolution scanning electron microscopy. *The Journal of protozoology* [Online] **32**:708–11. Available at: http://www.ncbi.nlm.nih.gov/pubmed/4067883.

Richardson, a J. *et al.* (1991). An outbreak of waterborne cryptosporidiosis in Swindon and Oxfordshire. *Epidemiology and infection* [Online] **107**:485–95. Available at: http://www.pubmedcentral.nih.gov/articlerender.fcgi?artid=2272087&tool=pmcentrez&rendertype=abstract.

Rosales, M., Cifuentes, J. and Mascaro, C. (1993). Cryptosporidium parvum Culture in MDCK Cells. *Experimental Parasitology* **76**:209–212.

Rosales, M.J. *et al.* (2005). Extracellular like-gregarine stages of Cryptosporidium parvum. *Acta Tropica* **95**:74–78.

Ryan, U. *et al.* (2016). It's official – Cryptosporidium is a gregarine: What are the implications for the water

industry? *Water Research* [Online] **105**:305–313. Available at: http://dx.doi.org/10.1016/j.watres.2016.09.013.

Ryan, U. and Hijjawi, N. (2015). New developments in Cryptosporidium research. *International Journal for Parasitology* [Online] **45**:367–373. Available at: http://dx.doi.org/10.1016/j.ijpara.2015.01.009.

Sifuentes, L.Y. and Di Giovanni, G.D. (2007). Aged HCT-8 cell monolayers support Cryptosporidium parvum infection. *Applied and Environmental Microbiology* **73**:7548–7551.

Singh, P. *et al.* (2015). Identification of invasion proteins of Cryptosporidium parvum. *World Journal of Microbiology and Biotechnology* **31**:1923–1934.

Slifko, T.R., Huffman, D.E. and Rose, J.B. (1999). A Most-Probable-Number Assay for Enumeration of Infectious Cryptosporidium parvum Oocysts. *Applied and Environmental Microbiology* **65**:3936–3941.

Spano, F. *et al.* (1997). Cloning of the entire COWP gene of Cryptosporidium parvum and ultrastructural localization of the protein during sexual parasite development. *Parasitology* [Online] **114 (Pt 5**:427–37. Available at: http://www.ncbi.nlm.nih.gov/pubmed/9149414.

Spano, F. *et al.* (1998). Molecular cloning and expression analysis of a Cryptosporidium parvum gene encoding a new member of the thrombospondin family. *Molecular and biochemical parasitology* [Online] **92**:147–62. Available at: http://www.ncbi.nlm.nih.gov/pubmed/9574918.

Sponseller, J.K., Griffiths, J.K. and Tzipori, S. (2014). The evolution of respiratory cryptosporidiosis: Evidence for transmission by inhalation. *Clinical Microbiology Reviews* **27**:575–586.

Thompson, R.C.A. *et al.* (2005). Cryptosporidium and cryptosporidiosis. *Advances in Parasitology* **59**:77–158.

Tumwine, J.K. *et al.* (2003). Cryptosporidium parvum in children with diarrhea in Mulago Hospital, Kampala, Uganda. *American Journal of Tropical Medicine and Hygiene* **68**:710–715.

Tzipori, S. and Ward, H. (2002). Cryptosporidiosis: Biology, pathogenesis and disease. *Microbes and Infection* **4**:1047–1058.

Umemiya, R. *et al.* (2005). Electron microscopic observation of the invasion process of Cryptosporidium parvum in severe combined immunodeficiency mice. *The Journal of parasitology* [Online] **91**:1034–9. Available at: http://www.ncbi.nlm.nih.gov/pubmed/16419745.

Upton, S.J., Tilley, M., Nesterenko, M. V, *et al.* (1994). A simple and reliable method of producing in vitro infections of Cryptosporidium parvum (Apicomplexa). *FEMS microbiology letters* **118**:45–49.

Upton, S.J. and Current, W.L. (1985). The species of Cryptosporidium (Apicomplexa: Cryptosporidiidae) infecting mammals. *The Journal of parasitology* [Online] **71**:625–9. Available at: http://www.ncbi.nlm.nih.gov/pubmed/4057006.

Upton, S.J., Tilley, M. and Brillhart, D.B. (1994). Comparative development of Cryptosporidium parvum (Apicomplexa) in 11 continuous host cell lines. *FEMS microbiology letters* [Online] **118**:233–6. Available at: http://www.ncbi.nlm.nih.gov/pubmed/8020747.

Upton, S.J., Tilley, M. and Brillhart, D.B. (1995). Effects of Select Medium Supplements on in-Vitro Development of Cryptosporidium-Parvum in Hct-8 Cells. *Journal of Clinical Microbiology* [Online] **33**:371–375. Available at: <Go to ISI>://A1995QC14800022.

Varughese, E.A. *et al.* (2014). A new in vitro model using small intestinal epithelial cells to enhance infection of Cryptosporidium parvum. *Journal of Microbiological Methods* [Online] **106**:47–54. Available at: http://dx.doi.org/10.1016/j.mimet.2014.07.017.

Villacorta, I. *et al.* (1996). Complete development of Cryptosporidium parvum in MDBK cells. *FEMS Microbiology Letters* **142**:129–132.

Vinayak, S. *et al.* (2015). Genetic modification of the diarrhoeal pathogen Cryptosporidium parvum. *Nature* [Online] **523**:477–80. Available at: http://dx.doi.org/10.1038/nature14651.

Wetzel, D.M. *et al.* (2005). Gliding motility leads to active cellular invasion by Cryptosporidium parvum sporozoites. *Infection and Immunity* **73**:5379–5387.

Woodmansee, D. and Joachim, P. (1983). Development of Cryptosporidium sp . in a human rectal tumor cell line. *The Proceedings of the Fourth International Symposium on Neonatal Diarrhea Sponsored by the Veterinary Infectious Diseases Organisation*.

Woods, K.M. and Upton, S.J. (2007). In vitro development of Cryptosporidium parvum in serum-free media. *Letters in Applied Microbiology* **44**:520–523.

Wu, Z. *et al.* (2000). Specific PCR primers for Cryptosporidium parvum with extra high sensitivity. *Molecular and Cellular Probes* [Online] **14**:33–39. Available at: http://www.ncbi.nlm.nih.gov/pubmed/10722790.

Yang, R. *et al.* (2015). Validation of cell-free culture using scanning electron microscopy (SEM) and gene expression studies. *Experimental Parasitology* [Online] **153**:55–62. Available at: http://dx.doi.org/10.1016/j.exppara.2015.03.002.

Yao, L. *et al.* (2007). Cryptosporidium parvum: Identification of a new surface adhesion protein on sporozoite and oocyst by screening of a phage-display cDNA library. *Experimental Parasitology* **115**:333–338.

Yoshida, H. *et al.* (2007). An outbreak of cryptosporidiosis suspected to be related to contaminated food, October 2006, Sakai City, Japan. *Japanese Journal of Infectious Diseases* **60**:405–407.

Zapata, F. *et al.* (2002). The Cryptosporidium parvum ABC protein family. *Molecular and biochemical parasitology* [Online] **120**:157–61. Available at: http://www.pubmedcentral.nih.gov/articlerender.fcgi?artid=321576&tool=pmcentrez&rendertype=abstract.

Zhang, H. *et al.* (2012). Transcriptome analysis reveals unique metabolic features in the Cryptosporidium parvum Oocysts associated with environmental survival and stresses. *BMC genomics* [Online] **13**:647. Available at: http://www.pubmedcentral.nih.gov/articlerender.fcgi?artid=3542205&tool=pmcentrez&rendertype=abstract.

Zhang, L., Sheoran, A.S. and Widmer, G. (2009). Cryptosporidium parvum DNA Replication in Cell-Free Culture. *Journal of Parasitology* [Online] **95**:1239–1242. Available at: http://www.bioone.org/doi/abs/10.1645/GE-2052.1.